DEVELOPMENT OF CARBON OXIDES SEQUESTRATION FROM YAMAHA EF1000 GENERATOR USING POST-COMBUSTION CAPTURE TECHNIQUE

BY

CHUKWU, MONDAY MORGAN

2011197001P

A PhD DISSERTATION

SUBMITTED TO

THE DEPARTMENT OF CHEMICAL ENGINEERING
FACULTY OF ENGINEERING
NNAMDI AZIKIWE UNIVERSITY, AWKA

IN PARTIAL FULFILMENT OF THE REQUIREMENTS FOR THE AWARD OF DOCTOR OF PHILOSOPHY (PhD) IN CHEMICAL ENGINEERING

MARCH, 2019.

CERTIFICATION

This is to certify that dissertation entitled '**Development of Carbon Oxides Sequestration from Yamaha EF1000 Generator Using Post – Combustion Capture Technique'**which is submitted by **CHUKWU MONDAY MORGAN** in partial fulfillment of the requirement for the award of doctorate degree in Chemical Engineering, Nnamdi Azikiwe University Awka, comprises my original work and due acknowledgment has been made in the text to all other materials used.

…… …….

Chukwu, Monday Morgan Date

APPROVAL PAGE

This dissertation titled '**Development of Carbon Oxides Sequestration from Yamaha EF1000 Generator using Post - Combustion capture Technique',** with registration number **2011197001P**which is submitted by Chukwu, Monday Morgan has been accepted and approved.

…….. ……
Engr. Prof. (Mrs) P.K. Igbokwe Date
Supervisor

…….. ……
Engr. Dr. M.C. Menkiti Date
Head, Chemical Engineering Department

…….. ……
Engr. Prof.V.I. Idigo Date
Dean, Faculty of Engineering

…….. …….
Prof. M.F.N. Abowei
External Examiner Date

…….. …….
Prof.P.K. Igbokwe Date
Dean, Postgraduate School

REPLACE this Page

DEDICATION

This research work is dedicated to Almighty God, my heavenly Father and maker, who is the Author of Life.

ACKNOWLEDGEMENTS

I will first attribute the success of this research to God Almighty for His help and Sustenance. To my research Supervisor, Engr. Prof. (Mrs.) P.K. Igbokwe, for her patience, invaluable assistance and encouragement during the course of this project work, I say a very big thank you.

Many thanks to the Head of Department, Engr. Dr. Mrs. M. C. Menkiti, for his words of encouragement towards the success of the research. I acknowledge the efforts and commitment of the former Head of Department, Engr. Dr. T.J. Nwabanne, towards the success of this research. He was there to encourage and guided me all through the work. I cannot thank enough all teaching staff of the department especially Dr. Ugonab for their unique support in various ways towards ensuring timely completion of the work.

I am grateful to all Panel members of the department that were there especially on their criticisms to the work when it was first presented at the department. You made me appreciate the work more.

I would like to appreciate efforts of the Chairman/CEO of New Concepts Lab - Engr. Clement Johnson. Many thanks to my friends - Engr. Jude Obijiaku and Engr J.C. Offurum for always being there for me while it lasted. My appreciation also goes to the Chairman, Ken Maduakor Group Ltd. for supporting immensely the course of this research.

Not forgetting the encouragements from my friends, my wife and wonderful kids, whose understanding and patience is immeasurable especially when they had to forgo the leisure of being with me during the yuletide period.

I sincerely thank you all.

ABSTRACT

This work aimed atdevelopment of carbon oxides sequestration from Yamaha EF1000 generator using post - combustion capture technique. The state of the art is the use of monoethanolamine as sorbent for carbon sequestration. The present study postulated reaction mechanism of sawdust ash leachate with CO_2 from flue gas and examined the use of the leachate as sorbent for capture of CO_2 and CO from Yamaha EF1000 generator as the source of flue gas. A prototype absorber was designed and fabricated to specifications of 8.2cm column diameter, overall column height of 11.4cm, column pressure drop of 1531.32N/m^2 and volumetric hold-up of 0.32cm^3 absorber liquid/cm^3 column. The Kipps apparatus were appropriately connected to the source of the flue gas in countercurrent movement of the flue gas with the sorbent. Modelling and optimization of the process were carried out using design expert version 10 with concentration of absorber liquids, process time and absorber liquid flow rate as the process variables. Quadratic models were obtained as the best models for the capture for each of the sorbents with CO_2 and CO of the exit flue gas as response. For the ash leachate, the CO_2 and CO composition of exit flue gas values of 3.557% and 16.768% as optima respectively, at sequestrant concentration of 21.795g/L, sequestration time of 9.997mins and sequestrant flow rate of 200.278cm^3/min respectively were achieved. Optimum CO_2 and CO composition of exit flue gas values of 4.139% and 18.959% respectively, and at the respective factors of 20.044g/L, 5.666mins and 223.848cm^3/min for sequestrant concentration, sequestration time and sequestrant flow rates respectively for monoethanolamine, were also obtained. From the results, the quadratic models best described the carbon sequestration process for both the leachate and the conventional monoethanolamine. CO_2 and CO capture achieved with the leachate was about 8% more than that achieved with the conventional monoethanolamine. The postulated mechanisms of the leachate appropriately described the behavior of the leachate with CO_2 from flue gas of Yamaha EF 1000 based on kinetics of the reaction obtained which agreed with the experimentally determined rate law. Capturing of CO with either monoethanolamine or sawdust ash leachate could not be seen published. This work has established that sawdust ash leachate can effectively be used as sorbent in place of the conventional monoethanolamine for Post – Combustion capture of CO_2 and CO.

TABLE OF CONTENTS

LIST OF TABLES

LIST OF FIGURES

Figures

NOMENCLATURE& SYMBOLS

Abbreviation	Description
ASU	Air Separation Unit
CCR	Carbonation Calcination Reaction
CCS	Carbon Capture and Storage
CPU	Compression and Purification Unit
DAF	Dry Ash Free
DEA	Diethanolamine
DECC	Department of Energy and Climate Change
EDTA	Ethylenedinitrilo-tetra-acetic-acid
ESP	Electro Static Precipitator
FGD	Flue Gas Desulphurisation
GHG	Greenhouse Gas
HHV	Higher Heating Value
LCPD	Large Combustion Plant Directive
LHV	Lower Heating Value
MEA	Monoethanolamine
mg/m^3	milligramme per cubic metre
MHI	Mitsubishi Heavy Industries
MMBtu	Million British thermal units
NETL	National Energy Technology Laboratory (US)
ng/J	Nanogramme/Joule
NOx	Nitrogen Oxides (NO and NO_2)
O&M	Operation and Maintenance
OPEX	Operating Expenditure
PC	Pulverised Coal
PM	Particulate Matter
ppmv	Parts Per Million by Volume
RFG	Recycled Flue Gas
SCR	Selective Catalytic Reduction
SDA	Spray Dryer Absorber
TIPS	ThermoEnergy Integrated Power System

CHAPTER ONE

INTRODUCTION

1.1 Background of the Study

One of the main global challenges in the years to come is to reduce the CO_2 emissions inview of the apparent contribution to global warming. Carbon dioxide capture and storage (CCS) from fossil fuel fired power plants is drawing increased interest as an intermediate solution towards sustainable energy systems in the long term. However, CCS is still facing some challenges, such as large scale implementation requires high energy demands and leads to high cost. Innovation and optimization of the capture process is needed to reduce the energy requirement and to minimize the investment cost in order to make CCS viable for application in the near future.

The CO_2 post-combustion capture based on the absorption/desorption process with monoethanolamine (MEA) solutions, is considered as the state-of-art technology. The MEA process has been defined as the reference case for the purposes of comparison and benchmarking (Davidson, 2007).

There is no question that carbon monoxide is a pollutant with potential to harm all living things. But does CO also affect Earth's climate. Unlike carbon dioxide, a compound that contains the same atoms as carbon monoxide, carbon monoxide is not known as a direct contributor to climate change (Metz et al., 2005). It does, however, play a role in this area and such roles will be investigated with the results of the sequestration.

Global warming is the increase in the average temperature of the earth. This effect is caused by anthropogenic greenhouse gases released to the atmosphere. The control of these greenhouse gases is arguably the most challenging environmental policy issue facing most countries. An approach that is gaining widespread interest is to control CO_2 emissions by capturing and sequestering CO_2 from fossil fuels to continue to be used without contributing significantly to greenhouse warming. There are ten primary greenhouse gases including water vapour (H_2O), Carbon dioxide (CO_2), methane (CH_4), and nitrous oxide (N_2O) that are naturally occurring. Hydrofluorocarbon and Sulphurhexaflouride (SF_6) are only present in the atmosphere due to industrial processes. Water vapour is the most abundant and dominant greenhouse gas, and CO_2 is the second – most significant one (Mohammad et al., 2014). This has been source of attention

for researcher for the past 30 years due to increasing global temperatures. Concentration of water vapour depends on temperature and other meteorological conditions, and not directly upon human activities.

CO_2accounts for 77% of the human contribution to the greenhouse effects in recent decades (26 to 30 percent of CO_2 emission). Main anthropogenic emissions of CO_2 come from the combustion of fossil fuel. CO_2 concentration in flue gases depends on the fuel such as coal (12 – 15 mol-% CO_2) and natural gas (3 – 4mol-% CO_2). In petroleum and other industrial plants, CO_2 concentration in exhaust stream, depends on the process such as oil refining (8 – 9mol% CO_2) and production of cement (14 – 33 mol% CO_2) and iron and steel (20 – 44 mol %).

From 2004 to 2011, global CO_2 emissions from energy uses were increased to 26% (Chiao et al., 2011; Zhao et al., 2008) as reported by Mohammad et al., 2014. While thoseof power plant (55% of global CO_2 emissions) transportation (33%), and industry (19%) have highest share in the CO_2 emission in USA. Cement and petro chemical plants are two major industries contributing about 5% to global anthropogenic CO_2 emission. Also, petrochemical industries have a large share of CO_2 emissions (Mohammad et al., 2014).

The atmospheric concentration of greenhouse gases (e.g. carbon dioxide, methane,nitrous oxide and chlorofluorocarbons) has increased gradually in the last century. The Intergovernmental Panel on Climate Changes (IPCC) has evaluated the size and impact of this increase. One of the conclusions is that the reasons behind the increased concentration of the greenhouse gases in the atmosphere are the human activities (Abu-Zahra et al., 2007a). As a result, the global atmospheric concentration of CO_2 increased from a pre-industrial value of about 280 parts per million by volume (ppmv) to 384 ppmv in 2007 (Abu-Zahra et al., 2007a). Moreover, the green houses gases concentration is expected to increase to about 600 ppmv by 2050 if no mitigation and emissions reduction options are applied 2007 (Abu-Zahra et al., 2009b). The emissions of the different greenhouse gases have been monitored and measured all around the globe. It is evident that carbon dioxide is the most important anthropogenic green house gas. Its annual emissions have grown between 1970 and 2004 by about 80%, from 21 to 38 gigatonnes, and represented 77% of total GHGs emissions in 2004&2007 (Abu-Zahra et al., 2009b).

There is a growing consensus that temperature increase due to climate change should be limited to around 2-3 degree celsius. There are many scenarios presented and discussed to evaluate the

required level of CO_2 emissions reduction to achieve this target (Abu-Zahra et al., 2007a; Abu-Zahra et al., 2009b). TheInternational Energy Agency (IEA) has considered two climate policy scenarios corresponding to long term stabilization of greenhouse gas in the year 2030 at 550 (an increase in global temperature of approximately 3^0C) and 450 (a rise of around 2^0C) ppm of CO_2(Suda et al., 1992). This can be achieved by combining different solutions (renewable, energy efficiency, CCS, nuclear) to cut down the CO_2emissions by 50-65% in 2030 comparing to the reference case level in 2006 (Suda et al., 1992). The European Union (EU) emphasizes the necessity to reduce CO_2emissions by developed countries by 30% in 2020 compared to 1990 levels (Abu-Zahra et al., 2009b; Suda et al., 1992). In addition, the EU is committed to achieve a 20% reduction of its greenhouse gas emissions by 2020 compared to 1990 (Sander and Mariz, 1992). To reach this ambitious goal, the focus is mainly on the CO_2 emissions from the consumption of fossil fuel, which is responsible of around 57% of the global green house gases emissions. The global intention is directed toward the fossil fuels that are used for electricity generation, which are responsible for 41% of the global CO_2 emission in 2004 (Imai, 2003). The transportation sector is the second largest CO_2 emitter and can contribute in reducing CO_2emissions (e.g. by the development of more efficient engines and by switching to more environmental friendly fuel like hydrogen, which is connected to an earlier CO_2 separation step).

Currently, fossil fuels provide around 80% of the world's total energy demand. Coal is playing a major role as the main source of electrical power (38% of the total electricity generation) (Mimura et al., 1995). The large dependency on fossil fuels makes it difficult to switch completely to other energy sources. Moreover, the international energy

y agency scenarios have expected the world energy demand to expand by 45% between now and 2030 (Herzog et al., 2009).

Many researchers are aiming to develop new solvent technologies to improve the efficiency of the CO_2 removal. Process model, simulation and evaluation are essential items to predict the maximization of the absorption process. Several researchers have modelled and studied the MEA absorption process (Abu-Zahra et al., 2007a). Most of their conclusions focused on reducing the thermal energy requirement to reduce the overall process expenses. This high-energy requirement makes the capture process energy intensive and costly considering the cost of procuring even the MEA (Rao et al., 2006). Therefore, it is important to study other alternative

solvents to achieving the capture.Also as part of an effort to reduce carbon monoxide poisoning, capturing carbon monoxide with the sawdust ash leachate will also be investigated.

1.2 Problem Statement

The control of greenhouse gases is arguably the most challenging environmental policy issue facing most countries today. The development of new technologies for the management of the aforementioned challenge is the key drive for this research, and this is even more imperative as there is now need for a shift from the conventional and commonly used chemicals to locally sourced waste materials, to accomplish the purpose. In this regard, sawdust ash is considered to be of advantage, since the problem of waste materials disposal have continually posed pollution and health problems to the public, and have been of great concern to researchers. To making sawdust ash useful, this research work concentrates on the viability of using sawdust ash leachate for $CO_2$and CO capturefrom flue gas and comparing the results with the capture achieved with the use of MEA.

1.3 Aim and Objectives

This research work aimed atdevelopment of carbon oxides sequestration from Yamaha EF1000 using Post – combustion capture technique.The specific objectives are as follows:

1) To produce and characterizesaw dust ash leachate.

2) To captureCO_2 and CO from flue gas using both sawdust ash leachate and MEA solutions.

3) To determine the effects of the varying ash leachate concentrations on the quantity of the CO_2 and CO absorbed.

4) To compare the efficiency of the commonly used MEA solution with the ash leachate at same concentrations and working conditions.

5) To determine the optimum process parameters, for sequestration of CO_2 and CO capture from flue gas.

6) To elucidate the design considerations for a prototype device for CO_2 and CO capture using the sawdust ash leachate and MEA.

1.4 Justification of the Study

Finding good and alternative approach for the capture of CO_2 and CO, on the quest to reduce green-house gases is an effort that will be much dependent on the development of new and dependable technologies that can handle the situation and yet making use of local and affordable sources to meet the target. Findings from this research and success in the test run of the design will sure go a long way to step up advances in this area of concern, exposing needed idea to this regard, thus enhancing general human health and environmental safety. Findings from this work will to a good extent serve to broaden knowledge that will be helpful in meeting the aforementioned purpose.

1.5 Scope of the Study

This research work focuses on the experimental investigation of the use of sawdust ash leachate in the sequestration of CO_2 and COfrom flue gas, and comparing result with the performance of conventional MEA solution used in the industries, for this purpose. Afterwards, modelling and optimization of the experimental data to obtain optimum process conditions for the sequestration of CO_2 and CO capture from flue gas will be conducted. Regression analysis will also be carried out to determine the model fit to the experimental data. The optimum process conditions will be used in the design and fabrication of a prototype device for CO_2 and CO capture from flue gas.

CHAPTER TWO

LITERATURE REVIEW

2.1 Carbon Capture

The main CO_2 source is the combustion of fossil fuels such as coal, oil, and gas in power plants, for transportation and in homes, offices, and industry. Fossil fuels provide more than 80% of the world's total energy demands (Rubin et al., 2012). It is difficult to reduce the dependency on fossil fuels and switch to other energy sources. Moreover, the conversion efficiency of other energy sources for power generation is mostly not as high as that of fossil fuels. A drastic reduction of CO_2 emissions resulting from fossil fuels can only be obtained by increasing the efficiency of power plants and production processes, and decreasing the energy demand, combined with CO_2 capture and storage (CCS). CCS is a promising method considering the ever-increasing worldwide energy demand and the possibility of retrofitting existing plants with capture, transport, and storage of CO_2(IEA GHG, 2005). The captured CO_2 can be used for enhanced oil recovery, in the chemical and food industries, or can be stored underground instead of being emitted to the atmosphere (Makino, 2006).

Technologies to separate CO_2 from flue gases are based on absorption, adsorption, membranes, or other physical and biological separation methods. Rao and Rubin (2002) showed that for many reasons, amine based CO_2 absorption systems are the most suitable for combustion based power plants. These can be used for dilute systems and low CO_2 concentrations. The technology is commercially available, it is easy to use and can be retrofitted to existing power plants. Absorption processes are based on thermally re-generable solvent, which have a strong affinity for CO_2. They are generated at elevated temperature. The process thus requires thermal energy to the regeneration of the solvent. Aqueous monoethanolamine (MEA) has been an available absorption technology for removing CO_2 from flue gas streams.

a. CO_2capture in industrial processes

Besides classical methods, some industries have already developed their ownCO_2capture method, based on their specific process. In some cases, the CO_2 capture process is still under development. The most significant example is briefly described below:

Natural gas sweetening: in order to preserve natural gas pipelines from corrosion, the CO_2 content in the gas must not exceed 2%. Depending on the initial CO_2 content, separation

membranes, physical or chemical absorption processes are applied. Natural gas sweetening is already a commercially available technology (IPCC, 2005).

b. In ammonia synthesis

Ammonia synthesis: this process is similar to pre-combustion capture with the difference that it is already commercially available. In ammonia plants, H_2 and N_2 react to form ammonia. Hydrogen is produced by steam reforming or gasification, depending on the fuel (light hydrocarbons or coal respectively). In order to purify the produced syngas, the CO_2 is generally captured by absorption. Carbon dioxide is then a by-product of the ammonia synthesis so that urea production plants – large CO_2 consumers – are usually associated with ammonia production plants (IPCC, 2005).

c. In steel production

Steel production: in 2008, the iron and steel industry accounted for 14% of the total industrial energy consumption (IEO, 2011). However, few large CO_2 capture projects have been identified in the steel industry. In the steel industry, the major part of the CO_2 production is not due to combustion, but to the reaction of iron ores with a reducing gas, usually carbon monoxide. The most promising method to cut down CO_2 emissions consists in capturing CO_2 from the gas exiting the blast furnace by vacuum pressure swing adsorption. The other components of the gas stream (CO and H_2) are recycled to the furnace. Moreover, the furnace can be operated with oxygen instead of air, so that the CO_2 content of the flue gas is increased (Zuo and Hirsch, 2008).

d. In cement production

Cement production: cement production plants are also large energy consumers. In cement plants, the CO_2 concentration in the flue gas varies between 15% and 30%. The post-combustion capture is the most adapted process for retrofitting existing plants, but it implies higher costs than in power plants due to the additional flue gas cleaning steps (Anderson et al., 2008). Consequently, the oxyfuel process is more adapted for a new cement production plant (Barker et al., 2009). This alternative technology takes place at high temperatures (carbonatation around 650°C, calcination around 900°C) but seems nevertheless promising, with a very low energy penalty compared to conventional capture methods (Bosoaga and John, 2009).

e. CO_2 utilization

The initial objective of CCS technologies is to capture CO_2 and to store it underground in order to limit its effect as greenhouse gas. However, capturing CO_2 is expensive so that valorizing it as a by-product instead of considering it as a waste would certainly be useful for the development of large scale CO_2 capture (IPCC, 2005).

2.1.1Overview of CO_2 Capture Systems

There are basically three systems for carbon dioxide capture and they are classified as shown in Figure 2.1**.**

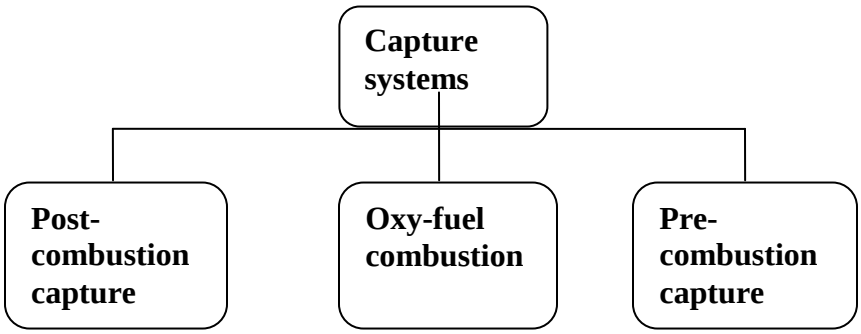

Figure 2.1: Carbon dioxide capture systems classification

a. Post-combustion capture

Post-combustion capture is a downstream process that is analogous to flue gas desulfurization. It involves the removal of CO_2 from the flue gas produced after the combustion of the fuel. A schematic of post-combustion capture is presented in Figure 2.2.

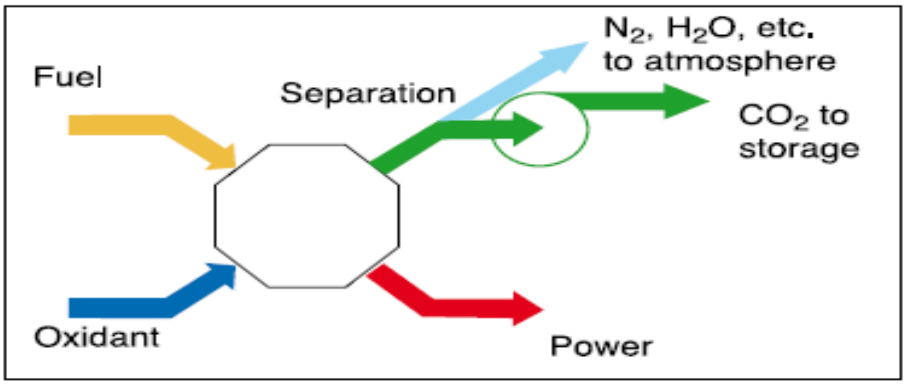

Figure 2.2: Schematic of post-combustion capture.(Adapted from Anderson and Newell (2004), *Prospects for carbon capture and storagetechnologies.*Annual Review of Environment and Resources**).**

The oxidant used for combustion is typically air and hence, the flue gases are diluted significantly with nitrogen. In addition, since the flue gases are at atmospheric pressure, a large volume of gas has to be treated. Table 2.1 shows the typical CO_2 percentage in the flue gases from different combustion systems.

Table 2.1: Typical CO_2 percentage in flue gas from different combustion systems

Flue gas source	**CO_2 Concentration, % vol (dry)**	**Pressure of gas Stream, Mpa**	**CO_2 partial Pressure, Mpa**
Natural gas fired boilers	7-10	0.1	0.007-0.01
Gas turbines	3-4	0.1	0.003-0.004
Oil fired boilers	11-13	0.1	0.011-0.013
Coal fired boilers	12-14	0.1	0.012-0.014
IGCC after combustion	12-14	0.1	0.012-0.014
IGCC synthesis gas after gasification	8-20	2-7	0.16-1.4

(Adapted from Anderson and Newell (2004), *Prospects for carbon capture and storage technologies.*Annual Review of Environment and Resources**).**

A number of methods exist for the post-combustion capture of CO_2 from flue gases. These include:

• Chemical absorption
• Physical absorptions
• Membrane separation
• Adsorption
• Cryogenic separation

b. Chemical Absorption

Chemical absorption systems at present are the preferred option for post combustion capture of CO_2. Chemical absorption systems have been in use since the 1930s for the capture of CO_2 from ammonia plants for use in food applications and hence, are a commercially realized technology, though not at the scale required for power plants.

CO_2 is separated from the flue gas by passing the flue gas through a continuous scrubbing system. Absorption processes utilize the reversible chemical reaction of CO_2 with an aqueous alkaline solvent, usually an amine. In the desorber, the absorbed CO_2 is stripped from the solution and a pure stream of CO_2 is sent for compression while the regenerated solvent is sent

back to the absorber. Heat is required in the reboiler to heat up the solvent to the required temperature; to provide the heat of desorption and to produce steam in order to establish the required driving force for CO_2 stripping from the solvent. This leads to the main energy penalty on the power plant. In addition, energy is required to compress the CO_2 to the conditions needed for storage and to operate the pumps and blowers in the process.

c. Oxy-fuel combustion

The main disadvantage of post-combustion capture systems is the dilution of the flue gases due to nitrogen. This problem can be mitigated if the combustion is carried out in the presence of oxygen instead of air. The burning of fossil fuel in an atmosphere of oxygen leads to excessively high temperatures – as high as 3500°C.

The temperature is moderated to a level that the material of construction can withstand by recycling a fraction of the exhaust flue gases. The flue gas contains mainly CO_2 and water. It may also contain other products of combustion, such as NO_x and SO_x, depending on the fuel employed. One of the advantages of oxy- fuel combustion is that the formation of NO_x is lowered since there is negligible amount of nitrogen in the oxidant. Any formation of NO_x will only arise from the nitrogen in the fuel. However, if the amount of fuel-bound nitrogen is high, the concentration of NO_x will be very high since it is not diluted by nitrogen. It is necessary that the NO_x be removed prior to recycle of the flue gas. After condensation of water, the flue gas contains 80-98% CO_2 depending on the type of the fuel used. This is then compressed, dried and sent for storage. The CO_2 capture efficiency is very close to 100% in these systems. It may be necessary to remove acidic gases such as SO_x and NO_x if their levels are above those prescribed for CO_2 sequestration. Removal of noble gases such as argon may be necessary depending on the purity of O_2 employed for combustion. Since there is less NO_x, the partial pressure of SO_x and HCl are increased leading to an increase in the acid dew point. Hence, it may be necessary to employ dry recycle of CO_2 if the sulfur content of the fuel is high. Since the stream is pure in CO_2 and is directly sequestered, it may be possible to store the SO_2 along with the CO_2 and claim mixed credits for this. This will avoid the need for a flue gas desulfurization unit (FGD). Water however needs to be removed. Complete dehydration of the flue gas will reduce mass flow and prevent corrosion and hydrate precipitation.

The main energy penalty in oxyfuel combustion occurs due to the energy intensive separation of oxygen from air in the air separation unit (ASU). Cryogenic separation is employed to obtain an oxygen stream of 95% purity. One of the methods is through the use of a boiler and a steam

cycle. To achieve this, boiler modifications are required with some redesign of the burner system. The air in leakage needs to be minimized and a recycle line needs to be provided for recycling flue gas to moderate the boiler temperature. In the case of natural gas, oxygen and natural gas can be sent to a gas turbine for combustion and power generation. However, for this to be implemented there needs to be commercialization of a gas turbine operating on CO_2 as the main working fluid.A feature of oxy-fuel combustion systems is that during start-up, air firing may be necessary so that sufficient recycle of the flue gas is established before oxygen firing is initiated. This necessitates the equipment for air firing and additional controls. The control of these systems is not yet well understood. In order, to evaluate the operability and reliability of these systems, large scale demonstration units need to be commissioned.

d. Chemical looping combustion

Chemical looping combustion (CLC) is an indirect combustion system that avoids the direct contact of fuel with the oxidant. Oxygen is transferred to the fuel via a solid oxygen carrier. The combustion system is split into two reactors. In the reduction reactor (also called the fuel reactor), the fuel reduces the solid oxide material which is then transported to the oxidation reactor where the reduced metal oxide is oxidized with air. A schematic of a CLC system is shown in Figure 2.3.

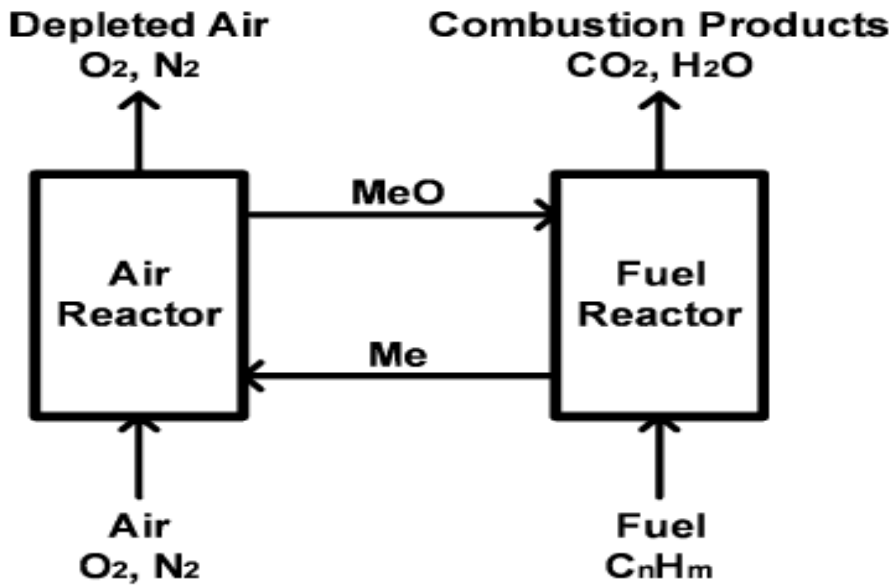

Figure 2.3: Schematic of chemical looping combustion. (Adapted from Herzog and Drake(1996).*Carbon dioxide recovery and disposal from large energy systems.*Annual Review of Energy and the Environment, 1996).

The reaction scheme is shown in equation 2-1 to 2-3:

The reduction reaction in the fuel reactor is:

$$CnH2m + (2n+m)MyOx \rightarrow (2n+m)MyOx-1 + nCO_2 + mH_2O \quad (2\text{-}1)$$

The oxidation reaction in the air reactor is:

$$(2n+m)MyOx-1 + [n + \tfrac{m}{2}]O_2 \rightarrow (2n+m)MyOx \quad (2\text{-}2)$$

The overall reaction is:

$$CnHm + [n + \tfrac{m}{2}]O_2 \rightarrow nCO_2 + mH_2O \quad (2\text{-}3)$$

The overall reactions (2-1to 2-3) are the equivalent of the combustion of the fuel.

(2-1) is usually endothermic while (2-2) is exothermic. Hence, there is need for transfer of heat from the oxidation reactor to the fuel reactor through the solid oxide particles. However, when CuO is used as the oxygen carrier, (2-1) is exothermic.The flue gases from the reduction reactor consist mainly of CO_2 and H_2O and a pure stream of CO_2 can be obtained by condensing the water. The flue gases can be integrated into the power cycle either via a steam boiler or via a CO_2/H_2O turbine (Herzog and Drake, 1996).

The oxygen depleted air in the oxidation reactor contains sensible heat due to the exothermic oxidation reaction. This stream is also integrated into the power cycle.

e. Pre- combustion capture

In pre -combustion capture, the carbon content of the fuel is reduced prior to combustion, so that upon combustion, a stream of pure CO_2 is produced. Pre combustion decarbonization can be used to produce hydrogen or generate electricity or both. A synthesis gas is produced in the first step of pre -combustion decarbonization. If natural gas is used as a fuel, this is obtained by either steam reforming or auto thermal reforming. If coal is used as the fuel, synthesis gas is obtained by gasification. In the next step, the synthesis gas is subjected to the water gas shift reaction to produce carbon dioxide and hydrogen. The hydrogen and carbon dioxide can be separated by pressure swing adsorption or physical absorption and the pure CO_2 stream is compressed and sent for storage. When pressure swing adsorption is used to produce a pure stream of CO_2 and another pure stream of H_2, an additional step is needed for CO_2 purification before the H_2 purification. The hydrogen stream is either used as a feedstock for a chemical process or is burnt to produce electricity.

f. Steam reforming

Natural gas can be steam reformed and then subjected to water gas shift reaction to produce a mixture consisting mainly of carbon dioxide and hydrogen. The reactions in steam reforming are outlined below:

$$CH_4 + H_2O + heat \rightarrow CO + 3H_2 \quad (2\text{-}4)$$

$$CO + H_2O \leftrightarrow CO_2 + H_2 \quad (2\text{-}5)$$

Steam reforming is endothermic and hence, some of the natural gas has to be used for firing in the reformer furnace to provide the heat required for the reforming reaction. This can lead to significant energy losses in the process. Since there is a more concentrated stream of CO_2 available, the energy penalty for absorption is not as high. The CO_2 can also be separated by pressure swing adsorption. However, the water gas shift reaction also requires steam to be withdrawn from the power cycle. Hence, this process is advantageous only if the energy savings made from capturing a purer stream of CO_2 are greater than the energy losses due to loss of natural gas used for firing and loss of steam from the steam cycle for the shift reaction. If a CO_2

free process is desired, it is necessary to use the produced hydrogen for firing in the reformer, and this would lead to even higher energy losses.

g. Auto - thermal reforming

Auto - thermal reforming is a combination of steam reforming and partial oxidation. Since the partial oxidation reaction is exothermic, it provides the energy required for the endothermic steam reforming and only minimal firing of additional natural gas as fuel is required. The reactions in auto thermal reforming are given below. The auto thermal reforming is the third reaction (2-8) and it is the sum of the first two reactions - (2-6) and (2-7).

$$CmHn + \frac{m}{2} O_2 \leftrightarrow mCO + nH \quad (2\text{-}6)$$

$$\frac{m}{2} H_2 + \frac{n}{4} O_2 \leftrightarrow \frac{m}{2} H_2O \quad (2\text{-}7)$$

$$CmHn + \frac{2m+n}{4} O_2 \rightarrow mCO + \frac{n}{2} H_2O \quad (2\text{-}8)$$

The flue gas contains mainly CO_2 and water. It may also contain other products of combustion, such as NO_x and SO_x, depending on the fuel employed. One of the advantages of oxyfuel combustion is that the formation of NO_x is lowered since there is negligible amount of nitrogen in the oxidant. Any formation of NO_x will only arise from the nitrogen in the fuel. However, if the amount of fuel-bound nitrogen is high, the concentration of NO_x will be very high since it is not diluted by nitrogen. It is necessary that the NO_x be removed prior to recycle of the flue gas. After condensation of water, the flue gas contains 80-98% CO_2 depending on the type of the fuel used. This is then compressed, dried and sent for storage. The CO_2 capture efficiency is very close to 100% in these systems. It may be necessary to remove acidic gases such as SO_x and NO_x if their levels are above those prescribed for CO_2 sequestration. Removal of noble gases such as argon may be necessary depending on the purity of O_2 employed for combustion. Since there is less NO_x, the partial pressure of SO_x and HCl are increased leading to an increase in the acid dew point. Hence, it may be necessary to employ dry recycle of CO_2 if the sulfur content of the fuel is high. Since the stream is pure in CO_2 and is directly sequestered, it may be possible to store the SO_2 along with the CO_2 and claim mixed credits for this. This will avoid the need for a flue gas desulfurization unit (FGD). Water however needs to be removed. Complete dehydration of the flue gas will reduce mass flow and prevent corrosion and hydrate precipitation.

2.2 Components of the Flue Gas

In addition to CO_2, N_2, O_2, H_2O, particulates, HCl, HF, mercury, other metals and other trace organic and inorganic contaminants, flue gas from coal combustion contains other acid gas components such as NOx and SOx. These acidic gas components have a chemical interaction with the alkaline solvent, similar to that of CO_2. This is not desirable as the irreversible nature of this interaction leads to the formation of heat stable salts and hence a loss in absorption capacity of the solvent and the risk of solids forming in the solution. In addition, it results in an extra consumption of chemicals to regenerate the solvent and the production of a waste stream such as sodium sulphate or sodium nitrate. Therefore, the removal of NOx and SOx to low levels before CO_2recovery becomes essential. For NOx, it is the NO_2which leads to the formation of heat stable salts. Fortunately, the level of $NO_2$is generally a small fraction of the overall NOx content in a flue gas (IPCC, 2005).

a. Nitrogen oxides

NOx produced from coal or lignite firing is mainly NO, with up to about 5% NO_2, but normally less. NO does not react with amines in CO_2 capture plant, but NO_2does. NO is not absorbed in plant but about 30% of the $NO_2$is. The concentration that results is acceptable for Fluor and is perhaps also low enough, although they have not stated a limit. It is therefore apparent that no additional NOx abatement is required to protect a Fluor amine scrubber.

b. Sulphur oxides

The allowable SOx content in the flue gas is determined primarily by the cost of the solvent – as this is consumed by reaction with SOx. SO_2 concentrations in the flue gas are typically around 300–5000 ppm. Commercially available removal plants remove up to 98–99% of the SO_2. Amines are relatively cheap chemicals, but even cheap solvents such as monoethanolamine (MEA) may require SOx concentrations of around 10 ppm to keep solvent consumption (around 1.6 kg of MEA/tonne CO_2 separated) and make up costs at reasonable values. The optimal SO_2 content, before the CO_2 absorption process, is acost trade-off between CO_2-solvent consumption and SO_2-removal costs.

2.2.1 Separation of CO_2 with MEA

The widely used chemical solvents are aqueous solutions of alkanolamines, of which the most recognised are monoethanolamine (MEA), diethanolamine (DEA) and methyldiethanolamine (MDEA). These alkanolamines arecommonly referred to as primary, secondary and

tertiaryamines according to the number of carbon-containing groups attached to the nitrogen atom. MEA, with only one carboncontaining group is classified as the primary amine, while DEA falls into the secondary amine category. MDEA is one of the tertiary amines having three carbon-containing groups (Veawab et al., 2003).

MEA has several advantages over other commercial alkanolamines, such as high reactivity, low solvent cost, low molecular weight and thus high absorbing capacity on a mass basis. It has a reasonable thermal stability and thermal degradation rate. Studies have been directed at finding new amines that are able to capture greater amounts of CO_2 than MEA and also to avoid its disadvantages. These include high enthalpy of reaction with CO_2 leading to higher desorber energy consumption, the formation of stable carbamate, andalso the formation of degradation products with carbonyl sulphide or oxygen-bearing gases, inability to remove mercaptans, vaporisation losses due to high vapour pressure, and more corrosive effects than many other alkanolamines, thus needing corrosion inhibitors when used in higher concentration (Davidson, 2007). Another major limitation of MEA is that its maximum CO_2 loading capacity based on stoichiometry is about 0.5mol CO_2/mol amine whereas tertiary amines, such as MDEA, have an equilibrium CO_2loading capacity that approaches 1mol CO_2/mol amine (Supap et al., 2009).

A comprehensive study has been conducted to evaluate the contributions of SO_2 and O_2 to the degradation of MEA during CO_2 capture from power plant flue gas (Uyanga and Idem, 2007). The authors noted that information on the effects of SO_2, NOx and fly ash on MEA degradation is scant. The aqueous MEA was contacted with gas mixtures that had SO_2 concentrations in the range 6–196 ppm. It was found that an increase in the concentrations of SO_2 and O_2 in the gas phase and MEA in the liquid phase resulted in an increase in MEA degradation, whereas an increase in CO_2 loading in the liquid phase inhibited degradation. It was pointed out that, if CO_2capture is carried out in the ‘rich mode’, whereby the lean MEA is still considerably loaded with CO_2 (for example, 0.25mol CO_2/mol MEA) rather than the ‘lean mode’ but maintaining the cyclic capacity, CO_2 could actually act as a degradation inhibitor, because this reduces the amount of $SO_2$and O_2 that could enter into the aqueous MEA solution to induce degradation. However, the detrimental corrosive effect of excess CO_2 in the system must be taken into account.

If the loaded amine solutions contact gas containing oxygen, the amine is subject to oxidative degradation. The degradationof MEA depends on temperature, initial MEA concentration, and

oxygen concentration. However, MEA degradation does not follow a simple rate equation; the reaction order changes from a low to a high value as the concentration of MEA increases. Even though the experimental conditions allowed the reaction to be modeled as a homogeneous liquid-phase reaction, it has been concluded that MEA oxidative degradation itself is not an elementary reaction (Davidson, 2007). Studies have shown that the degradation products are oxidized fragments of the amine including NH_3, formate, acetate, and peroxides. Other studies have shown that the oxidative degradation is catalyzed by the presence of various multivalent cations such as iron, copper, nickel and chromium (Goff and Rochelle, 2003). Dissolved iron will always be present in the absorber as a corrosion product and copper (II) salts are often added as corrosion inhibitors. The degradation rate of solutions with high CO_2 loadings increases with a rise in the concentration of dissolved iron. The addition of copper further catalyzes the degradation rates. At a lower CO_2loading, it was found that the degradation was faster (Davidson, 2007).

MEA undergoes degradation when exposed to coal-fired power plant flue gas composed of CO_2, fly ash, O_2, N_2, $SO_2$and NO_2. Fly ash is the fine particulates in flue gas consisting of inorganic oxides, such as SiO_2, Al_2O_3, Fe_2O_3, CaO, MgO, Na_2O, K_2O and P_2O_5. The breakdown of the amine makes the performance of the amine in the absorption process deteriorate. Not only does it reduce the CO_2 removal capacity, but corrosion and foaming are induced due to the presence of degradation products. The prediction of the extent and rate of amine degradation is vital in the estimation of the exact amine make-up rate needed to maintain the CO_2 absorption capacity of the capture process. It is also essential to evaluate the kinetics of the degradation process since this provides the elements for a better understanding of the degradation mechanism during the CO_2 absorption operation. A kinetic evaluation helps in the formulation of a degradation prevention strategy (Supap et al., 2009).

Since O_2 is known to be deleterious to most amines, considerable efforts have been focused on the O_2-induced degradation of MEA. Although the kinetic studies based only on the presence of O_2 in the flue gas could provide useful rate information, their application could be limited. If these kinetic models were applied to a coal-based application in which an aqueous amine was used to remove CO_2, a less than accurate degradation rate would result. This would be because of the presence of additional impurities such as SO_2 in the flue gas that also induce degradation. Other variables such as dissolved iron, NOx, corrosion inhibitors and fly ash could also be

present in the CO_2capture system. Supap et al., (2009), adopted a step-wise procedure of adding one variable at a time to determine their effects on amine degradation. They incorporated the effects of SO_2 with the well-studied effects of O_2. When the effects of all the parameters that affect amine degradation have been elucidated separately, it will be possible to determine whether there are interactions between these parameters. The negative effects of SO_2 in amine degradation have been reported in terms of its capability of forming heat stable salts such as thiosulphates and sulphates which reduce the CO_2 absorption capacity (Supap et al., 2009). Rao and Rubin (2002) recommended that SO_2concentration in the flue gas prior to being treated in a CO_2capture unit should not exceed 10 ppm in order to avoid excessive loss as amine solvent. Supap et al., (2009) used concentrations of SO_2 between 6 and 196 ppm that can be observed in a typical flue gas sequestration process.

Even though present in small amounts, SO_2 can dissolve and be carried in the amine solution to the regeneration section of the capture process at which point a high temperature can trigger serious degradation reactions with the amine solvent.

There are several ways in which an ideal post-combustion capture process could improve upon a generic MEA capture process. Improvements are possible for the solvent itself, and also for the process configuration. Starting with the characteristics of the solvent, the following aspects are of most interest (Moser et al., 2009):

- low regeneration duty;
- high stability against oxygen and thermal stress;
- low vapour pressure to reduce solvent losses;
- high cyclic capacity to reduce the solvent circulation rate;
- high reactivity to CO_2/fast reaction kinetics;
- uncritical safety data (such as non-toxic, high flash and ignition point);
- Good availability and low cost.

Puxty et al. (2009) screened 76 different amines for theirability to absorb CO_2. They included primary, secondary and tertiary amines; alkanolamines; polyamines of a mixed or single type; cyclic and aromatic amines; amino acids; and sterically free and hindered amines. Of the 76 amines tested, seven were found to have an outstanding CO_2 absorption capacity compared to modeling predictions. Of the four primary and secondary amines showing outstanding absorption

capacity, all showed initial absorption rates similar to MEA. More testing is required to evaluate further these amines as candidate molecules for large-scale CO_2 capture. Detailed information is required on CO_2 absorption rate as afunction of temperature, amine concentration and CO_2loading; the energy requirement of, and their capacity to, capture cyclically and release CO_2; their resistance to oxidative and thermal degradation; their corrosiveness; their resistance to degradation by flue gas impurities (SOx, NOx and trace elements); and their toxicity and the toxicity of degradation products.

Puxty et al. (2009) concluded from their work that there is still significant scope for improvement in the use of aqueous amine solutions for CO_2 capture by chemical absorption. However, it is also clear that there is a lack of understanding about the chemistry involved. Understanding how the amines that show outstanding CO_2 absorption capacities do so is fundamental to achieving an optimalformulation that maximizes efficiency and minimizes cost and sustainability for post-combustion capture on an industrial scale. Existing understanding of the reaction pathways is unable to account for these characteristics.

A study to improve post-combustion capture technology has been reported by Moser et al. (2009). Two factors characterizing the performance of the process were defined as necessary conditions for a future application of post-combustion technology. At present neither criteria are fulfilled by the post-combustion capture technology, particularly because of the large, unpressurised flue gas stream of a coal-fired power station that has to be treated and due to its special composition that differs from CO_2-rich gas streams. However, the feasibility study showed that both general goals could be achieved by an optimized post-combustion capture process based on a new scrubbing solvent.

2.2.2Environmental Impact of Carbon Monoxide

Carbon monoxide is different from most pollutants. It can persist in the atmosphere for about a month and can be transported along distances. Although carbon monoxide is only a weak greenhouse gas, its influence on climate goes beyond its own direct effects. Its presence affects concentrations of other greenhouse gases including methane, tropospheric ozone and carbon dioxide(Drew Shindell, 2007).

Carbon monoxide readily reacts with the hydroxyl radical (OH) forming a much stronger, greenhouse gas – carbon dioxide. This in turn, increases concentrations of methane, another

strong greenhouse gas; because the most common way methane is removed from the atmosphere is when it reacts with OH. So the formation of Carbon dioxide leaves fewer OH for methane to react with, thus increasing methane's concentration. A NASA report indicates that carbon monoxide is responsible for 13% reduction in hydroxyl concentrations and through other reactions, a 9% drop in sulfate concentrations (Drew Shindell, 2007).

Aboudheir et al. (2003) explained that these discrepancies are due to (among other factors) the assumptions of a pseudo first order reaction with respect to both mechanisms are needed to accurately describe the kinetics.

Three mechanisms were described by Vaidya and Kenig (2007).

- Zwitterions Mechanism
- Termolecular Mechanism
- Base catalyzed hydration mechanism

Davidson (2007) discussed three main degradation routes

a. Carbonate polymerization
b. Oxidant degradation
c. Chemical degradation

Carbonate polymerization is insignificant at temperature below 100^0C. Thermal degradation takes place at temperature above 205^0C, most degradation comes from the presence of oxygen in the flue gas. (Davidson, 2007) explains that for carboxylic (formate, glycolate, oxalate and acetate) are major amine degradation products while nitrates and ethylenediamine were also found in significant quantities.

Sexton and Rochelle (2009) described catalysts and inhibitors for MEA oxidation. They carried out studies at 55^0C and found that dissolved metals catalyze the oxidation process in the order of Copper > Chromium > Nickel > Iron >Vanadium.

They also identified effective degradation, inhibitors such as ethylenediamine ataractic acid (EDTA) and explained that some expected inhibitors such as formaldehyde formate and sodium sulphite actually increases MEA losses.

2.2.3Level of complexity in modelling

In modelling absorber and stripper, the two approaches are commonly used, the equilibrium based approach and the rate based approach. The former approach assumes a theoretical stage in which liquid and gas phase attain equilibrium and the performance of each stage is adjusted using tray efficiency correction factor (Schneilder et al., 1999). This is usually sufficient to model non-reactive system. In amine absorption, chemical reactions are involved and such equilibrium is rarely attained. As such the rate based approach is more appropriate. In the rate based approach actual rates of multi components mass and heat transfer as well as chemical reactions are considered directly (Noves, 2003). To model such a reactive absorption process, simple or complex representation can be used for mass transfer and reaction aspects differences between various forms of models are indicated. The two film theory assumes that the liquid and vapor phase both consist of film and bulk regions. Heat and mass transfer resistance are assumed to be restricted to these laminar film regions (Danckwerts, 1970).

The penetration theory originally proposed by Highie assumes that every element on the surface of the liquid is exposed to the vapor phase for the same length of time before it is replaced by liquid of the bulk composition. The exposure time encompasses the effects of the hydrodynamic properties of the system and is used to define their effect on the mass transfer coefficient (Danckwerts, 1970).

The performance of the absorber and the stripper, the two major components in the conventional CO_2 capture process has been studied by a number of researchers through modally and simulation. In Lawal et al (2009) a dynamic rigorous model was developed for the absorber. This assumed rate based mass transfer with reactions at equilibrium process analysis based on this model found that the absorber performance can be maintained during part load operation by Maintaining the ratio of the flow rate of the lean solvent and flue gas to the absorber in Kvamsdal et al. (2009), the absorber was modeled dynamically assuming rate based mass transfer and counting the impact of reaction with an enhancement factor, the dynamic model of absorber was then used to investigate two transient operation scenarios start up and load reduction. The authors also pointed out that a dynamic mode for the whole CO_2 capture process (i.e with the stripper and heat exchange units) is required to evaluate different operational challenges.

Lawal et al. (2009)developed a dynamic model for the stripper. This assumed rate based mass transfer and reaction at equilibrium, it was used to analyze the impact of the reboiler duty on the CO_2 loadings in the solvent at the bottom of the stripper modelled dynamically using rate based mass transfer and assuming reaction at equilibrium. This model was subsequently used to minimize the energy consumption of the stripper. The limitations of the publication so far (Lawal et al., 2009), (Kvamsdal et al., 2009) and (Ziali et al., 2009) is that process dynamic analysis was carried out with individual dynamic models for absorber or stripper independently without considering their possible interaction when operation together as a plant.

Uyanga and Idem (2007) demonstrated that an increase in SO_2 concentration would result in an increase in MEA degradation. The study also suggests that an increase in CO_2 loading in the liquid phase produced an inhibition effect to MEA degradation because this would reduce the amount of SO_2 and O_2 that could react with the MEA solution to induce degradation. It may therefore be of advantage to operate the absorption process with higher lean CO_2loading. However, in doing so consideration has to be made regarding the corrosive effect of more CO_2in the system (Davidson, 2007).

Davidson (2007) explained that the factors that influence corrosion rates in amines plants include CO_2loading, amine type and concentration, temperature, solution velocity and degradation products MEA is quite corrosive compared to the secondary or tertiary amines used for gas treating (Kittel et al, 2009). Corrosion is found to reduce in the following order MEA > Amp > DEA > MDEA (Davidson, 2007). Other solvents used for CO_2chemical absorption include methyldiethanol-amine (MDEA) MEA can react more quickly with CO_2than MDEA can, but MDEA has a higher of CO_2 absorption capacity and require lower energy to regenerate CO_2(Davidson, 2007).

Aroonwilas and Veawab (2007a) studied the performance of different amines such as MEA and MDEA is mixed at the appropriate ratio and used as solvent for CO_2 capture the energy consumption for regenerating $CO_2$is reduced significantly compared with MEA only, the whole power plant with CO_2capture can improve thermal efficiency around 3%. However, this study was carried out at steady state and when power plant is operated at full load; other solvents include the sterically hindered amines developed by the Kansai Electric Power Co. (Davidson, 2009). These solvents are claimed to offer lower energy consumption and solvent loss. These solvents however have higher cost (Reddy et al, 2008).

Process intensification can be used for the absorption of CO_2, this can be achieved with a novel technology called Higee (High gravity). This was first proposed when a rotating packed bed (RPB) was invented, to enhance distillation and absorption efficiencies. It takes advantage of centrifugal fields through RPB to generate high gravity and therefore boosts the mass transfer coefficients, resulting order of magnitude reduction in equilibrium size.

2.4Past Efforts and Research Directions of Carbon Capture Technologies

2.4.1Chemical Solvent

The most commonly used technology today for low concentration CO_2 capture is absorption with chemical solvents. This chemical absorption process is adapted from the gas processing industry where amine – based processes have been used commercially for the removal of acid gas impurities from process gas streams (Wang et al., 2011).

However, problems of scale, efficiency and stability become barriers when chemical solvents are used for high – volume gas flows with a relatively smaller fraction of valuable product. The processes require large amounts of material undergoing significant changes in conditions, leading to high investment costs and energy consumption. In addition, degradation and oxidation of the solvents over time produces products that are corrosive and may require hazardous material handling (Wang et al., 2011).

Research on improved chemical solvents that seeks a high absorption capacity for CO_2 without a corresponding large energy requirement for regeneration is necessitated. Other desirable proportion includes high chemical stability, low vapour pressure and low corrosiveness. It has been shown that solvents based on piperazine promoted K_2CO_3 can have reaction rates approaching that of monothenol amine – MEA, but currently have lower capacity. These modified amines attempt to balance good absorption and regeneration characteristics under some conditions due to the reduced chemical stability of the amine – CO_2 formed. Controlled species selectivity is also possible with these compounds.

Davidson (2007) established that chemical absorption of CO_2 is preferred for post combustion capture from fuel power plants because it is able to capture CO_2 in low partial pressures. MEA solvent is relatively cheap and chemical absorption process with MEA is backed up by commercially available and proven technology (Davidson and Santos, 2007).

Davidson (2007) highlighted some problems encountered using MEA such as:

(a) Degradation of solvents in the oxidizing environment of flue gas.

(b) Energy consumption for regeneration of solvents

(c) Corrosion

Alternative solvents to MEA should therefore have higher capacity for CO_2 capture and lower energy consumption. Other solvents used for CO_2 chemical absorption include methyldiethanolamine (MDEA). MEA can react more quickly with CO_2 than MDEA can, but MDEA has higher CO_2 absorption capacity and requires lower energy to regenerate CO_2 (Davidson, 2007; Aroonwilas and Veawab, 2009; Wang et al., 2011).

2.4.2Ideal Solvent Properties

In creating a CO_2 capture system that will be cost effective enough to be feasible economically, improvements to the current processes must occur. The most important of these advances will be the development of more effective solvents. Important solvent properties include fast CO_2 absorption rate, high CO_2 capacity, low regeneration energy requirements, low degradation rates, low solvent costs and low corrosivity. Solvents with a fast reaction rate will result in a smaller absorber, less packing and reduced pressure drop. The absorber could be operated closer to equilibrium, which would result in a CO_2 richer solution and thus a more efficient stripper and lower regeneration costs. Higher capacity solvents result in a lower circulation rate and a lower energy requirement for regeneration. A low corrosivity solvent can be used with equipment made of carbon steel, instead of stainless steel, which will reduce capital costs. There will be a tradeoff between solvent cost and benefits derived from its use, making the utilization of an inexpensive bulk material important (Cullinane and Rochelle, 2002).

Another class of solvents for CO_2 capture application is amino acid salts. They are being investigated because of their fast reaction kinetics, high achievable cyclic loadings, good stability towards oxygen and favorable CO_2 binding energy. One advantage of using these salts is for high CO_2 loading, precipitation will occur.

a. Chemistry of the MEA and Saw Dust Ash (SDA) Systems

In the MEA system, CO_2 is solubilized in the liquid phase either in a carbonate or bicarbonate form. The following reversible reactions occur in the MEA system:

$$2H_2O \leftrightarrow H_3O^+ + OH^- \quad (2\text{-}9)$$

$$CO_2 + 2H_2O \leftrightarrow HCO_3^- + H_3O^+ \quad (2\text{-}10)$$

$$MEA + HCO_3^- \leftrightarrow MEACOOH^- + H_2O \quad (2\text{-}11)$$

$$MEA + H_3O^+ \leftrightarrow MEA^+ + H_2O \quad (2\text{-}12)$$

$$HCO_3^- + H_2O \leftrightarrow CO_3^{2-} + H_3O^+ \quad (2\text{-}13)$$

A similar set of reactions can be proposed for the Saw Dust Ash (SDA) system:

$$2H_2O \leftrightarrow H_3O^+ + OH^- \quad (2\text{-}14)$$

$$CO_2 + 2H_2O \leftrightarrow HCO_3^- + H_3O^+ \quad (2\text{-}15)$$

$$Ca^{2+} + HCO_3^- \leftrightarrow CaCO_3 + H^+ \quad (2\text{-}16)$$

$$Ca^{2+} + H_3O^+ \leftrightarrow CaO + 3H^+ \quad (2\text{-}17)$$

$$HCO_3^- + 3H^+ \leftrightarrow CO_3^{2-} + 2H_2 \quad (2\text{-}18)$$

The equilibrium constants for the reaction are temperature dependent and follow the dependence given in (2-19).

$$In\ K_x = A + \frac{B}{T} + C\ In\ T + DT \quad (2\text{-}19)$$

b. Carbamate formation in the MEA system

Carbamate formation is an important reaction in CO_2 absorption. There is much discussion in the literature on the mechanism of formation of the carbamate. Two mechanisms have been proposed for the formation of the carbamate – the zwitterions mechanism and the termolecular mechanism.

c. Zwitterion Mechanism

This mechanism was proposed by Caplow (1968),and is shown in figure 2.4.

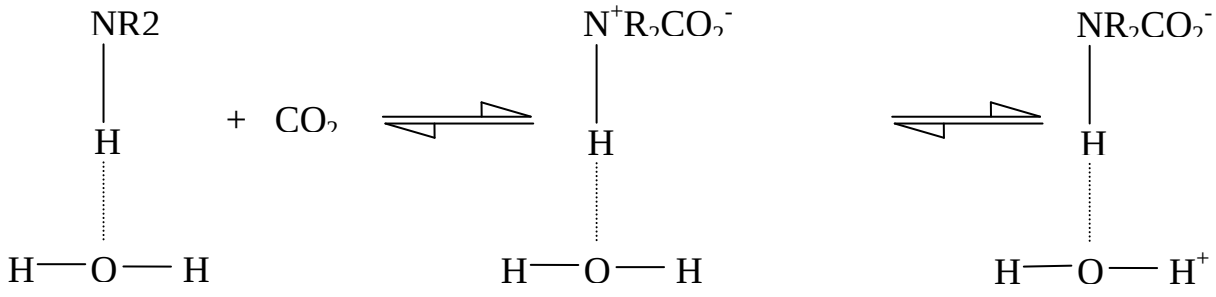

Figure 2.4: Zwitterion mechanism for carbamate formation

Caplow assumed that the amine molecule forms a hydrogen bond with the water molecule before reacting with CO_2. The first step was the formation of an unstable inter mediate by the bonding of the CO_2 molecule to the amine. In the second step, the amine proton is transferred to a basic molecule to form the carbamate. The base can be a water molecule or an amine.

The kinetic expressions for this have been elucidated by Kumar et al. (2003).

QSSA on zwitterions gives:

$$r_{CO_2} = \frac{k_2[CO_2][Am]}{1+\frac{k_{-1}}{\sum k_b[B]}} = \frac{[CO_2][Am]}{\frac{1}{k_2}+\frac{k_{-1}}{k_2}\frac{1}{\sum k_b[B]}} \qquad (2\text{-}20)$$

The summation term is the contribution of all the bases present in the solution for the removal of protons. In lean aqueous solutions, the amine, water, OH^- can act as bases causing the deprotonation of the zwitterions to form the carbamate specie.

1. For how amine concentrations, $k_b - k_{H2O}$

$$r_{CO_2} = k_2[CO_2][Am]\left(\frac{k_{H_2O}[H_2O]}{k_{-1}}\right) \qquad (2\text{-}21)$$

2. At moderately high amine concentrations, the contribution of the amine and the water to the zwitterion's deprotonations are equal important and hence the contribution of all must be considered.
3. At very high amine concentrations, the contribution of water to the deprotonation is insignificant and also $k_{-1}/(k_{Am}[am]$ is low. Hence,

$$r_{CO_2} = k_2[CO_2][Am] \quad (2\text{-}22)$$

d. Termolecular mechanism

A termolecular single-step mechanism for carbamate formation was proposed in 1989 and is shown in Figure 2.5.

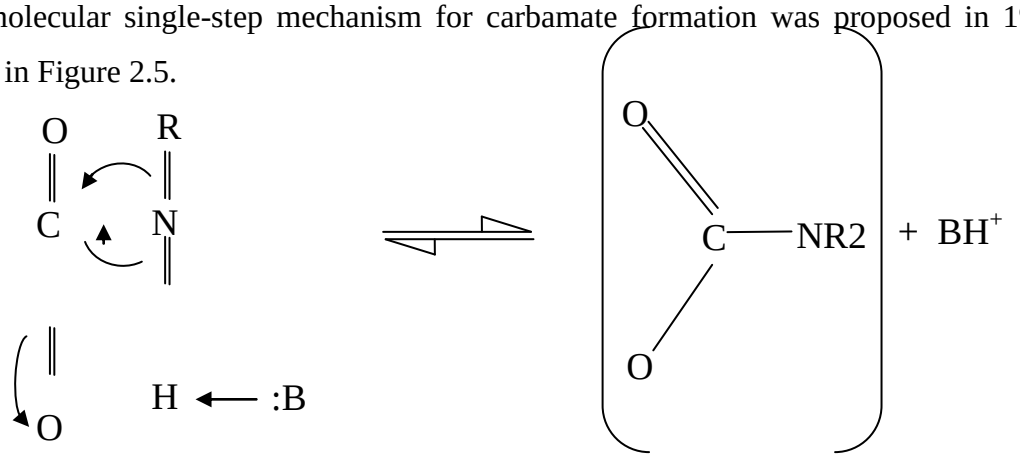

Figure 2.5: Termolecular mechanism for carbamate formation

In this mechanism, the bond formation with CO_2 and the proton transfer take place simultaneously. This mechanism is no very different from that proposed by Caplow in 1968. In this the formation of hydrogen bond with the base is ignored. If the lifetime of the zwitterions is very small, then Caplow's mechanism approaches the termolecular mechanism.

$$CO_2 + RRNH \rightleftharpoons RRN^+COO^- \qquad (2\text{-}23)$$

$$RRN^+HCOO^+ B \rightleftharpoons RRNCOO^- + BH^+ \qquad (2\text{-}24)$$

The experimental data can be represented by either mechanism. However, ab initio computations show that the single step termolecular reaction is more likely. In addition, for some systems reported in literature, the zwitterions mechanism gives implausible values of parameters. Other mechanisms have also been proposed to explain the carbamate formation and so as of yet, there is no consensus on which the correct mechanism is.

In the MEA system, CO_2 is solubilized in the liquid phase either in a carbamate, carbonate or bicarbonate forms.

2.4.3Process description of CO_2 capture using MEA

The process for CO_2 capture using MEA can be broken into three (3) different sections:

1. Flue gas cooling and compression
2. Absorption of CO_2 and regeneration of solvent
3. CO_2 compression

1. Flue gas cooling and compression:

The absorber in the MEA system operates at a temperature of approximately 40°C and hence, the inlet temperature of the gases to the absorber system needs to be around 40-50°C. In the case of natural gas combined cycle plants, the temperature of the flue gas at the exhaust of the power plant is around 110-120°C and these gases need to be cooled before being fed to the absorption system. Cooling is required for flue gases derived from coal-fired power plants as well unless the flue gases have been through a wet flue gas desulfurization scrubber, in which case they may already have been cooled to the requisite temperature.

The flue gas is typically cooled by passing it through a direct contact cooling tower (DCC). The DCC is a packed tower in which there is counter-current flow of cooling water and the flue gases. The flue gases enter at the bottom of the tower with the cooling water entering at the top. In the tower, the flue gas is cooled by evaporation of water and hence, the water content of the flue gas is reduced at the exit of the tower. The cooling water is collected at the bottom of the

DCC and is sent to a cooling water in order to have its temperature reduced before being used in the DCC again. The flue gas exits at the top of the DCC and is sent to a blower where it is slightly compressed. Since the flue gas stream has to flow upward through a packed absorber, it is necessary to increase the pressure of the flue gas before sending it to the absorber. This is also accompanied by attendant temperature increase. It is necessary that prior to chemical absorption with MEA, the flue gas be scrubbed to remove NOx, SOx and similar impurities. The presence of NOx and SOx in the flue gas is undesirable since they react irreversibly with the amine solvent to form heat stable salts that cannot be reclaimed. In NOx, it is NO_2 which is responsible for the irreversible reaction. A NO_2 level of less than 20 ppmv is recommended. Most modern plants produce a flue gas with a NO_2 content lower than this and hence, this does not pose too much of a problem. For SOx, there is a trade -off between the cost of the flue gas desulfurization and the cost of the makeup solvent required to compensate the degradation of the solvent due to SOx.

Reclaiming of solvent

Particularly in the case of flue gas from coal fired power plants, it will be necessary to use a MEA reclaimer to treat some of the heat stable salts that from due to the NOx and SOx. The continued buildup of these salts in the amine stream is undesirable since it lowers the capacity of the solvent for CO_2 absorption. A purge stream of the solvent is removed and taken to a reclaimer where in the presence of a strong alkali like NaOH and with the application of heat, some of the heat stable salts can be dissociated, resulting in the recovery of some of the solvent. The sludge that is produced in the reclaimer is sent for disposal in a landfill.

3. CO_2 compression:

The CO_2 gas that is released from the desorber needs to be dried and compressed before being sent for storage. Drying is an important step since the presence of moisture in the stream can cause corrosion in the pipelines used for CO_2 transport. Typically, a 4-stagereciprocating compressor is used with cooling between the stages. The compressor is used to compress the CO_2 to 90 atm, beyond which the supercritical liquid CO_2 can be pumped to the discharge pressure of 130 atm.

2.4.4Advantages and drawbacks of post-combustion capture with amine solvents

The main advantage of CO_2 post-combustion capture is its availability for retrofitting existing power plants (Figueroa et al., 2008). Among the different post-combustion techniques and at the current state of technology, reactive absorption in amine solvents is often considered as the most efficient method for CO_2 capture, or at least the most feasible route to large-scale implementation (Rubin et al., 2012; Svendsen et al., 2011). The main reason for that is the large experience gained in various applications like natural gas sweetening or commercial CO_2 capture from flue gas. Moreover, the development of CO_2 capture with amine solvents was based on MEA, an amine that rapidly reacts with CO_2 and that possesses a high CO_2 capacity on a mass basis (Brúder and Svendsen, 2012). However, two main drawbacks still affect the CO_2 chemical absorption in amine solvents, and especially in MEA: the high cost of the process and its environmental safety (Svendsen et al., 2011).

Besides cost issues, the environmental safety of post-combustion capture with amine solvents also represents a critical issue. Creating a new environmental problem when solving an initial one must be strictly avoided (Svendsen et al., 2011). Two types of environmentally harmful chemicals may be emitted by the CO_2 capture process: the amine solvent and its degradation products.

The vapour pressure of the amine solvent above its aqueous solution can be significant, so that some amine may exit the process with the cleaned flue gas. In the case of MEA, solvent emissions can be kept very low by an optimal operation of the washing section (Mertens et al., 2012; Moser et al., 2011). In comparison, significant emissions of AMP solvent were recorded during a pilot plant test with AMP/PZ (Mertens et al., 2012). This is in accordance with the higher volatility of AMP compared to MEA and PZ (Nguyen et al., 2010). Thus, volatility is a further essential parameter when selecting a new solvent. Based on unpublished data, Svendsen et al. (2011) claim that optimal washing sections could bring amine emissions down to 0.01-0.05 ppm in the cleaned flue gas.

Amine degradation products may also be emitted by the capture process. Indeed, during the absorption, the amine solvent is in contact with oxygen from the flue gas, inducing oxidative degradation of the amine. The solvent is also heated in presence of CO_2 during the regeneration, inducing thermal degradation with CO_2. If SOx and NOx impurities have not been correctly removed from the flue gas before the absorber, they may also cause amine solvent degradation. The amine solvent can degrade into gaseous as well as liquid degradation products that are

classified as environmentally harmful emissions. Some recent studies at lab and pilot scale have evidenced that the operating conditions of the capture process have a direct impact on the formation and emission of degradation products (Mertens et al., 2012; Voice and Rochelle, 2013). However, there still remains a knowledge gap about the environmental impact of post-combustion CO_2 capture with amines (Shao, 2009).

2.5Influence of Dissolved Metals

Several works have reported that the presence of dissolved metals like iron (Fe), copper (Cu), chromium (Cr), nickel (Ni), manganese (Mn) and vanadium (V) catalyzes solvent degradation. Fe, Cr, Ni and Mn may leach from columns and pipes walls, and Cu and V are sometimes deliberately added to amine solutions as corrosion inhibitors (Cheng & Meisen, 1996).

No published results could be found about the influence of metals on thermal decomposition or on MEA reactions with flue gas contaminants. In the case of MEA thermal degradation with CO_2, different studies have evidenced that the presence of metal has no influence on the degradation.

On the contrary, dissolved metals play a major role in oxidative degradation. Indeed, the presence of metals catalyzes the formation of free radicals, and thus the initiation of chain reactions. Bedell (2009) proposes three main pathways:

Dissolved metals show varying potentials as catalysts for the oxidative degradation of MEA. Moreover, combinations of metals may increase the respective catalytic effects of the different metals, like in the presence of both iron and copper. Metals can be classified in decreasing order of oxidative potential as following:

Mn7+ > Fe2+/Cu2+ ≥ Cu2+> Cr3+/Ni2+ > Fe2+ > Cr3+ > V5+ > Ti, Co, Mo, Ni, Sn, Se, Ce, Zn

Ag2+ also shows an oxidative potential, but it has not been compared to other metals. On the contrary, it has been reported that Mn2+ has an inhibiting effect on degradation. This highlights the need for further studies to better understand metal catalyzed degradation pathways. Moreover, degradation products are observed in different proportions according to the metal catalyst used.

Finally, there is still a knowledge gap in the interactions between corrosion and degradation, inducing an important challenge for post-combustion CO_2 capture. Indeed, there is a vicious circle between both phenomena. Degradation causes the apparition of corrosive products that corrode the pipe walls, thus releasing more metal ions into the solution. Considering that

oxidative degradation is catalysed by those metal ions, degradation is then worsened by the corrosion and vice-versa.

2.6Possible Answers to Amine Degradation

Various solutions have been proposed to limit the influence of degradation on the operation of a CO_2 capture plant. Usual solutions in commercial plants are referred to as reclaiming processes. They aim at purifying the amine solvent that contains degradation products. However, it is also possible to act preventively in order to avoid solvent degradation, which is the objective of degradation inhibitors.

2.6.1 Reclaiming methods

The most commonly used reclaiming methods are described below based on the work of Cummings et al. (2007).

Solvent purge and make-up: as mentioned by Cummings et al. (2007), "this method might not be opposed by your amine supplier". It is a simple and widely used solution in commercial CO_2 capture processes but it implies a large consumption of fresh amine. Moreover, the purged solvent must be properly disposed of, inducing additional waste treatment costs and a low environmental efficiency.

Thermal distillation: the amine solvent is vaporized in a distillation column, and the non-volatile degradation products are recovered in the sump of the column. This is an interesting technique if the concentration of degradation products is high. There is less waste generated in comparison to the first method but the energy requirement of distillation is an important drawback in this method, especially for less degraded solutions. Thermal reclaiming may also induce additional thermal degradation with CO_2 since the temperature in the bottom of the reclaimer may reach 150°C. Thermal distillation may be performed under vacuum for low volatile amine. It is not the case for MEA.

Neutralization: a strong base, usually NaOH is added to the solution. The undesired acid contaminant that has formed a salt with MEA associates with the strong base and releases the amine. This method limits the effect of degradation products, but does not remove them, so that solvent properties may remain affected. An interesting alternative to NaOH has been proposed by Xu and Rochelle (2009). KOH is used as the strong base, leading to the precipitation of

K_2SO4 crystals easily removable from the solvent. However, this method mainly addresses heat stable salts so that non-ionic degradation products are unaffected.
Ion exchange: the same principle as for neutralization is used. The undesired acid contaminant that has formed a salt with MEA is exchanged with a friendly anion brought into the system by a resin. This is an interesting method from the economic point of view, but it only addresses ionic degradation products.

Electrodialysis: Ionic degradation products migrate through ion-selective membranes placed in an electric field. The energy requirement of this technique is advantageous but it produces more waste than ion exchange.
Independently of their efficiency, these methods are only used with already degraded amine solvents, so that they do not prevent degradation. As a consequence, many negative effects induced by degradation are not addressed by such techniques.

2.6.2 Degradation inhibitors

The use of degradation inhibitors may be an interesting alternative to reclaiming techniques. Indeed, some chemicals show the ability of inhibiting amine degradation, especially oxidative degradation. This attractive approach prevents the formation of degradation products, so that the fresh amine consumption is reduced, as well as the waste volume. However, degradation inhibitors may modify the solvent properties, and more research is needed to assess this effect. Indeed, the biodegradability of amine solvents should be preserved in order to limit the environmental penalty of solvent emissions (either due to solvent volatility or to accidental release) so that a trade-off is necessary between solvent stability and environmental safety.
The role of a degradation inhibitor is to prevent or minimize the solvent degradation during the CO_2 capture process. However, no degradation inhibitor has been proposed so far to prevent MEA thermal decomposition, thermal degradation with CO_2 or NOx degradation, and only few studies have considered SO_2 degradation. The reasons are the following: Experimental study of amine solvent degradation. Thermal decomposition of MEA occurs at temperatures higher than 200°C (Epp and Bathen, 2011), so that there is no need to consider it in usual CO_2 capture processes.

Degradation due to CO_2 results from the CO_2 absorption in MEA, a mechanism that is desired, so that inhibiting this mechanism does not make much sense. Degradation with NOx and SOx

has rarely been studied because of the low SO_2 and NOx content achievable in power plant flue gas.

As a consequence, most studies about degradation inhibitors address oxidative degradation. Oxidative degradation inhibitors may be separated into three main categories based on the oxidative degradation mechanisms (Bedell, 2009).

Chelating agents: they form a complex with dissolved metals, inhibiting their catalytic activity and limiting the initiation/propagation steps of the chain reaction.

Radical and O_2 scavengers: dissolved O_2 forms peroxides in water. Radical scavengers react with the peroxides to form stable products and stop the chain reaction. They are also called O_2 scavengers since they stoichiometrically react with dissolved O_2. Disadvantage of many radical scavengers is that they are consumed during the reaction and must be renewed.

Stable salts like KCl, KBr or KCOOH increase the ionic strength of water, so that the solubility of gases in the solvent decreases (Goff and Rochelle, 2003). However, these salts appeared to be poor inhibitors, decreasing the NH_3 production by only 15% in the best case.

2.6.3Degradation of MEA Solvent

One of the concerns with using MEA as a solvent is that it is prone to degradation at high temperatures by a number of mechanisms as outlined in this section.

a. Carbamate Polymerization

Carbamate polymerization is the most common mechanism of amine degradation. It occurs in the presence of CO_2 and high temperature. The rate of degradation is a strong function of CO_2 partial pressure and temperature. Carbamate polymerization is initiated by the formation of an oxazolidone. This forms as a five-member ring by the internal reaction of an alcohol and a carbamate. The parent amine then reacts with the oxazolidone to produce a substituted ethylenediamine. The final step in the degradation is the condensation of the substituted ethylenediamine to a substituted piperazine. Sterically hindered amines and tertiary amines do not have a strong tendency to form carbamate and hence, are not subjected to his form of degradation.

Degradation by carbamate polymerization is insignificant at temperatures lower than 100^0C and hence, will be important only around the stripper and the reboiler sump. Since, the degradation reactions are favored at high CO_2loading, the degradation is more probable at the rich end of the stripper. In addition, the rate of polymerization has a high dependence on amine concentration

and hence, solvents that use a lower amine concentration will have a lower rate of degradation. Carbamate polymerization has been studied by a number of authors, however there is not much literature on the kinetics of the carbamate polymerization react.

b. Oxidative degradation

Oxidative degradation occurs due to the presence of oxygen in the flue. Neither carbon dioxide nor high temperature is required for oxidative degradation to occur. The products of oxidative degradation include various aldehydes, organic acids such as acetate, formate, glycolate, acetate and oxalate amines, NH_3 and nitrosoamines. These products can have significant environmental impacts if released into the environment. Nitrosoamines are known to be carcinogens. Oxidative degradation also results in the formation of heat stable salts and loss of the solvent. The degraded solvent has to be replaces with make-up and this can be a significant cost in the process. In addition, the degradation reactions can significantly enhance the corrosion of the column and its internals. In industrial applications, Fe and Cu are likely to be catalysts that promote the degradation of the amine.

Oxidative degradation will most likely occur at short times and low temperature with contact in the absorber and at longer times and high temperature in the stripper. A number of authors have studied the oxidative degradation of MEA. A study at the University of Texas has identified that the oxidative degradation of MEA under industrial conditions is controlled by O_2 mass transfer and that the degradation rate is likely to be 0.29 - 0.73kg MEA/m ton of CO_2. In general, inhibitors are added to the system to prevent the oxidative degradation of MEA.

2.7Chilled Ammonia System

The use of ammonia as a solvent for absorption of CO_2has seen increasing interest over the past few years. Two variation of this process have been discussed in this literature. The first is the Aqua ammonia process in which an aqueous ammonia solution is used to capture $CO_2$with the absorption occurring at room temperature. In this process, the absorption of CO_2 in the ammonia solution is carried out under refrigerated conditions in the temperature range of 0 to 10^0C. The process engineering for the chilled ammonia process has been carried out by Alston power. The focus of this chapter is on an analysis of the energy consumption in the chilled ammonia process.

2.7.1 Chemistry of the chilled ammonia system

The chemistry of the system is based on the reaction of CO_2 with an ammonium carbonate solution. The chilled ammonia process also involves the precipitation of ammonium bicarbonate due to the low temperature in the absorber. The reactions involved are detailed under:

$$NH_3(g) \leftrightarrow NH_3(aq) \quad (2\text{-}25)$$

$$CO_2(g) \leftrightarrow CO_2(aq) \quad (2\text{-}26)$$

$$2H_2O(aq) \leftrightarrow H_3O^+(aq) + OH^-(aq) \quad (2\text{-}27)$$

$$CO_2(aq) + 2H_2O(aq) \leftrightarrow H_3O^+(aq) + HCO_3^-(aq) \quad (2\text{-}28)$$

$$HCO_3^-(aq) + H_2O(aq) \leftrightarrow H_3O^+(aq) + CO_3^{2-}(aq) \quad (2\text{-}29)$$

$$NH_3(aq) + H_2O(aq) \leftrightarrow NH_4^+(aq) + OH(aq) \quad (2\text{-}30)$$

$$NH_3(aq) + HCO_3^-(aq) \leftrightarrow NH_2COO^-(aq) + H_2O(aq) \quad (2\text{-}31)$$

$$NH_4^+(aq) + HCO_3^-(aq) \leftrightarrow NH_4HCO_3(s) \quad (2\text{-}32)$$

CO_2 is solubilized in the solution in the carbonate, bicarbonate and carbonate forms. It is important to consider the carbonate formation since this is a significant reaction. Many studies of the ammonia system ignore the formation of the carbonate species and this result in a much lower estimated heat of reaction.

2.8Discussion on Mass Transfer Considerations

In the modelling of the chilled ammonia system, the absorber was modeled as made up of a number of equilibrium stages – both from the kinetics viewpoint as well as the mass transfer view. However, it is important to consider the mass transfer implications in the chilled ammonia system, particularly given the precipitation that occurs in the system. In this section, a preliminary discussion on the comparison of the mass transfer coefficient in the chilled ammonia system with the MEA system is presented.

2.8.1 Intrinsic mass transfer coefficient

If the reaction of CO_2 with the solvent is assumed to be a pseudo-first order reaction as an approximation, then:

$$r_{CO_2} = k_1[CO_2] \quad (2\text{-}33)$$

With

$$k_1 = k_2[C_s] \quad (2\text{-}34)$$

Where:

K_1 is the pseudo-first order rate constant

K_2 is the second order rate constant

C_s is the concentration of the solvent

The differential equation representing the steady state transfer is then given by:

$$D_{CO_2} \frac{\partial^2 [CO_2]}{\partial x^2} - k_1 [CO_2] = 0 \qquad (2\text{-}35)$$

Where:

D_{CO_2} is the diffusivity of CO_2

The boundary conditions are:

$$\{co_2\} = \{co_2\}_{I\,@}\ x = 8 \qquad (2\text{-}36)$$

Where:

X=0 and x=8 are the boundaries of the liquid film

The general solution of this equation as given by Danckwerts is:

$$[CO_2] = \frac{1}{\sinh\sqrt{M}} \left[[CO_2]_b \sinh\left(x\sqrt{\frac{k_1}{D_{CO_2}}} \right) + [CO_2]_i \sinh\left(\frac{D_{CO_2}}{k_1} - x \right) \sqrt{\frac{k_1}{D_{CO_2}}} \right] \qquad (2\text{-}37)$$

Where
$$M = \frac{D_{CO_2} k_1}{k_1^2} \qquad (2\text{-}38)$$

Where

M = (hatta number)^2

KI is the mass transfer coefficient in m/s

Now applying fick's law at the gas-liguid interface, we have

$$N_{CO2=-} \frac{d[co_2]}{dx}_{x=0} \qquad (2\text{-}39)$$

Where:

Nco_2 is the flux of co_2

This gives us an expression for co_2 flux under first and pseudo first-order conditions:

$$N_{CO2} = KI\left([CO_2]i - \frac{[co_2]b}{csh\sqrt{M}} \right) \frac{\sqrt{M}}{\tanh\sqrt{M}} \qquad (2\text{-}40)$$

As the rate of the reaction increases, the hatta number increases and the reaction

Becomes completed in the film and $[co2]b$ ----->0 and the rate tanh contribution tends to 1.

Hence we obtain,

$$Nco_2 = kI\sqrt{M[co_2]i}$$
$$Nco_2 = \sqrt{kDco_2[co_2]i} \quad (2\text{-}41)$$

Equation (2-34) can be combined to give equation (2-36))

$$Nco2 = \sqrt{K2C_sDco_2[co_2]}\,i \quad (2\text{-}42)$$

The equation for the co_2 flux can also be given as in (2-37))

$$Nco_2 = k_L * (CO_2 - CO_2) \quad (2\text{-}43)$$

Since CO_2b--→0, we have

$$Nco_2 = k_L[co_2]i \quad (2\text{-}44)$$

comparing (2-43) and (2-45) we have

$$kL = \sqrt{k_2[C_S]D_{co2}} \quad (2\text{-}45)$$

Thus using the above equations it is possible to compare the mass transfer coefficients that are obtainable in different solutions.

a. Kinetic constant for MEA system

A number of researchers have investigated the kinetic of CO_2absorption in MEA. Bishnoi(2011) provides a compilation of the various results and suggests that the rate expression provided by Hikita (2009) fits the data the best. The rate expression is.

$$\log_{10} K_2 = 10.99 - \frac{2152}{T} \quad (2\text{-}46)$$

b. Kinetic constant for ammonia system

For the rate constant for the reaction of CO_2 with NH expression of Pinsent (2009) was utilized the reaction constant is given by:

$$\log_{10} K_2 = 11.13 - \frac{2530}{T} \quad (2\text{-}47)$$

c. Comparison of mass transfer coefficient in MEA with chilled ammoniasystem

Using (2-45), we have

$$\frac{^{K}L,MEA}{^{K}L,NH,} = \sqrt{\frac{K_2,MEA^{C}MEA}{K_2NHMEA^{C}NH}} \quad (2\text{-}48)$$

Thus, the mass transfer coefficient in the chilled ammonia process is times lower than in the MEA process.

2.8.2 Inhibition of mass transfer by precipitation

The second issue with the ammonia absorbers is that of precipitation. Since there is significant solid precipitation, it may not be appropriate to use a packed tower to avoid problems with the clogging of packing. A design such as a spray tower may have to be employed. However, the mass transfer obtained in spray towers is inherently poorer than in packed columns. Given the lower intrinsic mass transfer mass coefficient in the ammonia.

Process as compared to the MEA process, this will pose a significant problem. Alternative absorber designs that will allow sufficient mass transfer without being inhibited by solid precipitation will need to be investigated.

2.9Wood and Sawdust Ash

Wood ash is the inorganic and organic residue remaining after combustion of wood or unbleached wood fiber. The physical and chemical properties of wood ash vary significantly depending on many factors. Hardwoods usually produce more ash than softwoods, and the bark and leaves generally produce more ash than the inner woody parts of the tree (Hakkila, 1989). On average, the burning of wood results in 6 to 10 percent ashes. When ash is produced in industrial combustion systems, the temperature of combustion, cleanliness of the fuel wood, the collection location, and the process can also have profound effects on the nature of the ash material (Arends & Donkersloot-Shouq, 1985). Therefore, wood ash composition can vary depending on geographical location and industrial processes. This makes testing the ash extremely important.

Ash is composed of many major and minor elements which trees need for growth. Since most of these elements are extracted from the soil and atmosphere during the tree's growth, they are common in our environment and are also essential in production of crops and forages.

Calcium is the most abundant element in wood ash and gives ash properties similar to agricultural lime (Moller and Ingerslev, 2001). Ash is also a good source of potassium, phosphorus, and magnesium. In terms of commercial fertilizer, average wood ash would be about 0-1-3 (N-P-K)(Korpinen andFardim, 2006). In addition to these macro-nutrients, wood ash is a good source of many micronutrients needed in trace amounts for adequate plant growth. Wood ash contains few elements that pose environmental problems. Heavy metal concentrations are typically low.

Field and greenhouse research confirms the safety and practicality of recycling wood ash on agricultural lands. Wood ash has a liming effect of between 8 and 90 percent of the total neutralizing power of lime, and can increase plant growth up to 45 percent over traditional limestone(Richmond, 1993). The major constraints to land application of wood ash are transportation costs, low fertilizer analysis, and handling constraints. With ever-increasing disposal costs, land application of wood ash will probably be the disposal choice in the coming century as it results in savings for the industry, an opportunity for agriculture and conservation of our resources (Rikala and Jozefek, 1990).

Sawdust ash is an organic waste resulting from the mechanical milling or processing of timber (wood) into various shapes and sizes. The dust is mostly used as domestic fuel. The resulting ash is known as saw-dust ash (SDA). Dry sawdust concrete weighs only 30% as much as normal weight concrete and its insulating properties approximate those of wood.

The quality of sawdust depends on the saw type, method of sawing, type of tree used, and the storage method of logs including temperature, moisture and season (Isomaki, 1970; Rantasuo, 1976; Liiri, 1979). Thus, sawdust from different mills can be very heterogeneous raw materials. The quality of sawdust is mainly dependent on the particle size of sawdust. The particle size of sawdust is not uniform and the distribution is usually concentrated on the smallest size fractions (Isotalo et al., 1964; Surewicz, 1974; Bublitz and Yang, 1975; Taylor,1977; Joshi et al., 1982; MacLeod and Kingsland, 1990; Korpinen andFardim, 2006; Bergström et al., 2008). However, there may be some difficulties comparing the different studies due to the different fractionation processes. The fibre length is greatly affected by the particle size of the wood material. The average length of softwood fibres is about 3 mm, whereas the average fibre length of softwood sawdust is approximately 1.0–1.2mm (Isotalo et al., 1964; Uusvaara,1975; Arends and Donkersloot-Shouq, 1985; Korpinen, 2002). The shortening of the fibre length is due to the cutting that appears in sawing (Bausch and Hartler, 1960). Bark that exists in sawdust is harmful, especially when sawdust is used in the production of Kraft pulp. Bark consumes cooking chemicals, causes discolouring and impairs the quality of pulp. In addition, the cooking yield of bark is low (Uusvaara, 1975).

It has been found that pine sawdust contained 0.4% bark in summer, 1.3%in winter and the annual mean bark content was 0.7%. It has also been found that Nigeria spruce contained 0.5% bark in summer, 2.7% in winter and the annual mean bark content of Nigeria spruce sawdust was

1.3% (Uusvaara, 1975). Sawdust originates normally from older parts of the tree stem. Saw logs typically represent a diameter exceeding 150 mm, as pulpwood logs have an acceptable diameter of around 70 mm (Lukkari, 1998). Subsequently, sawdust may contain a larger proportion of heartwood. Juvenile wood including heartwood compared to mature wood has shorter and narrower cells, thinner cell walls, higher early wood/latewood ratio, lower cellulose content, higher hemicellulose content, higher lignin content and higher extractives content (Mimms et al., 1995; Parham, 1983; Zobel and Sprague, 1998).

2.10 Models and Modelling

According to Fredrick, model is a miniature representation of something, a pattern of something to be made, an example for imitation, emulation, a description or analogy used to help visualize something that may or may not be directly observed, a system of postulates, data and inferences presented as a mathematical description of an entirety or state of affairs. While modelling is the concise description of the total variation in one quantity by partitioning it into a deterministic component given by a mathematical function of one or more other quantities plus a random component that follows a particular probability distribution. It is therefore the mathematical representation of physical systems.

a) Types of Models

Numerous models exist depending on their application. They include sequence and series models, limit and continuity (i.e. finite and infinite), static and dynamic models, growth and decay models, cycles and oscillation models, deterministic and probabilistic stochastic models, and linear and nonlinear models.

b) Uses of Models

Models are used basically for estimation, prediction, calibration and optimization. Estimation is to determine the value of the regression function that is associated with a specific combination of prediction variable values which are the parameters. Prediction determines future values of the response variables. It yields the variables (dependent and independent) using the parameter values. Calibration allows for the quantitative conversion of measurements made on one of the scale while optimization addresses the substitution of an output value for the response variable and solving for the associated predictor variable values.

c) Steps in Modelling

The basic steps for every model building are data collection, model development, model fitting and model validation. Models are developed following some basic steps which provide universal framework. Although details may vary from method to method, an understanding of the common steps combined with underlying assumptions needed for the analysis is essential. In the model development stage, plots of the data process knowledge and assumptions about the process are used to determine the form of the model to be fitted to data. Using the develop model, an appropriate model fitting method is used to estimate the unknown parameters in the model. The model is now assessed to see if the assumptions are valid, the model can now be used to answer scientific or engineering questions that prompted the model effort.

d)Properties of Models

Model development is based on fundamental physical and chemical laws. They are often characterized by assumptions which are indispensable, provided they are made with sound judgment since a model containing all parameters will be very complex. Furthermore, mathematical consistency must be followed (with zero degree of freedom) for models to be solvable and their verification is essential in order to ensure the workability.

e) Assumptions of Models

These are implicit assumptions in form of statements, based on properties inherent to the process modeling methods. A particular model has its own specific assumptions but in general, typical assumptions for process modeling are:

The process is physical, chemical or statistical in nature

The means of the random error are zero

The random errors have a constant standard deviation and follow a normal distribution

The data are randomly sampled from the process

The exemplary variables are observed without error.

f) Prediction using Models

Models serve as prediction tools in engineering application. In order to determine future values of the dependent variables, fitted models with estimated parameters are used to compute uncertainties by plugging the values of the prediction or independent variables. This gives the idea of the future of the process in question with the assumption in place.

g) Optimization using Models

It involves the substitution of an output value for the response variable and solving for the associated predictor variable values. The model becomes a link between input and output. Models for optimization require a cause and effect relationship between the predictor and the response variable. Quadratic models are usually used for the calculus determination of maximum and minimum for the applicable optimization decision.

h) Verification of Models

Verifying if a model fits a data is an exercise for effective modeling. Model validation is probably the most important step in the model building sequence. Often, the validation of a model is seen to consist of nothing more than quoting the statistics from the fit which measures the fraction of total variability in the response that is accounted for by the mode. However, a high value does not guarantee that the model fit the data well and the use of such model will rather not generate answers to the underlying engineering questions.

i) Statistical Modelling

A statistical model is a class of mathematical model, which embodied a set of assumptions concerning the generation of some sample data, and similar data from a larger population. A statistical model represents often in considerably idealized form the data-generating process.

The assumption embodied by a statistical model describe a set of probability distribution, some of which are assumed to adequately approximate the distribution from which a particular data set is sampled. The probability distributions inherent in statistical models are what distinguishes statistical models from other non-statistical, mathematical models.

A statistical model is usually specified by mathematical equations that relate one or more random variables and possibly other non-random variables. As such, a statistical is "a formal representation of a theory" (Adȅr, 2008).

2.11Theory for Prototype Equipment Design and Specifications

All process plants consist of various units which are compound in such manner that the desired throughput is achieved in an efficient, safe and economic way.

Equipment used the chemical process industries can be classified as:

(a) Proprietary and

(b) Non-propriety

The proprietary equipment are such as pumps, compressors, etc, which are usually designed and manufactured by specialist firms. While the Non-proprietary equipment are designed and manufactured by special, one-off, items for particular process; such as the prototype device designed in this research, for the CO_2 absorption from flue gas of small generator set. The chemical engineer is not normally involved in the detailed design of propriety equipment. Our concern will be to select and/or specify the equipment needed for a particular duty (Sinnott, 2005).

However, the selection of any equipment required in process plant depends on certain parameters like the temperature of the process, power requirement, pressure to be withstood and the desired throughput.

Design data have been developed, giving sizes, operating conditions number and location of opening, types of flaps and heads, codes variation allowances and other information which may be necessary. Many of the machine design details was handled by the fabricator, even though that we as chemical/process engineers supplied the very basic design information.

In this chapter, we have restricted our write-up to the design and/or specification of our plant non-propriety equipment. The design calculations are reserved in the Appendix C, tabulated in well-mannered design and specification sheets for each of the process equipment.

2.11.1 General Design Considerations

a. Design Temperature

The design temperature at which the design stress is evaluated is taken as the maximum working temperature of the material of construction with due allowance for any uncertainty in predicting vessels wall temperature.

b. Design Pressure

The design pressure could be regarded as the pressure which is use in the design of a pressure containing system or any piece of equipment. Usually, the design pressure is chosen a little higher than the operating pressure, as a general rule of thumb is to have the maximum expected operating pressure to be 10-15% less than the design pressure.

c. Design Stress

The design engineer ensures that the stress developed in a structure or equipment due to service loads does not exceed the elastic limit. This limit is usually chosen by ensuring that stresses remain within the limit through the uses of factors of safety.

d. Corrosion Allowances

Corrosion allowance is the tribute to corrosion damage paid by the design engineer to compensate for the inevitable effects of corrosion on process equipment, especially those exposed to the environment. For carbon and low alloy steels where severe corrosion is not expected, a minimum allowance of 2.0mm is used, while where more severe conditions are anticipate, this value may be increased to 4.0mm.

e. Minimum Practical Wall Thickness

Almost always, a minimum wall thickness is required to ensure that vessels are sufficiently rigid to withstand their own height and/or any incidental loads.

2.11.2 Material Balances

Material balances are the single most important component of a process design. In any given process of industrial importance, it is the overall material balance taken over the complete process that determines the amount of raw material required for specified quantities of various products in the process. Material balance is the basic tool for process and plant design in that it is the overall material balances and balances over individual process units that determine the process stream flow and their composition which are required for specification of the various pieces of equipment used in the process.

Material balances are indispensible tools in the optimization and simulation of plant operation, troubleshooting and in the location of plant performance against design data. They are equally useful in the extrapolation of data obtained from plant instrumentation where such data are insufficient, in monitoring of instrument performance and in the economic analysis.

a. Fundamentals of Material Balance Calculations

The fundamental law governing the material balance calculations is the principle of conservation of mass which states that matter can neither be created nor be destroyed except for nuclear reaction where it can be see that mass and energy are equivalence and so can take any of the either form. The general conservation equation for any process system is given

Material Out = Material In + Generation – Consumption - Accumulation

For a steady state process without reaction, the generation, consumption and accumulation terms are zero so that the above equation becomes:

Material Out = Material In

In material balance calculations, the choice of the correct basis for the calculation often determines whether the calculation proves to be simple or complex. The selection of correct basis for calculations is usually enhanced by long experience. It may be more convenient to carry out the material balance calculations in gmol/s or g/s while the results may be presented in kg/hr or tonne/hr.

b. Solution to Material Balance Problems

There are several approaches to material calculations depending on the complexities of the problem to be solved. The best way to solve a particular material balance problem depends largely on the information provided, the information desired from the problem, and the constraints that apply to the problem. Simple material balance calculations involving only a few streams and with a few unknown can usually be solved by simple direct algebraic methods. In this case, the relationship between the unknowns and the information provided can usually be clearly identified. However, for more complex cases involving several processing steps or several recycle, purge and by-pass stream, more complex algebraic methods are usually required.

c. Material Balances for Processes with Recycle Streams

The presence of recycle, purge and by-pass streams makes material balance calculations more difficult. The more recycle streams there are, the more complex and difficult the material balance calculations become. If no recycle streams are present, the material balance on a series of processing steps can be carried out sequentially, taking each processing step one after the other. The calculated flow rates out of one processing step become the feed flow rates to the next step. If a recycle stream is present, then at a point where the recycle stream is returned to the process, the flow rates of the recycle stream is unknown, as its value depends on downstream flow rate which have not yet been calculated. Since the recycle flow rate is unknown, the sequence of calculations cannot continue to the point where the flow rate of the recycle stream can be determined.

There are basically two traditional approaches to material balance problems involving recycle streams(Miller et al., 2002). These are the cut and Try method and the Formal Algebraic Method.

In the former, the recycle stream flow rates are estimated and the calculations are continued until the recycle flow rates are calculated. The estimated flow rates are then compared with the calculated values and a better estimate of the recycle flow rates is made. In the latter however, a set of material balance equations are set up with the recycle flow rates as unknowns and solved simultaneously to determine the flow rates in each stream.

d. The Split Fraction Method

The split fraction method is one of the formal algebraic method is based on the realization that the basic function of most chemical processing units (unit operations) is to divide the inlet flow of a component between two or more outlet streams. It is therefore, possible, when setting up the equations describing a unit operation to express the flow of any component in any outlet stream as a function of the flow of that component in the inlet stream.

In fig 2.6, the block shown represents any unit in an information flow diagram and the whole figure shows the nomenclature used in setting up the material balance equations in the split fraction method:

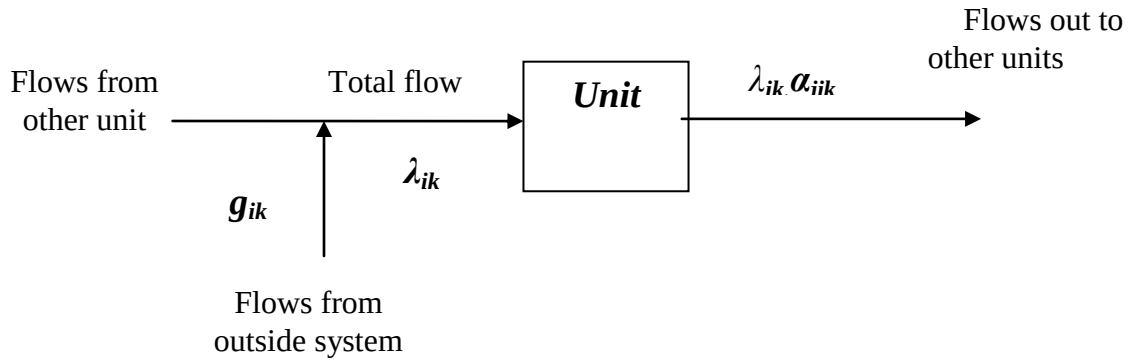

Fig 2.6: An information flow diagram showing the nomenclature used in setting up the material balances

i = Unit number

λ_{ik} = Total flow of component k into unit i

α_{jik} = The fraction of the total flow of component k entering unit i that leaves in the outlet stream from unit i and is connected to unit j; that is "the split fraction co-efficient of component k that enters unit i and is connected to j.

g_{iok} = any fresh feed of component k that goes into unit i.

The value of the split fraction co-efficient depends on the nature of the unit and the inlet stream composition. The outlet streams from a unit can feed forward to other units or backwards to other units (recycle).

In this design, the split fraction method has been used to carry out the material balance calculations. This method is chosen not only because of the presence of recycle stream but also due to the numerous components and processing units involved. The advantage of this split fraction method is that a set of n x n simultaneous linear material balance equations only need to be solved for each component regardless of the complexities of the recycle streams present. See Appendix A for the details of the material balance calculations for this process. The results of the material balance are summarized section 3.4.

2.11.3Energy Balances

The Energy balance provides a detailed account of all the energy requirements of the process equipment, and is based on the principle of conservation of energy. The principle states that energy can neither be created nor destroyed but can be transformed from one form to another. Also, energy can be transferred from one body to another.

The conservation of energy however differs from the mass in that energy can be generated (or consumed) in a chemical process. Material can change form; new molecular specie can be formed in a process unit and must be equal to the one out at steady state. The same is not true for energy. The total enthalpy of the outlet stream will not be equal to that of the inlet stream if energy is generated or consumed in the processes, such as that due to heat of reaction.

Energy can exist in various forms; head, mechanical, electrical energy, and it is the total energy that is conserved. In plant operation, an energy balance on the plant will show the patterns of energy usage and suggest area of conservation and saving.

a. Conservation of Energy

As in the case of material balance, a general equation can be written for energy balance;

Energy out – Energy in + Generation – Consumption = Accumulation

This is a statement of the first law of thermodynamics. An energy balance can be written for any process step. Chemical reactions will evolve energy (exothermic) or consume energy (endothermic). For steady state process usually, the accumulation of both mass and energy will be zero.

Energy Balance Assumptions

1. The process operation is at steady state
2. Heat losses are negligible, due to proper insulation (adequate lagging) of process equipment, vessels and pipe networks.
3. Negligible effect of pressure on heat capacities.
4. Potential and kinetic Energy contributions are ignored.

b. Choice of Standard State

As in any proper thermodynamics analysis, accurate values can be determined relative to some arbitrary chosen state. This is due to the fact that absolute values of the energy terms are not easily obtainable. We will specify the temperature, state of aggregation, and pressure of the substance at the standard state.

For the purpose of this design (as in the process analysis), our standard state is taken to be 298K and 1atm, for all gaseous and liquid streams. And where phase changes, heats of phase change will be considered. Also where stream pressures are not 1atm, the effect on its enthalpy of changing its pressure to the standard state pressure of 1atm we must also put into consideration unless where we have assumed that the effect of pressure on the enthalpy of the stream is negligible.

Table 2.8: Heat Capacity Constants for the stream components

S/N	Components	A	B	C	D	E
1	CO_2	-8,304,300	104,370	-433.33	0.60052	-
2	H_2O	276,370	-2,090.1	8.125	-0.01412	$9.37x10^{-6}$
3	O_2	175,430	-6,152.3	113.92	-0.92382	0.0027963
4	CO	65.429	28,723	-847.39	1,959.6	-
5	NO	-2,979.600	76,602	-652.59	1.8879	-
6	SO_2	85,743	5.7443	-	-	-
7	N_2	281,970	-12,281	248	-2.2182	0.00749

Source: Chemical Engineers Handbook by Perry, 2007

2.12 Summary of Literature Review

Many researchers are aiming to develop new solvent technologies to improve the efficiency of the CO_2 capture.Imai(2003) is of the view that better and more advanced solvents for CO_2capture from flue gas will in the future be developed from biological sources, which is in line with the essence of the investigation in this work, by comparing the capture performance of SDA leachate with that of the conventionally used MEA for the purpose. While many related research works have been reviewed extensively, none of the conventional solvents for carbon sequestration has been found as ideal solvent, in terms of efficiency, cost effectiveness and energy involvement. This is due to the fact that they are toxic, non - readily available and not even cheap as in the case of the conventional monoethanolamine solution used as benchmark for this research.Therefore, it is important to study other alternative solvent to achieving the capture. Also in this work, sawdust ash leachate has been proposed as alternative solvent for CO_2 and CO capture, and its effectiveness would be investigated in the course of this research.

CHAPTER THREE

MATERIALS AND METHODS

3.1 Materials

3.1.1 Sample/Material Collection

Saw dust was gathered from a carpentry workshop within Umuagwo locality of Ohaji LGA of Imo State. Also MEA stock solution was purchased from Head Bridge Market Onitsha.The various components of the laboratory scale absorber column set up (including a laboratory glass absorber with baffles, kips apparatus base, glass tubes, retort stand, rubber corks) were also made available for the sequestration experimental runs. A dosing pump, a diversion valve and a generating set (Yamaha EF1000), were provided for the experimental runs.

3.1.2 Material Preparation

To produce saw dust ash of required particle size and quality, 2kg of saw dust sample was weighed and dried in an electric oven at 130^0Cfor 2 hours. The sample was later charred using a low flame in a fume cupboard until it has ceased smoking. The charred sample which was in crucibles were placed in a cold muffle oven (electric furnace) and the temperature was set at 550^0C. The sample was treated for 12 hours at 550^0C. After that, the muffle furnace was turned off and allowed to cool to at about 150^0C before it was opened. Safety tongs was used to transfer the crucibles containing the sample to a desiccator with porcelain plate and desiccant. The crucibles were covered and the desiccator was closed. The crucibles were allowed to cool prior to weighing. Finally, the saw dust ash was screened through a mesh size of 0.1mm to obtain particulates suitable for the ash leachate preparations.

The various concentrations (in g/L) of the ash leachates were then prepared by weighing required quantities of the saw dust ash and dissolving same accordingly in predetermined volumes of deionized water to obtain appropriate ash leachate concentrations, for the experimental runs.

Similarly, the MEA stock solution was diluted to obtain various concentrationsof the sequestrant(similar to those of the ash solutions) for the CO_2 and CO capture experiments from flue gas (exhaust) ofYamaha EF1000.

3.1.3 Materials/Apparatus used for the sequestration experiments

a. Materials/Reagents

- Monoethanolamine stock solution
- Saw dust ash
- De-ionized water
- Distilled water
- 0.1M NaOH Solution
- Phenolphthalein indicator

b. Apparatus/Equipment

- Laboratory scale absorber column set up
- Dosing pump(Model: JM 15.77/4.2)
- Yamaha(Model: EF1000)
- Gas analyzer(Model:Ambro 2000)
- Analytical balance (Model: Adventurer Pro A35, Make: OHAUS)
- Electro-thermal Oven (Model: HG 9023A, Make: B.BRANC, scientific and instrumental company, England)
- Heating mantle (Model: ZDHW-250, Make: PEC Medical, USA)
- Multi-Parameter Bench Photometer (Model: HI 83200, Make: Hanna)
- Atomic Absorption Spectrophotometer (AAS)
- Muffle furnace
- 0.1mm size screening mesh
- Desiccator
- Ceramic pestle and mortar
- Stop watch
- pH meter
- Retort stand
- 250ml and 500ml conical flasks
- 100ml, 250ml, 500ml and 1000ml beakers
- Measuring cylinders
- 100ml volumetric flask
- Pipettes
- Test tubes

- Specific gravity bottle
- Whatman filter papers
- Glass funnel
- Stirring rod
- Spatula

3.2Methods

3.2.1 Method for the Ash Compositional Analysis

a) Physical Parameters

i. pH

ISO:3025 Electrometric Method was used. The pH electrode used in the pH measurement was of a combined glass electrode. It consists of sensing half-cell and reference half-cell, together form an electrode system. The sensing half-cell is a thin pH sensitive semi permeable membrane,separating two solutions, viz: the sample to be analyzed, and the internal solution,enclosed inside the glass membrane and has a known pH value. An electrical potential is developed inside and another electrical potential outside, the difference in the potential is measured and is given as the pH of the sample. ThepH meter was switched on about 30 minutes before the test. The buffer solutions of pH 4.0, 7.0 and 9.0 were prepared, and the pH meter calibrated to 9.2 using the buffer and by adjusting the calibration knob. Again the pH meter was calibrated to 7.0 using the buffer and by adjusting the calibration knob. Then the pH meter was calibrated to 4.0 using the buffer and by adjusting the calibration knob. Finally the pH meter was read by inserting the probe into the sample.

ii. Conductivity and Total Dissolved Solids

ISO: 3025 Electrometric Method was used. Conductivity was measured with a probe and a meter. A voltage was applied between the two electrodes in the probe, and then in the immersed in the sample water. The drop in voltage caused by the resistance of the water was used to calculate the conductivity per centimeter. Conductivity (G), the inverse of resistivity (R), is determined from the voltage and current values according to Ohms law. i.e. R=V/I, then G=1/R=I/V. The meter converts the probe measurement to micro ohms per centimeter and displays the result for the user.Theconductivity meter was switched on about 30 minutes before the test. 0.1M potassium chloride was prepared, and the conductivity meter calibrated to 14.12ohms using the standard 0.1M KCl by adjusting the calibration knob.The conductivity meter was read by inserting the probe in the sample (µS/cm). After this, it was switch over to the TDS mode and the reading taken and recorded in mg/l.

iii. Salinity

Salinity wasdetermined using the hand-held Refractometer, Model: E-Line Refractometer ‘ATC Range’, Order Code 44-803, Range 0 - 32^0Brix ATC, Scale Division 0.2. The refractometer was calibrated with distilled water. Twodrops of sample was left on the refractive surface of the

refractometer. The sample was covered and the refractive index read off, which has been scaled as salinity values, (Marine pollution monitoring manual, 2009).

vi. Moisture Content

A clean and dry crucible was weighed to 0.01g as W_1. 10g of saw dust ash was weighed and transferred into the pre-weighed crucible, and the crucible and content reweighed to 0.01g as W_2. Then the crucible and content was placed in the oven and dried to constant weight between 105 °C and 110 °C.The crucible and content was thereafter removed from the oven and placed in a desiccator to cool. Finally, the crucible and content was weighed to 0.01g W_3.

Calculation: Moisture Content (%) $= \frac{W2-W3}{W3-W1} \times 100$ (3-1)

(AOAC, 2016).

b) Particulate Analysis

i. Bulk Density

10g of sawdust ash was weighed out with a weighting balance. It was then completely transferred into a 50ml measuring cylinder filled with distilled water. The volume of the distilled water displaced was recorded, and the bulk density was calculated by dividing the mass of the sawdust ash by the volume of water displaced.

$$\text{Bulk Density (B.D)} = \frac{\text{mass of saw dust ash}}{\text{volume of water displaced}} \quad (3\text{-}2)$$

ii. Pore Volume and Porosity

5g of sawdust ash (sample) was weighed and transferred into a 10ml measuring cylinder in order to determine the total volume of the particles. The sawdust ash was further transferred into a beaker containing 20ml of distilled water, and was boiled for 5 minutes to displace air in the sample. The content in this beaker was filtered, superficially dried, and weighed. The increase in weight of the sawdust ash was recorded, and divided by the density of water to obtain the pore volume of the saw dust ash.

$$\text{Pore Volume (P.V)} = \frac{\text{increase in mass of saw dust ash}}{\text{density of water}} \quad (3\text{-}3)$$

Porosity was calculated by dividing the pore/void volume of the particles with the total volume of the particles.

$$\text{Porosity (ɧ)} = \frac{\text{volume of void}}{\text{Total volume}} \quad (3\text{-}4)$$

c) Mineral Content Analysis

i. Nitrate/Nitrate-nitrogen

Nitrates react with phenol disulphonic acid and produce a nitrate derivative, which in alkaline solution develops yellow colour due to rearrangement of its structure. The colour produced is directly proportional to the concentration of nitrates present in the sample. The photometer was switched on, and the program for nitrate was selected at a wavelength of 525 nm. Theprepared sample was poured into two separate 10ml cuvettes to the mark.One of the sample cuvette was used to zero the photometer. One sachet of nitrate reagent (HI83200) was added to the second cuvette and was inserted into the cell compartment.After a reaction time of 4 minutes 30 seconds, the READ button was pressed to display the result in mg/l NO_3^-. (AOAC, 2016).

ii. Phosphate/Phosphorus

The photometer was put on, and the program for phosphate was selected at a wavelength of 525 nm.The prepared sample was poured into two separate cuvettes to the 10ml mark. One of the samples (blank) was used to zero the photometer.10 drops of molybdate reagent and one packet of HI93717B, was added to the second cuvette. The lid of the cuvette was closed and shaken vigorously to dissolve the reagent.The first sample (blank) was replaced with the reacted sample cell in the light shield and timed for 5 minutes.The READ button was pressed at the end of the countdown time to display the result in mg/l PO_4^{3-}. (AOAC, 2016).

iii. Sulphate

Sulphate is precipitated in hydrochloric acid medium as barium sulphate by the addition of barium chloride solution: $BaCl_2 + SO_4 + 2Cl^-$

The barium sulphate is insoluble and because of this, it can be washed with water until chloride free and then dried to constant weight. Interference: Small quantities of Fe (II) iron, Mg, and Al may be tolerated. But Fe (III) iron and Ca may exert an adverse effect on the precipitation. However, they can removed by passing them through caution removing ion – exchange column. The photometer was put on and the wavelength selected at 466 nm. 10ml of prepared sample was poured into 2 separate cuvettes, and one of the samples (blank) was used to zero the photometer. One packet of barium chloride reagent was added to the second sample cuvette. The first cuvette was then replaced with the second reacted sample cell cuvette and timed for 5 minute.The READ

button was pressed at the end of the countdown time to display the reading in mg/l SO^{2-}_4.(AOAC, 2016).

Determination of metals

5g of the ash sample was dissolved in a 250ml conical flask, and about 60ml of 0.1M HCl was added and the solution filtered through a filter paper into a 100ml volumetric flask. It was then made up to mark with distilled-deionized water. The sample was then analyzed using flame photometer for Na, K, Ca and Mg. While for Fe, Cu, Pb, Mn, and Cr were analyzed using AAS (Atomic Absorption Spectrophotometer).

Flame Photometric Method for Metal Determination

iv. Sodium

The flame photometer was placed in a place where there are no direct rays of sunlight or constant light emitted by an overhead fixture and free from dust and tobacco smoke. It was ensured that sweats, traces of soap or detergent etc which are known to contain Na were not allowed into water sample whose sodium was desired.Blank and sodium calibration standard were prepared in steps in the 0 – 10mg/l application range, starting with the highest concentration and then working towards the most dilute solution. The emission on the photometer was measured at 589nm, and the calibration curves constructed from the standards. The samples were run on the photometer at 589nm and the readings noted.

Calculation: Na (mg/l) is calculated as given by the equation below,

$$\text{mg/l cation} = \frac{\text{concentration reading on curve x D (dilution factor)}}{\text{volume (ml)}\,of\ sample}$$

$$= \frac{\text{vol.ume (ml) of sample + volume (ml) of distilled water added}}{\text{volume (ml)}\,of\ sample} \qquad (3\text{-}5)$$

D was taken as 1, as there was no dilution.

v. Potassium

Stock potassium solution: KCl crystal was dried at 110^0C to constant weight in an oven. 1.907g accurately weighed and diluted to 1 liter with distilled water (1ml = 1mg K).Intermediate potassium solution: 10ml of stock potassium solution was diluted to 100ml with distilled water (1ml = 0.1mg = 100µg Na). This solution was used for preparing the calibration curve in the potassium range of 1.0 to 10mg/l.Standard potassium solution: 10ml of the intermediate potassium solution was obtained and diluted it to 100ml with distilled water. This gives 1ml =

10µg Na. This was used to prepare calibration curve in thepotassiumrange of 0.1 to 1.0mg/l. Similar procedure was carried out as in the case of sodium above.

Calculation: K (mg/l) is calculated as given by the equation 3.5.

Principles of Atomic Absorption Spectrophotometer

Working principles: Atomic absorption spectrometer's working principles is based on the sample being aspirated into flame and atomized when the AAS's light beam is directed through the flame into monochromator, and onto the detector that measures the amount of light absorbed by the atomized element in the flame. Since metals have their own characteristic absorption wave length a source lamp composed of that element is used, making the method relatively free from spectral or radiational interferences. The amount of energy of the characteristic wavelength absorbed in the flame is proportional to the concentration of the element in the sample.

vi. Iron

5.0503 g of IRON (11) ammonium sulphate was dissolved in distilled water and madeup to 1 litre. (1 ml=1 mg Fe).

vii. Copper

3.9296 g of copper sulphate pental hydrate was weighed and dissolved in some distilled water and made up to 1 litre (1 ml=1 mg Cu).

viii. Lead

1.5985 g of lead in nitrate was dissolved with distilled water and made up to 1 litre (1 ml = 1 mg Pb).

ix. Chromium

2.8285 g of anhydrous potassium dichromate was dissolved in distilled water and made up to 1 litre (1 ml= mg Cr).

x. Zinc

100 g of 30 mesh zinc metals was dissolved in slightly excess (1+1) HCl (about 1 ml) and was diluted to 1 liter with distilled water (1 ml = 1 mg Zn). (AOAC, 2016).

3.2.2 Method for the Sequestration Experiments

a) CO_2/CO sequestration with SDA Leachate and MEA Solution

Seventeen (17) sets of SDA leachate and MEA solutionrespectively, were prepared to concentrations of 1.25, 11.88 and 22.50g/L, depending on the run concentration as suggested by the 3-level experimental design. The prepared sequestrants weremade available for the

absorption/sequestration experiments. The experimental glass absorber was mounted on a table, and the gas and liquid inlets and outlets were connected appropriately.The dosing pump (for the sequestrant/absorber liquid transport) was then connected accordingly and the equipment connected to a power source and set to the required % stroke value (depending on the flow rate of the experimental run to be carried out), for the required optimal flow.A generating set (Yamaha EF1000) was put on, and after about two minutes the exhaust gas was analyzed for the $CO_2$and CO composition, then the flue gas exhaust was connected through to the absorber column gas inlet pipe. After this, the dosing pump was switched on for the sequestrant/absorber liquid circulation through the column, and in a counter current flow with that of the entry flue gas. This CO_2 and CO absorption process was monitored for a period of 5 - 10 minutes (depending on the experimental run performed), after which the gas analyzer,Ambro 2000 was used to check both the $CO_2$and CO composition of the exiting gas (lean gas) from the column. As the absorber exit gas was analyzed, exit absorber liquid (rich liquid) sample was collected and CO_2 test carried out on it using a classical method of the liquid titration with NaOH solution and phenolphthalein as indicator, as a means of confirming dissolution of the gas in the circulated absorber liquid (sequestrant).

For the classical evaluation of the dissolved CO_2 in the sequestrant, it is understood to follow the reaction mechanism described below as proposed by the Hack Kit Method.

Equation of Reaction: $CO_{2\,(aq)} + NaOH_{(aq)} \leftrightarrow NaHCO_{3(aq)}$ (3-6)

(Hach Kit Method)

In the end, experimental results were carefully recorded and other required parameters calculated as required, and accordingly.

b) Determination of CO_2 and CO in flue gas

The Gas Analyzer (Model: Ambro 2000) was put on and allowed to boot for about five minutes, after which the equipment was set on the program for the parameter to be tested (programs for $CO_2$and CO respectively), and the equipment gas sensor brought to the gas exit point of the absorber set up, in order to detect the $CO_2$and CO composition of the flue gas. Also the $CO_2$and CO composition of the flue gas coming out directly from the generating set (Yamaha EF1000) exhaust was determined and recorded.

However, for the SDA leachates and MEA solutions respectively, the reduction in the CO_2 contents of the flue gas exiting the absorber column and the enrichment of the absorber liquid were both monitored, results found useful in understanding the phenomenon, and discussed.

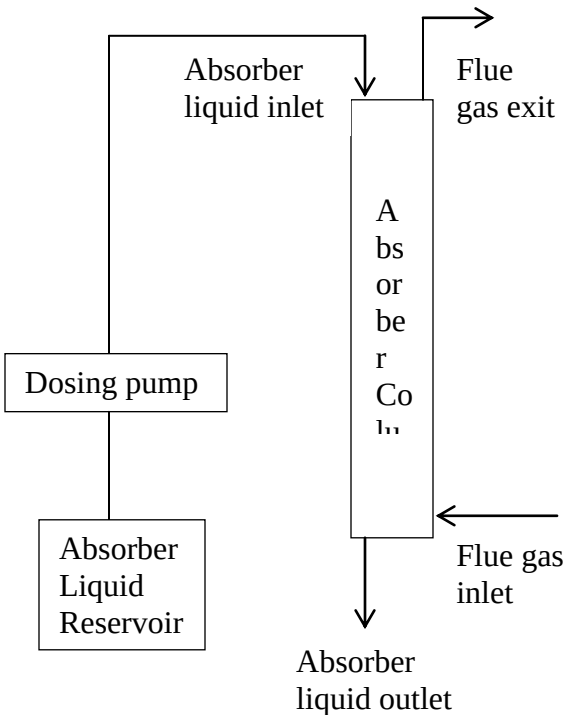

Plate 3.1:The Experimental set-up (Pictorial) **Fig 3.1: Block flow diagram of absorber**

c) Proposed reaction mechanisms and kinetics for the SDA Leachate with CO_2

In order to provide improved theoretical understanding of the kinetics of the dissolution of CO_2 in water and the subsequent chemical reactions, and to offer systematic approximations that may be exploited in multi-scale modelling tools, Mitchell *et al.*(2010) simplified the complex kinetic modelling of these key reactions, by using the method of matched asymptotic expansions to identify the distinct time scales over which the reactions take place and to provide simple expressions for the resulting dynamic and equilibrium concentrations. It is on the basis of the understanding of the compositions of the saw dust ash leachate that the following reaction mechanisms are postulated:

$$CO_2(g) \leftrightarrow CO_2(aq) \qquad (3\text{-}7)$$

$$CO_2(aq) + H_2O \leftrightarrow H_2CO_3 \quad (3\text{-}8)$$

$$H_2CO_3 \leftrightarrow H^+ + HCO_3^- \quad (3\text{-}9)$$

$$HCO_3^- \leftrightarrow H^+ + CO_3^{2-} \quad (3\text{-}10)$$

$$Ca^{2+} + CO_3^{2-} \leftrightarrow CaCO_3(aq) \quad (3\text{-}11)$$

In reaction (3-7), gaseous carbon dioxide is dissolved in water, reacting to form carbonic acid (3-8). Hydrogen ions dissociate from the carbonic acid, to give bicarbonate (3-9), and then a carbonate ion (3-10), which then reacts with acalciumcationtoformcalciumcarbonate(3-11).

d) Determination of Experimental Rate Law for the Carbon Sequestration

The experimental rate law for the carbon capture with SDA leachate was determined using excerpts of the original phenomenal experimental runs.

Rate = $k[CO_2(aq)]^x[H_2O]^y$

Experimental Rate Law: Rate = $k[CO_2]^1[H_2O]^1$ (3-27)

(See Appendix C for detailed calculations)

e) Determination of Overall Rate Constant (Second Order Rate Constant, k_2) and Mass Transfer Coefficient

The overall rate constant *k* was determined by substituting values from the result excerpts of the carbon capture with SDA leachate (table C1).

Choosing values for Trial 7, which represents an average of the three trials (or experimental serial numbers), and/or a mid-representative of the entire experimental trial runs, the overall rate constant (second order rate constant) and mass transfer co-efficient were obtained as:

$k = k_2 = 0.53 M^{-1}min^{-1}$

The mass transfer coefficient was determined by substituting appropriate values into eqn (2-45):

$K_L = \sqrt{(k_2[C_S]D_{CO2})}$

Where,

$K_L$is mass transfer coefficient (cms^{-1})

$k_2$is the second order reaction rate constant = $0.53M^{-1}min^{-1} = 8.83 \times 10^{-3} M^{-1}s^{-1}$

$C_S$is the optimal concentration of the solvent (sequestrant) = 22.5g/L = 1.25M

$D_{CO2}$is the diffusivity of CO_2in mineralized water = $1.88 \times 10^{-5} cm^2s^{-1}$

Hence, the mass transfer coefficient was obtained as:

$K_L = 4.56 \times 10^{-4} cms^{-1}$

3.3 Optimization

3.3.1 Modeling and Optimization of the CO_2 and CO capture process

The Design Expert Software was used in the Regression Statistical Analysis of the results for the wood ash and MEA absorption processes. The experimental data were gathered in the required format for the statistical study, and the collated data were used in the analysis to generate the necessary statistical parameters useful in the statistical model development and optimization.

Also, the software was employed in the surface response plots of the experimental data which served as visual aid in the judgment for the data variability and optimization values.

3.3.2 Process Variables

The process variables (X) used for the computer analysis are as follows:

X_1 = Concentration of SDA leachate or MEA solution (g/L)

X_2 = Sequestration time(mins)

X_3 = Flow rate of sequestrant (cm^3/min)

3.3.3 Response Variables

The response variables (Y) for the computer analysis are:

Y_1 = CO_2 composition of exit flue gas (%)

Y_2 = CO composition of exit flue gas (%)

3.3.4 Optimum Process Conditions

For 'CO_2 composition of exit flue gas (%)' as response variable; the optimum process conditions are theX_1, X_2, X_3 values that yield the optimum (minimum) Y_1 value.

While, for 'CO composition of exit flue gas (%)' as response variables; the optimum process conditions are the X_1, X_2, X_3 values that yield the optimum (minimum) Y_2 value.

3.3.5 Experimental Design

Table 3.1: Experimental design code and boundary/limit for the factors (Independent variables)

S/N	Variable	Code (X)	Boundary	
			Lower	Upper
1	Concentration of SDA/MEA solution (g/L)	X1	1.25	22.5
2	Sequestration time (mins)	X2	5	10
3	Flow rate of sequestrant (cm^3/min)	X3	200	250

Table 3.2: Experimental design code for the responses (Dependent variables)

S/N	Variable	Code (Y)
1	CO_2 composition of exit flue gas (%)	Y_1
2	CO composition of exit flue gas (%)	Y_2

Table 3.3: Experimental design matrix (codes showing three factors and three levels; Box Behnken design)

S/N	Run	Block	X_1 (g/L)	X_2 (mins)	X_3(cm^3/min)	Y_1 (%)	Y_2 (%)
1	16	(1)	-1.000	-1.000	0.000		
2	12	(1)	1.000	-1.000	0.000		
3	2	(1)	-1.000	1.000	0.000		
4	6	(1)	1.000	1.000	0.000		
5	4	(1)	-1.000	0.000	-1.000		
6	1	(1)	1.000	0.000	-1.000		
7	17	(1)	-1.000	0.000	1.000		
8	10	(1)	22.50	0.000	1.000		
9	5	(1)	0.000	-1.000	-1.000		
10	15	(1)	0.000	1.000	-1.000		
11	14	(1)	0.000	-1.000	1.000		
12	9	(1)	0.000	1.000	1.000		
13	7	(1)	0.000	0.000	0.000		
14	3	(1)	0.000	0.000	0.000		
15	8	(1)	0.000	0.000	0.000		
16	13	(1)	0.000	0.000	0.000		
17	11	(1)	0.000	0.000	0.000		

Table 3.4: Experimental design matrix (with actual values; Box Behnken design for three factors and three levels)

S/N	Run	Block	X_1 (g/L)	X_2 (mins)	X_3(cm^3/min)	Y_1 (%)	Y_2 (%)
1	16	Block 1	1.25	5.00	225.00		
2	12	Block 1	22.50	5.00	225.00		
3	2	Block 1	1.25	10.00	225.00		
4	6	Block 1	22.50	10.00	225.00		
5	4	Block 1	1.25	7.50	200.00		
6	1	Block 1	22.50	7.50	200.00		
7	17	Block 1	1.25	7.50	250.00		
8	10	Block 1	22.50	7.50	250.00		
9	5	Block 1	11.88	5.00	200.00		
10	15	Block 1	11.88	10.00	200.00		
11	14	Block 1	11.88	5.00	250.00		
12	9	Block 1	11.88	10.00	250.00		
13	7	Block 1	11.88	7.50	225.00		
14	3	Block 1	11.88	7.50	225.00		
15	8	Block 1	11.88	7.50	225.00		
16	13	Block 1	11.88	7.50	225.00		
17	11	Block 1	11.88	7.50	225.00		

CHAPTER FOUR

RESULTS ANDDISCUSSION

4.1 Results for the Sawdust Ash Compositional Analysis

The results for the characterization of the saw dust ash/leachate are presented herein in Tables 4.1-4.3.

4.1.1 Characterization of the Sawdust Ash/Leachate

Table 4.1: Result for the physical parameters of SDA

S/N	Parameter	Trial 1	Trial 2	Trial 3	Trial 4	Average Value
1	pH	10.12	10.14	10.17	10.18	10.15
2	Conductivity, µs/cm	1920	1900	1960	1880	1915
3	Total Dissolved Solids, mg/l	1248	1234	1274	1222	1245
4	Salinity, mg/l	115.20	82.29	65.83	98.75	90.52
5	Total organic matter, %	99.24	99.17	99.17	99.19	99.19
6	Moisture content, %	50.362	51.080	50.792	50.934	50.792
7	Ash content, %	75.5	82.9	83.3	81.0	80.7

In Table 4.1, the compositional analysis of the saw dust ash/leachate used for the absorption experiments has revealed that the physical parameters analyzed produced results which agree with works of Huang et al. (1992) and Ohno, 1992 as expected for effectiveness for the purpose of capturing CO_2 which is a weak acid. The leachate is seen to be alkaline in nature, with a very high conductivity value of 1915µs/cm on the average. The total dissolved solids produced a high result as expected and the salinity was also high. The saw dust ash had a total organic

matter content of over 99% with moisture content of about 50% which indicates its ability to corrode absorber device.

In line with the alkaline result obtained for the SDA, Huang *et al*. (1992) asserted wood ash as a soil addictive and liming agent.Ohno (1992) noted that acidity of soil can be neutralized by addition of wood ash, and phosphorus and potassium nutrients could be augmented by the application equally.

Table 4.2: Result for the particulate analysis of SDA

S/N	Parameter	Trial 1	Trial 2	Trial 3	Trial 4	Average Value
1	Bulk density, g/cm^3	0.10018	0.10014	0.10018	0.10019	0.10017
2	Pore volume, cm^3	0.3476	0.3468	0.3477	0.3469	0.3472
3	Porosity	0.01738	0.01734	0.01740	0.01740	0.01738

For the particulate analysis, from Table 4.2, the bulk density is seen to be as low as $0.1g/cm^3$ with pore volume of approximately $0.35cm^3$ and porosity value of 0.017.These properties indicate good absorptive capacity of the leachate.Someshwar (1996) established that depending on the method with which sawdust ash is obtained, it is usually found to have a bulk density of ±0.1 and porosity almost as low as 0.02, which is perfectly in line with what has been obtained in the sawdust ash sample analysis. The corroboration of the obtained results with established literature shows that the prepared ash possess the ability necessary for the sequestration of CO_2.

Table 4.3: Result for the mineralcontent analysis of SDA

S/N	Parameter	Trial 1	Trial 2	Trial 3	Trial 4	Average Value
1	Chloride, mg/kg Cl^-	63.77	45.55	36.44	54.66	50.105
2	Nitrate, mg/kg NO^-_3	10.60	21.71	15.60	12.00	14.98
3	Nitrate-nitrogen, mg/kg NO^-_3-N	2.40	4.90	3.60	2.70	3.40
4	Phosphate, mg/kg PO_4^{3-}	2.30	1.90	1.30	1.50	1.75
5	Phosphorus, mg/kg P	0.70	0.60	0.40	0.50	0.55
6	Sulphate, mg/kg SO_4^{2-}	5.00	5.00	5.00	5.00	5.00
7	Sodium, mg/kg Na	5.05	5.10	5.15	6.00	5.33
8	Potassium, ppm K	3.00	3.10	3.30	4.20	3.40
9	Calcium, mg/kg Ca	484.97	432.86	476.95	501.00	473.95
10	Magnesium, mg/kg Mg	44.506	48.883	44.749	41.344	44.871
11	Iron, mg/kg Fe	0.20	0.22	0.14	0.17	0.18
12	Copper, mg/l Cu	3.62	3.22	3.81	3.29	3.49
13	Lead, mg/l Pb	0.132	0.086	0.100	0.626	0.236
14	Manganese, mg/l Mn	0.50	0.40	0.80	0.30	0.50
15	Chromium, mg/l Cr	0.041	0.026	0.030	0.036	0.033
16	Zinc, mg/l Zn	28.68	28.54	27.91	28.04	28.29

As seen in Table 4.3, the mineral content analysis showed good content for chloride and nitrate, and low contents as obtained for the phosphates and sulphate values. Among the light metals, calcium was found to be more available in the saw dust ash with value of over 400mg/l. The heavy metals as expected are in trace amounts (Ruhling, 1996), except for zinc which was as high as 28mg/l. Most of the parameter values obtained in the SDA characterization are found to be about similar values as outlined by Etiegni and Mahler (1991).

However, Misra *and Baker* (1993) noted wood ash composition to be a function of the furnace temperature during the processing. It therefore indicates that for the furnace ash processing temperature used, these values obtained could be slightly varied depending on the ashing (furnace) temperature used.

4.2 Results for CO_2 and CO Sequestration using SDA Leachate and MEA

Table 4.4: Result for CO_2 and CO Sequestration using SDA Leachate as Absorber Liquid (Sequestrant)

S/N	Run	X_1 (g/L)	X_2 (mins)	X_3(cm^3/min)	Y_1 (%)	Y_2 (%)
1	16	1.25	5.00	225.00	33.35	6.48
2	12	22.50	5.00	225.00	29.99	5.72
3	2	1.25	10.00	225.00	26.81	4.83
4	6	22.50	10.00	225.00	25.80	4.89
5	4	1.25	7.50	200.00	26.20	5.15
6	1	22.50	7.50	200.00	21.40	4.88
7	17	1.25	7.50	250.00	23.80	5.00
8	10	22.50	7.50	250.00	21.05	4.47
9	5	11.875	5.00	200.00	34.92	6.78
10	15	11.875	10.00	200.00	19.01	3.64
11	14	11.875	5.00	250.00	23.02	4.92
12	9	11.875	10.00	250.00	25.36	5.06
13	7	11.875	7.50	225.00	28.40	5.68
14	3	11.875	7.50	225.00	28.00	5.60
15	8	11.875	7.50	225.00	28.80	5.70
16	13	11.875	7.50	225.00	30.50	6.01
17	11	11.875	7.50	225.00	28.40	5.69

Where,

X_1 = Concentration of SDA leachate (g/L)

X_2 = Sequestration time (mins)

X_3 = Flow rate of sequestrant (cm^3/min)

Y_1 = CO_2 composition of exit flue gas (%)

Y_2 = CO composition of exit flue gas (%)

Table 4.5: Result for CO_2 and CO Sequestration using MEA Solution as Absorber Liquid (Sequestrant)

S/N	Run	X_1 (g/L)	X_2 (mins)	X_3(cm^3/min)	Y_1 (%)	Y_2 (%)
1	16	1.25	5.00	225.00	23.56	5.67
2	12	22.50	5.00	225.00	19.26	4.16
3	2	1.25	10.00	225.00	28.31	6.12
4	6	22.50	10.00	225.00	19.77	5.07
5	4	1.25	7.50	200.00	27.22	5.98
6	1	22.50	7.50	200.00	20.61	4.90
7	17	1.25	7.50	250.00	29.79	6.52
8	10	22.50	7.50	250.00	21.35	5.04
9	5	11.875	5.00	200.00	23.25	5.73
10	15	11.875	10.00	200.00	24.54	5.83
11	14	11.875	5.00	250.00	24.28	5.59
12	9	11.875	10.00	250.00	29.38	6.75
13	7	11.875	7.50	225.00	21.60	4.48
14	3	11.875	7.50	225.00	22.01	4.51
15	8	11.875	7.50	225.00	21.80	4.58
16	13	11.875	7.50	225.00	22.01	4.59
17	11	11.875	7.50	225.00	19.99	4.48

Where,

X_1 = Concentration of MEA solution (g/L)

X_2 = Sequestration time (mins)

X_3 = Flow rate of sequestrant (cm^3/min)

Y_1 = CO_2 composition of exit flue gas (%)

Y_2 = CO composition of exit flue gas (%)

In the result tables for the experimental runs (Tables 4.4 and 4.5) for the SDA leachate and MEA solutions, absorber liquid/sequestrant concentrations within the range of 1.25g/L and 22.50g/L were used. This was due to the ash dissolution difficulty encountered in preparing SDA leachate concentrations above 22.5g/L, and below 1.25g/L concentration no clear change in the dissolved CO_2 concentration of the absorber liquid.

Again for the preliminary runs set up, after some initial trials have been carried out, the optimal sequestrant flow rate were found to be within the range of 200cm^3/min to 250cm^3/min, for the successful operation of the laboratory scale glass absorber without flooding. The pump settings at which the aforementionedoptimal liquid flow were established were 30%, 40% and 50% strokes, which were subsequently adopted in the design of experiments.

Box Behnken design for three factors and three levels was used in the design of experiments (for both SDA leachate and MEA solution) for the laboratory experimental runs, producing seventeen (17) runs. The factors (independent variables; X_1, X_2 and X_3) weretaken to be the concentration of sequestrant (g/L), sequestration time (mins) and flow rate of sequestrant (cm^3/min) respectively,while the responses (Y_1 and Y_2) were taken to be the CO_2 and CO compositions of the exiting flue gas from the absorber column, respectively. For the factors (with box bekhen design), experimental design data points of 1.25, 11.88 and 22.50g/L were used for the concentration of the sequestrants, data points of 5, 7.5 and 10mins for the sequestration time, and for the flow rate of sequestrants, 220cm^3/min, 225cm^3/min and 250cm^3/min were used.

The CO_2 compositions of the flue gas from the absorber column (when SDA leachate was used as sequestrant) were found to be within the values of 19.01% and 34.92%, and between values of 3.64% and 6.78% for CO compositions. When MEA solution was used as sequestrant, CO_2 compositions of the flue gas from the absorber column had values between 19.26% and 29.79%, and the CO compositions with values between 4.16% and 6.75. However, the CO_2 and CO compositions of the flue gas exiting directly from the generating set (Yamaha EF1000) were measured by the Ambro2000 Gas Analyzer to be 41% and 8.2% respectively. According to Gale (2002), domestic power generating sets could form part of the well-known potential CO_2 emission sources from which it is a possibility to capture and store carbon. Gielen and Moriguchi (2003) reiterated that absorption (or scrubbing) remains one of the effective approaches to carbon capture from flue gases of both large and medium scale industrial plants.

From the results, the effects of each of the factors were better understood when statistical analysis were done based on the results with which statistical models were developed and

response surface methodology carried out for the purpose of optimizing the capture process conditions under investigation in this work. The respective discussions are outlined in the subsequent section 4.3 that follows.

Imai(2003) is of the view that better and more advanced solvents for CO_2capture from flue gas will in the future be developed from biological sources, which is in line with the essence of the investigation in this work, by comparing the capture performance of SDA leachate with that of the conventionally used MEA for the purpose.

Mimuraet al.(1995) showed immense concern through their research on energy saving technology for flue gas carbon dioxide recovery and steam system in power plant. Their effort was geared towards minimizing the energy requirement for the capture process which happens to be a major advantage of the quest for this work.

Moser et al. (2009) worked on enabling post combustion captureoptimization with the pilot plant project at Niederaussem. Even though they used conventional liquid for capture, their optimization approach involved setting out process factors and performing the capture at the various defined factor combinations, which is an analogue of what has been done in this work.

Rao and Rubin (2002) after working ona technical, economic and environmental assessment of amine-based CO_2 capture technology for power plant greenhouse gas control, agree to the fact that the exercise with the chemical based liquid even though technically effective and environmental assessment commendable, the economics of the process remains a factor of concern. This present quest to ascertain the replaceability of conventional chemical liquids with locally (prepared) sourced alternatives seeks to address that.

4.3 Results for the Statistical Analysis, Modelling and Optimization

4.3.1 SDA Leachate – 'CO_2 and CO Composition of Exit Flue Gas' as Response

Table 4.6: Results of Experimental Runs recoded for SDA Leachate

		Factor 1	Factor 2	Factor 3	Response 1	Response 2
Std	Run	A: Conc. of SDA Leachate	B: Sequestration time	C: Flowrate of sequestrant	CO_2 composition of exit flue gas	CO composition of exit flue gas
		g/L	Mins	cubic cm per min	%	%
1	5	1.25	5	225	33.35	6.48
2	2	1.25	10	225	26.81	4.83
3	6	22.5	5	225	29.99	5.72
4	9	22.5	10	225	25.80	4.89
5	3	11.875	5	200	34.92	6.78
6	17	11.875	10	200	19.01	3.64
7	4	11.875	5	250	23.02	4.92
8	12	11.875	10	250	25.36	5.06
9	1	1.25	7.5	200	26.20	5.15
10	8	22.5	7.5	200	21.40	4.88
11	7	1.25	7.5	250	23.80	5.00
12	16	22.5	7.5	250	21.05	4.47
13	15	11.875	7.5	225	28.40	5.68
14	13	11.875	7.5	225	28.00	5.60
15	10	11.875	7.5	225	28.80	5.70
16	11	11.875	7.5	225	30.50	6.01
17	14	11.875	7.5	225	28.40	5.69

On the response columns of table 4.6, the responses obtained from the different experimental runs carried out by combining the three variables in a unique manner for each of the runs are

tabulated. It is seen that the three experimental variable interactions gave a total of 12distinct runs and 5 centre points. The responses obtained from various runs are however significantly exceptional implying that each of the factors have a substantial effect on the response, as observed from the results.

Table 4.7: Fit Summary Table (SDA Leachate)

	Sequential	**Lack of Fit**	**Adjusted**	**Predicted**	
Source	**p-value**	**p-value**	**R-Squared**	**R-Squared**	
Linear	0.1306	0.0047	0.1903	-0.2942	
2FI	0.1044	0.0074	0.4155	-0.5318	
Quadratic	**0.0002**	**0.4384**	**0.9446**	**0.8020**	**Suggested**
Cubic	0.4384		0.9474		Aliased

Table 4.8: Lack of Fit Test (SDA Leachate)

	Sum of		**Mean**	**F**	**p-value**	
Source	**Squares**	**Df**	**Square**	**Value**	**Prob > F**	
Linear	188.78	9	20.98	21.8	0.0047	
2FI	103.11	6	17.18	17.86	0.0074	
Quadratic	**3.25**	**3**	**1.08**	**1.13**	**0.4384**	**Suggested**
Cubic	0	0				Aliased
Pure Error	3.85	4	0.96			

Table 4.9:Model Summary Statistics (SDA Leachate)

	Std.		**Adjusted**	**Predicted**		
Source	**Dev.**	**R-Squared**	**R-Squared**	**R-Squared**	**PRESS**	
Linear	3.85	0.3421	0.1903	-0.2942	378.93	
2FI	3.27	0.6347	0.4155	-0.5318	448.52	
Quadratic	**1.01**	**0.9758**	**0.9446**	**0.8020**	**57.99**	**Suggested**
Cubic	0.98	0.9869	0.9474		+	Aliased

DF = degree of freedom

CV = Coefficient of variance

PRESS = Predicted residual sum of squares

ANOVA Analysis and Model Fitting

The F-value tests performed using analysis of variance (ANOVA),were useful in evaluating the significance of each type of model. Based on the results of F-value, the highest order model with significant terms showing the relationship between parameters well and normally werechosen.

Again, the adequacy of the models was evaluated by applying the lack-of-fit test. The lack-of-fit test is used in the numerator in an F-test of the null hypothesis, and it indicates whether a proposed model fits well or not. The test for lack-of-fit compares the variation around the model with pure variation within replicated observations. The lack-of-fit test measured the adequacy of the different models based on response surface analysis (Lee *et al.*, 2006). In Table 4.8, it is observedthere was a significant difference (F-value = 188.78and 103.11) lack of fit for Linear and 2FI models. However, the test was not significant (F-value = 3.25 and 0.00) for quadratic and cubic models respectively. The significant results of lack of fit for linear and 2FImodels have shown that these models are not adequate for predicting the CO_2 composition of the exit flue gas.Moreso, apart from the F-value and the lack of fit, it is also seen that the R-squared, adjusted R-squared and the predicted R-squared values for the quadratic model produced high values of 0.9758, 0.9446, 0.8020 respectively when compared to those for the other models (linear, 2FI and cubic) as found in table 4.9. The measure of how efficient the variability in the actual response values can normally be explained by the experimental variables and their interactions which is given by the R-Squared value. It is established statistically that the closer the R^2 value is to unity, the better the model predicts the response. Adjusted-R^2on the other hand is a measure of the amount of variation around the mean explained by the model, adjusted for the number of terms in the model. Further, the adjusted-R^2decreases as the number of terms in the model increases, if those additional terms do not add value to the model. Predicted-R^2 is a measure of the amount of variation in new data explained by the model. The predicted-R^2 and the adjusted-R^2 should be within 0.20 of each other, otherwise there may be a problem with either the data or the model, (Taran and Aghaie, 2015).

Based on these results, the effect of each parameter was evaluated using quadratic model as shown in Table 4.10.

Table 4.10: ANOVA for Response Surface Quadratic model(SDA Leachate)

	Sum of		**Mean**	**F**	**p-value**	
Source	**Squares**	**Df**	**Square**	**Value**	**Prob > F**	
Model	285.7	9	31.74	31.31	< 0.0001	significant
A-Conc. of SDA leachate	73.8	1	73.8	72.79	< 0.0001	
B-Sequetration time	17.78	1	17.78	17.53	0.0041	
C-Flowrate of sequestrant	8.6	1	8.6	8.48	0.0226	
AB	1.38	1	1.38	1.36	0.2814	
AC	83.24	1	83.24	82.11	< 0.0001	
BC	1.05	1	1.05	1.04	0.3426	
A^2	7.31	1	7.31	7.21	0.0313	
B^2	5.57	1	5.57	5.49	0.0516	
C^2	87.47	1	87.47	86.28	< 0.0001	
Residual	7.1	7	1.01			
Lack of Fit	3.25	3	1.08	1.13	0.4384	not significant
Pure Error	3.85	4	0.96			
Cor Total	292.79	16				

It is seen from table 4.10 that the Model F-value of 31.31implies the model is significant, and there is onlya 0.01% chance that an F-value this large could occur due to noise.It has been established that values of "Prob > F" less than 0.0500 indicate model terms are significant.In this case A, B, C, AC, A^2, C^2 are significant model terms.Values greater than 0.1000 indicatethe model terms are not significant.However, if there are many insignificant model terms (not counting those required to support hierarchy),model reduction may improve our model.

The "Lack of Fit F-value" of 1.13 implies the Lack of Fit is not significant relative to the pureerror. There is only a 43.84% chance that a "Lack of Fit F-value" this large could occur dueto noise. Non-significant lack of fit is good because we want the model to fit.Further, the insignificant model terms could be eliminated to improve the model efficiency. Using backward elimination model with alpha to exit term equal to 0.100, the insignificant model terms were eliminated from the ANOVA terms.

After removing the insignificant model terms, the reduced quadratic model was obtained as shown on Table 4.11.

Table 4.11: ANOVA for Reduced Response Surface Quadratic model(SDA Leachate)

Source	**Sum of Squares**	**Df**	**Mean Square**	**F Value**	**p-value Prob > F**	
Model	283.27	7	40.47	38.23	< 0.0001	significant
A-Conc. of SDA leachate	73.8	1	73.8	69.71	< 0.0001	
B-Sequestration time	17.78	1	17.78	16.79	0.0027	
C-Flowrate of sequestrant	8.6	1	8.6	8.12	0.0191	
AB	83.24	1	83.24	78.63	< 0.0001	
AC	7.31	1	7.31	6.9	0.0275	
A^2	5.57	1	5.57	5.26	0.0476	
C^2	87.47	1	87.47	82.62	< 0.0001	
Residual	9.53	9	1.06			
Lack of Fit	5.68	5	1.14	1.18	0.4486	not significant
Pure Error	3.85	4	0.96			
Cor Total	292.79	16				

Std. Dev.	1.03	R-Squared	0.9675
Mean	26.75	Adj R-Squared	0.9422
C.V. %	3.85	Pred R-Squared	0.8611
PRESS	40.66	Adeq Precision	21.533
-2 Log Likelihood	38.4	BIC	61.07
		AICc	72.4

The Model is significant with an F-value of 38.23. And there is onlya 0.01% chance that an F-value this large could occur due to noise.Values of "Prob > F" less than 0.0500 indicate model terms are significant.In this case A, B, C, AB, AC, A^2, C^2 are all significant model terms.Values greater than 0.1000 indicate the model terms are not significant.If there are many insignificant model terms (not counting those required to support hierarchy),model reduction may improve the model.

The "Lack of Fit F-value" of 1.18 implies the Lack of Fit is not significant relative to the pureerror. There is a 44.86% chance that a "Lack of Fit F-value" this large could occur dueto noise. While non-significant lack of fit is good because it means the model would fit.

The F-values of the independent variables (sequestrantconcentration,sequestration time, flow rate of sequestrant) were estimated as 69.71, 16.79, and8.12 respectively, showing that the single effects ofthe independent variablesare significantly high on the response (CO_2 composition of the exit flue gas stream). The CV called coefficient of variation which is defined as the ratio of the standard deviation of estimate to the mean value of the observed response is independent of the unit. It is also a measure of reproducibility and repeatability of the models (Chen *et al.,* 2010; Chen *et al.,* 2011). The calculations indicated the CV value of 3.85% which illustrated that the model can be considered reasonably reproducible (because its CV was not greater than 10%), (Chen et al., 2011). The signal to noise ratio which is given as the value of the adequacy precision is 21.533. This indicates that an adequate relationship of signal to noise ratio exists and model can be used to navigate the design space.

The selected models in terms of the coded and actual values are given in the equations 4.1 and 4.2.

$$CO_2 = 28.82 - 3.037A - 1.490B - 1.036C + 4.5618AC + 1.317A^2 - 1.149B^2 - 4.557C^2 \quad (4.1)$$

$$CO = 5.729 - 0.685A - 0.187B - 0.125C + 0.205AB + 0.820AC - 0.241B^2 - 0.621C^2 \quad (4.2)$$

The equation in terms of coded factors can be used to make predictions about the response forgiven levels of each factor. By default, the high levels of the factors are coded as +1 and thelow levels of the factors are coded as -1. The coded equation is useful for identifying therelative impact of the factors by comparing the factor coefficients.

In terms of Actual values, the model terms are given by equations 4.3 and 4.4;

$$CO_2 = -186.667 - 20.79888^{*}A + 0.10158^{*}B + 2.69274^{*}C + 0.07299A^{*}C + 0.21075^{*}A^2 - 0.010184^{*}B^2 - 7.29E^{-3\,*}C^2 \quad (4.3)$$

$$CO = -18.68163 - 3.31765^{*}A - 0.024761^{*}B + 0.34395^{*}C + 0.00772A^{*}B + 0.01312A^{*}C - 0.00214^{*}B^2 - 0.000994^{*}C^2 \quad (4.4)$$

The equation in terms of actual factors can be used to make predictions about the response for given levels of each factor. Here, the levels are specified in the original units for each factor. This equation should not be used to determine the relative impact of each factor because the coefficients are scaled to accommodate the units of each factor and the intercept is not at the centre of the design space.

The response values obtained by inserting the independent values are the predicted values of the model. These values are compared to the actual and experimental values. The result of this comparison is shown in the figures 4.1 and 4.2.

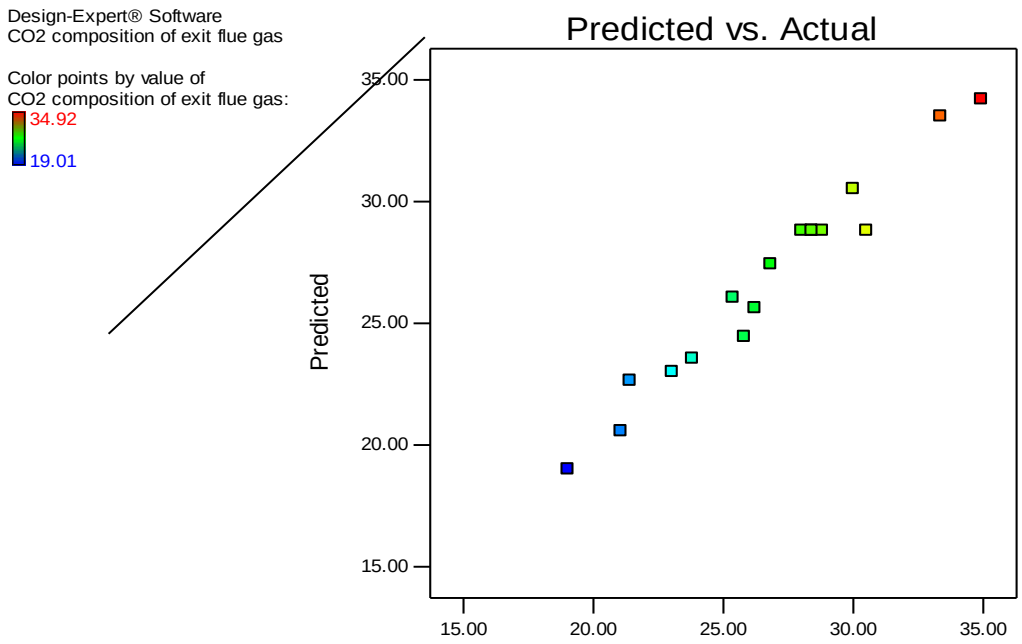

Figure4.1: Linear correlation between predicted vs. actual values for effect of CO_2 reduction using SDA leachate

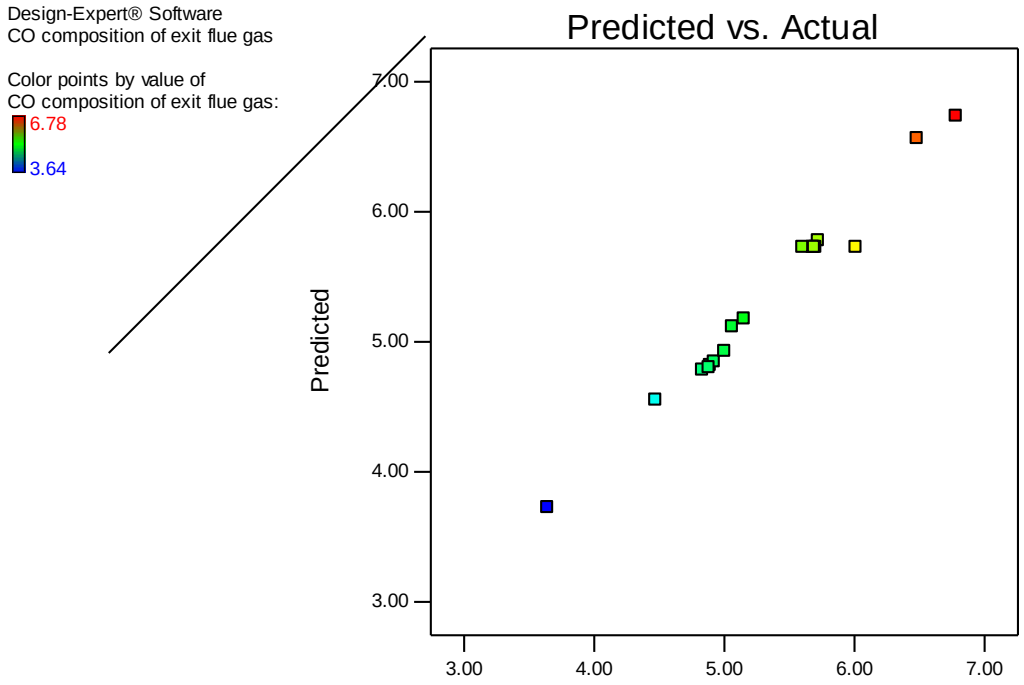

Figure4.2: Linear correlation between predicted vs. actual values foreffect of CO reduction using SDA leachate

From Figures 4.1 and 4.2, it can be seen that the actual values were relatively distributed near to the predicted value lineshowing that there is a good correlation between the actual values and the

predicted values. This observation shows that thecentral composite design (CCD) is well fitted for the developed model and can be used to perform the optimisation for the process.

3D surface and interaction plots

In order to visualize the relationship between the experimental variables and the response, and to study individual and interaction effects of the three factors consisting of the SDA leachate concentration, sequestration time, and flowrate of sequestrant, response surfaces and interaction plots were generated from the quadratic model, as shown in figures 4.3 – 4.8. These figures illustrate the response of different experimental variables and can be used to identify the major interactions between the variables.

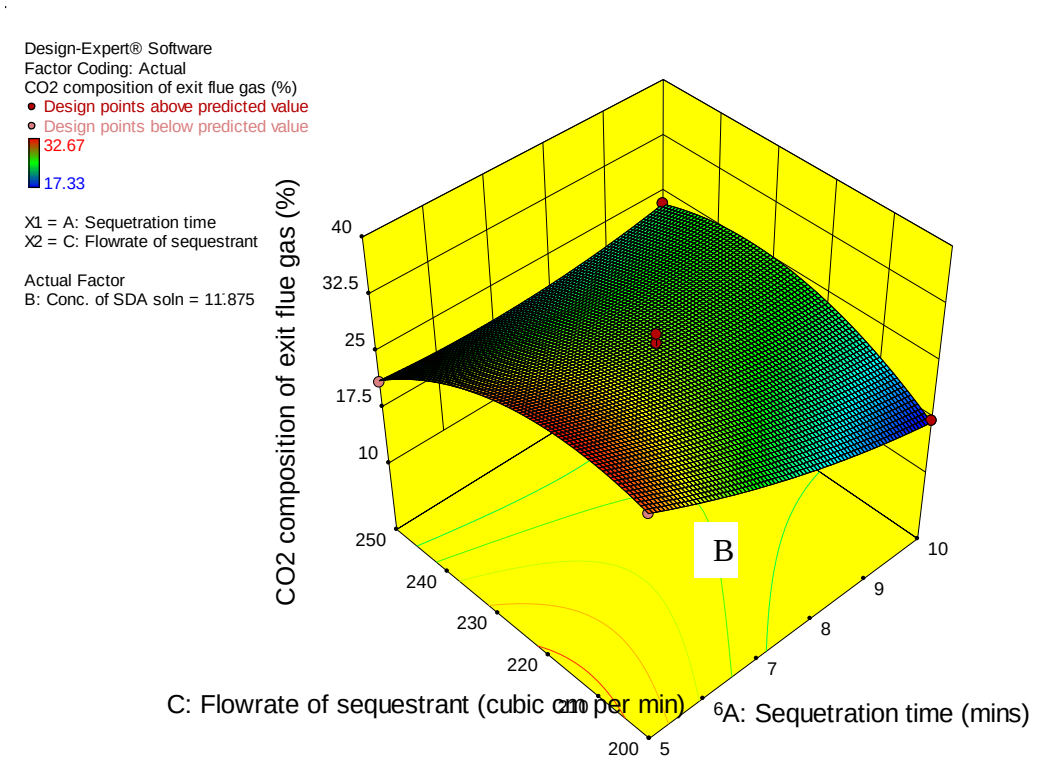

Figure4.3: Surface Response Plot (SDA Leachate) – Using Sequestration time (B, mins)and Flow Rate of Sequestrant (C, cubic cm) as Factors, with 'CO_2 Composition of Exit Flue Gas' as Response

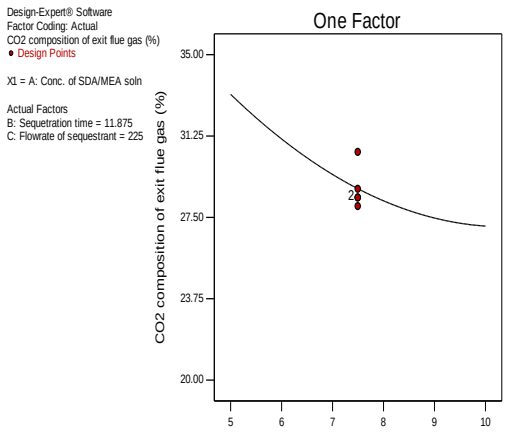

Figure4.4: One Factor plot of CO_2 comp. against sequestration time

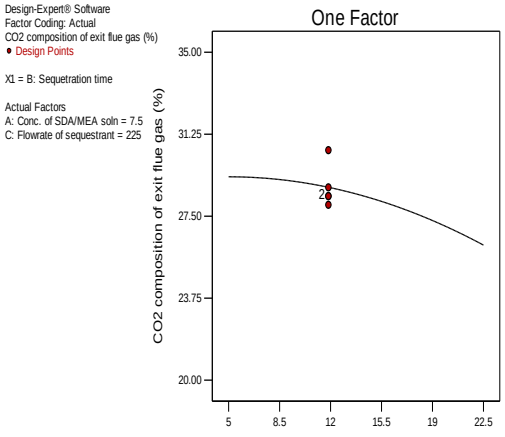

Figure4.5: One Factor plot of CO_2 comp. against concentration of SDA Leachate

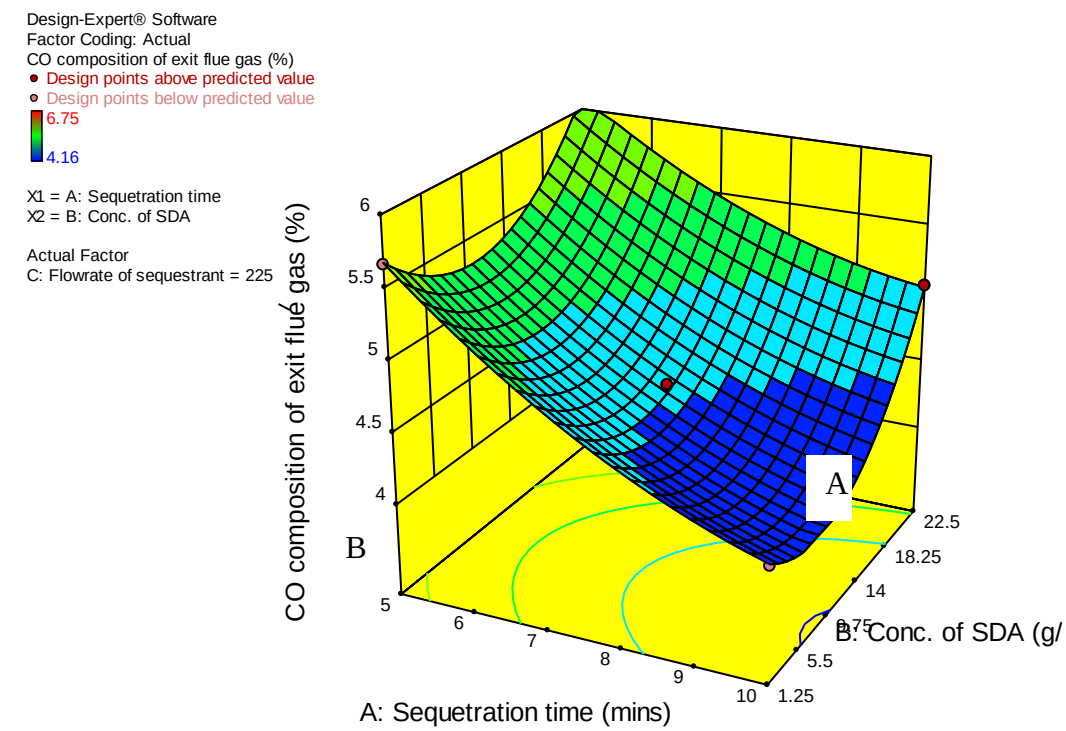

Figure4.6: Surface Response Plot (SDA Leachate) – Using Concentration of SDA Leachate (A, g/L) and Sequestration time (B, mins) as Factors, with 'CO Composition of Exit Flue Gas' as Response

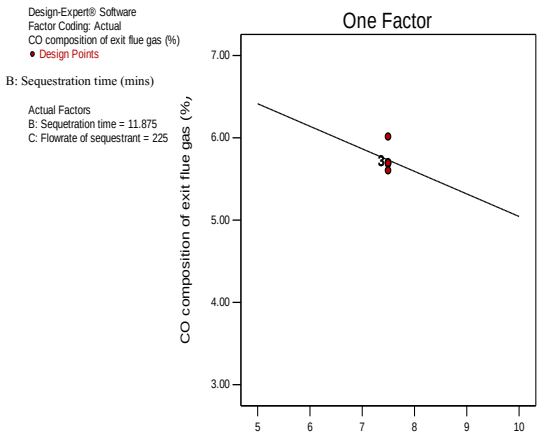

Figure4.7: One Factor plot of CO comp. against sequestration time

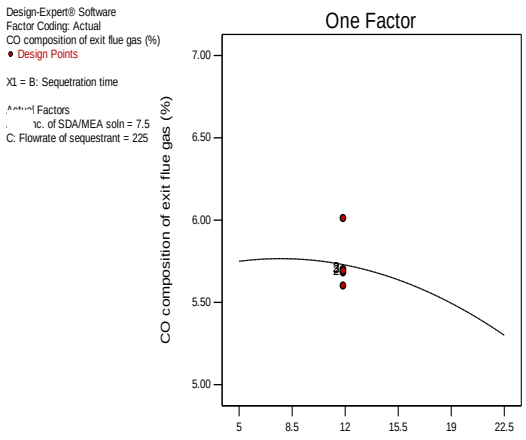

Figure4.8: One Factor plot of CO comp. concentration of SDA Leachate

Figures4.3 to 4.8 show the 3D plot and its corresponding interactions for the effects of SDA leachateconcentration on composition ofCO_2 and CO in the exit flue gas stream. The graphs show that the least recorded value for $CO_2$and CO in the exit streams occur between 16.8g/L and 11.6g/L SDA Leachate concentration, which is in accordance with the model. As the SDA leachate concentration is increased from 8.3g/L to 15.4g/L, the amount of CO_2 in the exit stream steadily decreases from 21.68% to 20.26% as seen in figure 4.5. This is similar to the report of several researchers (Moser et al., 2009) who agree that increase in sequestrant concentration results in decrease in CO_2 and CO composition of the exit flue gas stream. A similar trend was observed in the measurement of CO in the exit flue gas stream as seen figure 4.8.

It is evident that the SDA Leachate concentration has a significant effect on the response. Increasing the SDA Leachate concentration beyond 18.5g/L at all levels of sequestration time results in the increase of CO_2 and CO composition of the exit flue gas stream. As expected, the CO_2 and CO levels decreased linearly with increase in sequestration time (figures 4.4 and 4.7). This effect is independent of the SDA Leachate concentration as seen on the 3D plots of figures4.3 and 4.6.

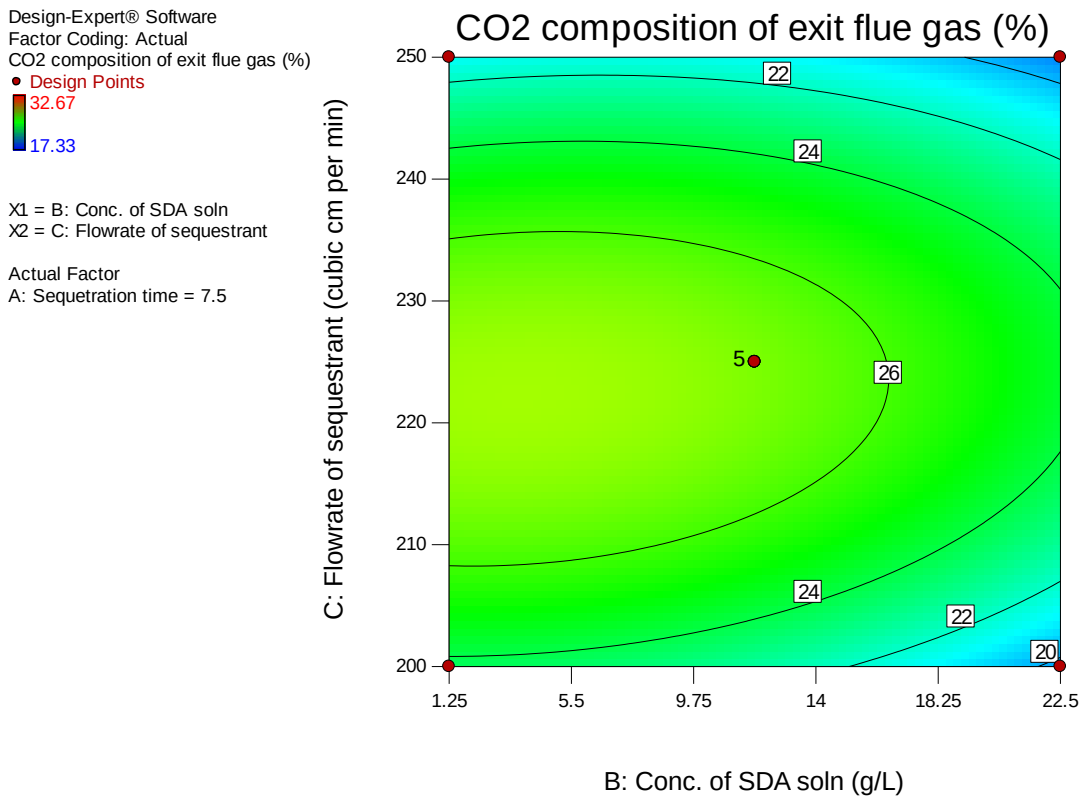

Figure 4.9: 2D contour plot for the effect of sequestrant flowrate and conc. of SDA leachate on CO_2composition of exit flue gas

The effect of sequestrant flowrate and sequestration time on the CO_2composition of exit flue gas is shown on the 2D contour plot of fig. 4.9.

This process was carried out at sequestration time of 7.5 minutes. The lowest CO_2composition of the exit flue gas is found to be 24% at SDA flowrate of 223cubic centimeters per minute and 22.5g/L SDA concentration. Between 225 - 250 cm^3/min sequestrant flowrate, at all values of SDA leachate concentration, the flue gas CO_2 composition decreased steadily as seen on isolines of the 2D contour plot. The decrease in CO_2composition of the exit flue gas is associated with its consequent dissolution in the SDA leachate and the subsequent affinity for the calcium ions in the leachate. At higher values of sequestrant flowrate (230 cm^3/min - 250 cm^3/min), the flue gas CO_2 composition decreased steadily from 26 - 22% at 7.5g/L SDA leachate concentration.

This decrease can be attributed to the improved interaction of the dissolved CO_2 with the ions in leachate, due to increased flow.

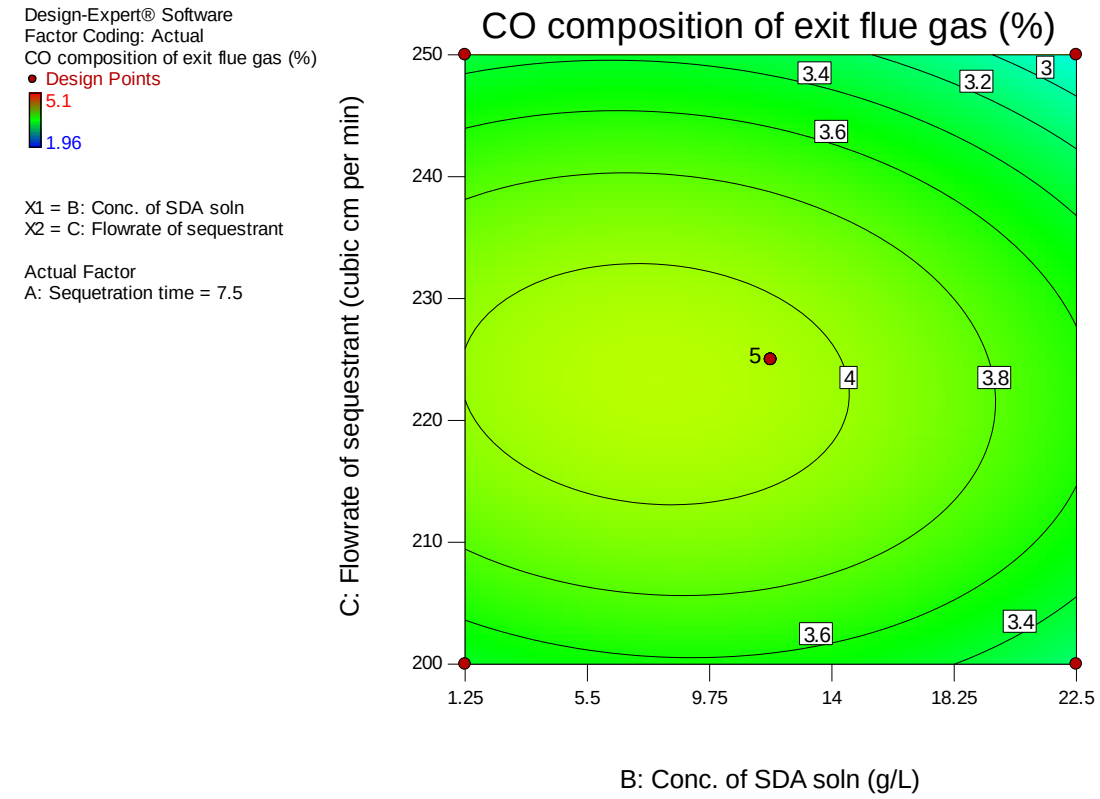

Figure 4.10: 2D contour plot for the effect of sequestrant flowrate and conc. of SDA leachate on CO composition of exit flue gas

The effect of sequestrant flowrate and sequestration time on the CO composition of exit flue gas is shown on the 2D contour plot of fig. 4.10.

The sequestration was carried out at sequestration time of 7.5 minutes. The exit flue gas CO compsition is seen to decrease steadily with increasing sequestrant flowrate from 200 - 225 cm^3/min, where the lowest value of 3.6% CO is recorded. Beyond 225 cm^3/min, the amount of CO captured in the exit stream begins to increase steadily with increasing sequestrant flowrate. This trend is observed for all values of SDA leachate concentrations. However, the lowest value of 3.6% for CO composition of exit flue gas was recorded at sequestration time of 22.5g/L and 225 cm^3/min flowrate. It is good to

note that the decrease in the composition of exit flue gas with corresponding decrease in flowrate is as a result of an enhanced interaction created which further enhances the capture process.

Optimisation

The tables 4.12 and 4.13 outline the contraints and solutions for the optimisation results of the sequestration with SDA leachate.

Table 4.12: Optimisation Contraints Values for Factors and Responses

Name	Goal	Lower Limit	Upper Limit	Lower Weight	Upper Weight	Importance
A: Conc. of SDA leahate	is in range	1.25	22.5	1	1	3
B:Sequetration time	is in range	5	10	1	1	3
C:Flowrate of sequestrant	is in range	200	250	1	1	3
CO_2 composition of exit flue gas	minimize	19.01	34.92	1	1	3
CO composition of exit flue gas	minimize	3.64	6.78	1	1	3

Table 4.13: Optimisation Solutions Values for Factors and Responses

Number	Conc. of SDA leahate	Sequetration time	Flowrate of sequestrant	CO_2 composition of exit flue gas	CO composition of exit flue gas	Desirability
1	21.795	9.997	200.278	16.768	3.557	1 Selected
2	19.694	9.997	200.022	17.315	3.614	1
3	22.180	9.929	201.046	17.148	3.634	1
4	19.444	9.989	200.198	17.493	3.639	1
5	22.346	9.929	201.159	17.143	3.635	1
6	20.427	9.973	200.195	17.225	3.616	1
7	21.130	9.959	200.479	17.166	3.619	1
8	20.640	9.950	200.269	17.239	3.626	1

From table 4.13, the obtained and selected optimum values for the sequestration with SDA leachate have CO_2 and CO composition of exit flue gas values of 16.768% and 3.557% as optima (i.e minima) respectively, at sequestrant concentration of 21.795g/L, sequestration time of 9.997mins and sequestrant flow rate of 200.278cm^3/min respectively.

4.3.2 MEA Solution – 'CO_2 and CO Composition of Exit Flue Gas' as Response

Table 4.14: Results of Experimental Runs recoded for MEA Solution

		Factor 1	Factor 2	Factor 3	Response 1	Response 2
Std	Run	A: Conc. of MEA soln	B: Sequestration time	C: Flowrate of sequestrant	CO_2 composition of exit flue gas	CO composition of exit flue gas
		g/L	Mins	cubic cm per min	%	%
1	9	1.25	5	225	23.56	5.67
2	2	22.5	5	225	19.26	4.16
3	5	1.25	10	225	28.31	6.12
4	1	22.5	10	225	19.77	5.07
5	3	1.25	7.5	200	27.22	5.98
6	14	22.5	7.5	200	20.61	4.90
7	15	1.25	7.5	250	29.79	6.52
8	4	22.5	7.5	250	21.35	5.04
9	8	11.875	5	200	23.25	5.73
10	16	11.875	10	200	24.54	5.83
11	7	11.875	5	250	24.28	5.59
12	17	11.875	10	250	29.38	6.75
13	10	11.875	7.5	225	21.60	4.48
14	6	11.875	7.5	225	22.01	4.51
15	13	11.875	7.5	225	21.80	4.58
16	11	11.875	7.5	225	22.01	4.59
17	12	11.875	7.5	225	19.99	4.48

The responses obtained from different experimental runs carried out by combinations of the three variables unique to each of the runs are tabulated on the response columns of table4.14. The three experimental variable interactions gave a total of 12distinct runs and 5 centre points. The

responses obtained from various runs are significantly exceptional which implies that each of the factors have substantial effect on the response.

Table 4.15: Fit Summary Table (MEA Solution)

	Sequential	Lack of Fit	Adjusted	Predicted	
Source	**p-value**	**p-value**	**R-Squared**	**R-Squared**	
Linear	0.0013	0.0291	0.6177	0.4691	
2FI	0.6107	0.0208	0.5823	0.1543	
Quadratic	**0.0006**	**0.5855**	**0.9434**	**0.8347**	**Suggested**
Cubic	0.5855		0.936		

Table 4.16:Lack of Fit Test (MEA Solution)

	Sum of		Mean	F	p-value	
Source	**Squares**	**Df**	**Square**	**Value**	**Prob > F**	
Linear	53.33	9	5.93	8.18	0.0291	
2FI	44.36	6	7.39	10.2	0.0208	
Quadratic	**1.59**	**3**	**0.53**	**0.73**	**0.5855**	**Suggested**
Cubic	0	0				
Pure Error	2.9	4	0.72			

Table 4.17:Model Summary Statistics (MEA Solution)

	Std.		Adjusted	Predicted		
Source	**Dev.**	**R-Squared**	**R-Squared**	**R-Squared**	**PRESS**	
Linear	2.08	0.6894	0.6177	0.4691	96.12	
2FI	2.17	0.739	0.5823	0.1543	153.11	
Quadratic	**0.8**	**0.9752**	**0.9434**	**0.8347**	**29.93**	**Suggested**
Cubic	0.85	0.984	0.936		+	

DF = degree of freedom

CV = Coefficient of variance

PRESS = Predicted residual sum of squares

ANOVA Analysis and Model Fitting

The F-value tests were performed using analysis of variance (ANOVA) to calculate the significance of each type of model. Based on the results of F-value, the highest order model with significant terms which shows the relationship between parameters well and normally would be chosen.

The adequacy of the models was evaluated by applying the lack-of-fit test. This test is used in the numerator in an F-test of the null hypothesis and indicates that a proposed model fits well or not. The test for lack-of-fit compares the variation around the model with pure variation within replicated observations. This test measured the adequacy of the different models based on response surface analysis (Lee *et al.,* 2006). As shown in Table 4.16there was a significant difference (F-value = 53.33 and 44.36) lack of fit for Linear and 2FI models. However, the test was not significant (F-value = 1.59 and 0.000) for quadratic and cubic models respectively. The significant results of lack of fit for linear and 2FImodels showed that these models are not adequate for predicting the CO_2 composition of the exit gas.Apart from the F-value and the lack of fit, the R-squared, adjusted R-squared and the predicted R-squared values for the quadratic model produced a high value of 0.9752, 0.9434, 0.8347 respectively when compared to other models (2FI, linear, and cubic) as shown on table 4.17. The measure of how efficient the variability in the actual response values can be explained by the experimental variables and their interactions is given by the R-Squared value. The closer the R^2 value is to unity, the better the model predicts the response. Adjusted-R^2 is a measure of the amount of variation around the mean explained by the model, adjusted for the number of terms in the model. The adjusted-R^2decreases as the number of terms in the model increases, if those additional terms don't add value to the model. Predicted-R^2 is a measure of the amount of variation in new data explained by the model. The predicted-R^2 and the adjusted-R^2 should be within 0.20 of each other. Otherwise there may be a problem with either the data or the model, (Taran and Aghaie, 2015).

Based on these results, the effect of each parameter was evaluated using quadratic model as shown in Table 4.18.

Table 4.18:ANOVA for Response Surface Quadratic model(MEA Solution)

Source	Sum of Squares	Df	Mean Square	F Value	p-value Prob > F	
Model	176.55	9	19.62	30.61	< 0.0001	significant
A-Conc. of MEA soln	16.96	1	16.96	26.46	0.0013	
B-Sequestration time	97.3	1	97.3	151.83	< 0.0001	
C-Flowrate of sequestrant	10.55	1	10.55	16.47	0.0048	
AB	4.51	1	4.51	7.03	0.0329	
AC	3.63	1	3.63	5.67	0.0489	
BC	0.83	1	0.83	1.29	0.2928	
A^2	3.65	1	3.65	5.7	0.0484	
B^2	0.42	1	0.42	0.65	0.4468	
C^2	36.6	1	36.6	57.11	0.0001	
Residual	4.49	7	0.64			
Lack of Fit	1.59	3	0.53	0.73	0.5855	not significant
Pure Error	2.9	4	0.72			
Cor Total	181.04	16				

From the table 4.18, it could be seen that the Model F-value of 30.61 implies the model is significant. There is onlya 0.01% chance that an F-value this large could occur due to noise.Values of "Prob > F" less than 0.0500 indicate model terms are significant.In this case A, B, C, AB, AC, A^2, C^2 are significant model terms.Values greater than 0.1000 indicate the model terms are not significant.If there are many insignificant model terms (not counting those required to support hierarchy),model reduction may improve your model.

The "Lack of Fit F-value" of 0.73 implies the Lack of Fit is not significant relative to the pureerror. There is a 58.55% chance that a "Lack of Fit F-value" this large could occur dueto noise. Non-significant lack of fit is good because we want the model to fit.The insignificant model terms could be eliminated to improve the model efficiency. Using backward elimination model with alpha to exit term equal to 0.100, the insignificant model terms were eliminated from the ANOVA terms.

After removing the insignificant model terms, the reduced quadratic model was obtained as shown in Table 4.19.

Table 4.19: ANOVA for Reduced Response Surface Quadratic model(MEA Solution)

Source	**Sum of Squares**	**Df**	**Mean Square**	**F Value**	**p-value Prob > F**	
Model	175.31	7	25.04	39.33	< 0.0001	significant
A-Conc. of MEA solution	16.96	1	16.96	26.63	0.0006	
B-Sequetration time	97.3	1	97.3	152.8	< 0.0001	
C-Flowrate of sequestrant	10.55	1	10.55	16.57	0.0028	
AB	4.51	1	4.51	7.08	0.026	
AC	3.63	1	3.63	5.7	0.0407	
A^2	3.79	1	3.79	5.96	0.0373	
C^2	37.12	1	37.12	58.28	< 0.0001	
Residual	5.73	9	0.64			
Lack of Fit	2.83	5	0.57	0.78	0.6111	not significant
Pure Error	2.9	4	0.72			
Cor Total	181.04	16				

Std. Dev.	0.8	R-Squared	0.9683
Mean	23.46	Adj R-Squared	0.9437
C.V. %	3.4	Pred R-Squared	0.8877
PRESS	20.33	Adeq Precision	19.245
-2 Log Likelihood	29.76	BIC	52.43
		AICc	63.76

The Model F-value of 39.33 implies the model is significant. There is onlya 0.01% chance that an F-value this large could occur due to noise.Values of "Prob > F" less than 0.0500 indicate model terms are significant.In this case A, B, C, AB, AC, A^2, C^2 are significant model terms.Values greater than 0.1000 indicate the model terms are not significant.If there are many insignificant model terms (not counting those required to support hierarchy),model reduction may improve your model.

The "Lack of Fit F-value" of 0.78 implies the Lack of Fit is not significant relative to the pureerror. There is a 61.11% chance that a "Lack of Fit F-value" this large could occur dueto noise. Non-significant lack of fit is good because it means the model would fit.

The F-value of the independent variables (sequestrantconcentration,sequestration time, flow rate of sequestrant) was estimated as 26.63, 152.80, and16.57 respectively, showing that the single effects ofthe independent variablesare significantly high on the response (CO_2 composition of the exit flue gas stream). The CV called coefficient of variation which is defined as the ratio of the standard deviation of estimate to the mean value of the observed response is independent of the unit. It is also a measure of reproducibility and repeatability of the models (Chen *et al.,* 2010; Chen *et al.,* 2011). The calculations indicated the CV value of 3.4% which illustrated that the model can be considered reasonably reproducible (because its CV was not greater than 10%) (Chen et al., 2011). The signal to noise ratio which is given as the value of the adequacy precision is 19.245. This indicates that an adequate relationship of signal to noise ratio exists and model can be used to navigate the design space.

The selected models in terms of the coded and actual values are given in the equations 4.5 and 4.6:

$$CO_2 = 21.61 + 1.46A - 3.49B + 1.15C - 1.06AB + 0.95AC + 0.95A^2 + 2.96C^2 \quad (4.5)$$

$$CO = 4.528 + 0.3275A - 0.64B + 0.1825C + 0.115AB + 0.265AC - 0.100BC + 0.546A^2 + 0.181B^2 + 0.901C^2 \quad (4.6)$$

The equation in terms of coded factors can be used to make predictions about the response forgiven levels of each factor. By default, the high levels of the factors are coded as +1 and thelow levels of the factors are coded as -1. The coded equation is useful for identifying therelative impact of the factors by comparing the factor coefficients.

In terms of Actual values, the model terms are given by;

$$CO_2 = 281.66 - 4.65^{*}A - 0.0285^{*}B - 2.2031^{*}C + 0.648A^{*}B + 0.01524A^{*}C + 0.1517^{*}A^2 + 0.00474^{*}C^2 \quad (4.7)$$

$$CO = 87.27409 - 2.184812^{*}A - 0.04608^{*}B - 0.66875^{*}C + 0.004329A^{*}B + 0.00424A^{*}C - 0.000376B^{*}C + 0.08736^{*}A^2 + 0.001603^{*}B^2 + 0.001442^{*}C^2 \quad (4.8)$$

The equation in terms of actual factors can be used to make predictions about the response for given levels of each factor. Here, the levels have been specified in the original units for each factor. This equation should not be used to determine the relative impact of each factor because the coefficients are scaled to accommodate the units of each factor and the intercept is not at the centre of the design space.

The response values obtained by inserting the independent values are the predicted values of the model. These values are compared to the actual and experimental values. The result of this comparison is shown in the figures 4.11 and 4.12.

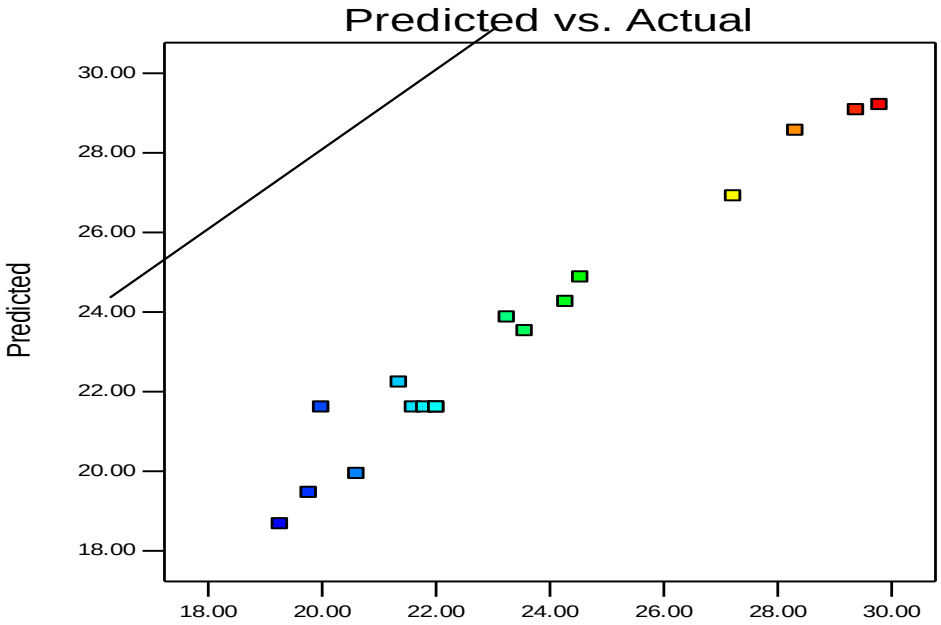

Figure4.11: Linear correlation between predicted vs. actual values for effect of CO_2 reduction using MEA solution

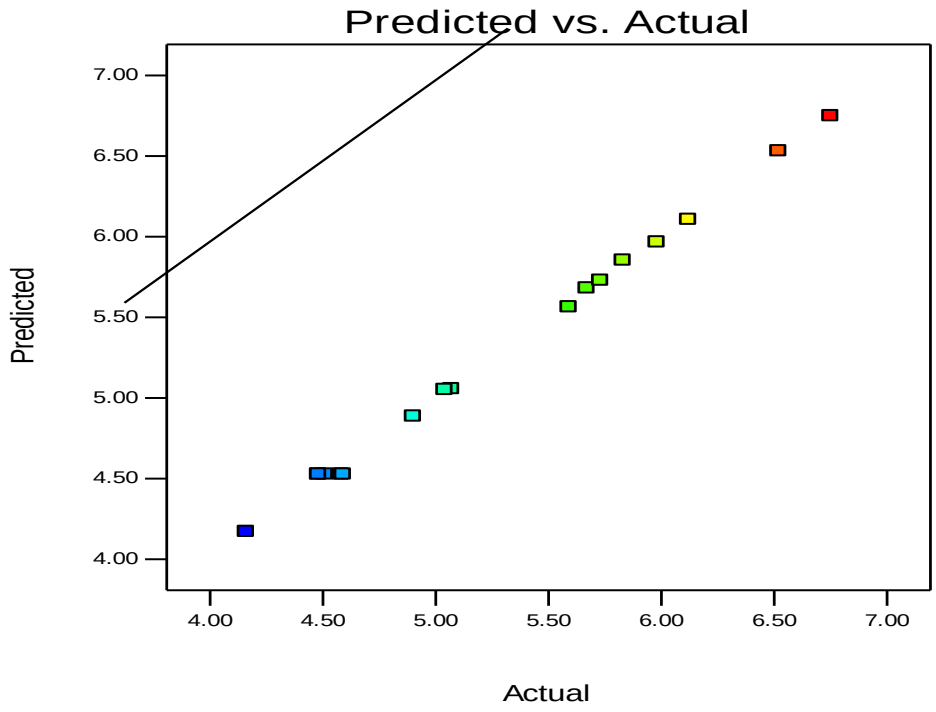

Figure4.12: Linear correlation between predicted vs. actual values foreffect of CO reduction using MEA solution

As it can be seen in Figures 4.11 and 4.12, the actual values were distributed relatively near to the predicted value line, showing that there is a good correlation between the actual and the predicted values. This observation shows that thecentral composite design (CCD) is well fitted into the model and thus can be used to perform the optimisation operation for the process.

3D surface and interaction plots

In order to visualize the relationship between the experimental variables and the response, and to study individual and interaction effects of the three factors consisting of the MEA conc., sequetration time, and flowrate of sequestrant. Response surfaces and interaction plots were generated from the quadratic model, as shown in figures 4.13 – 4.18. These figures illustrate the response of different experimental variables and can be used to identify the major interactions between the variables.

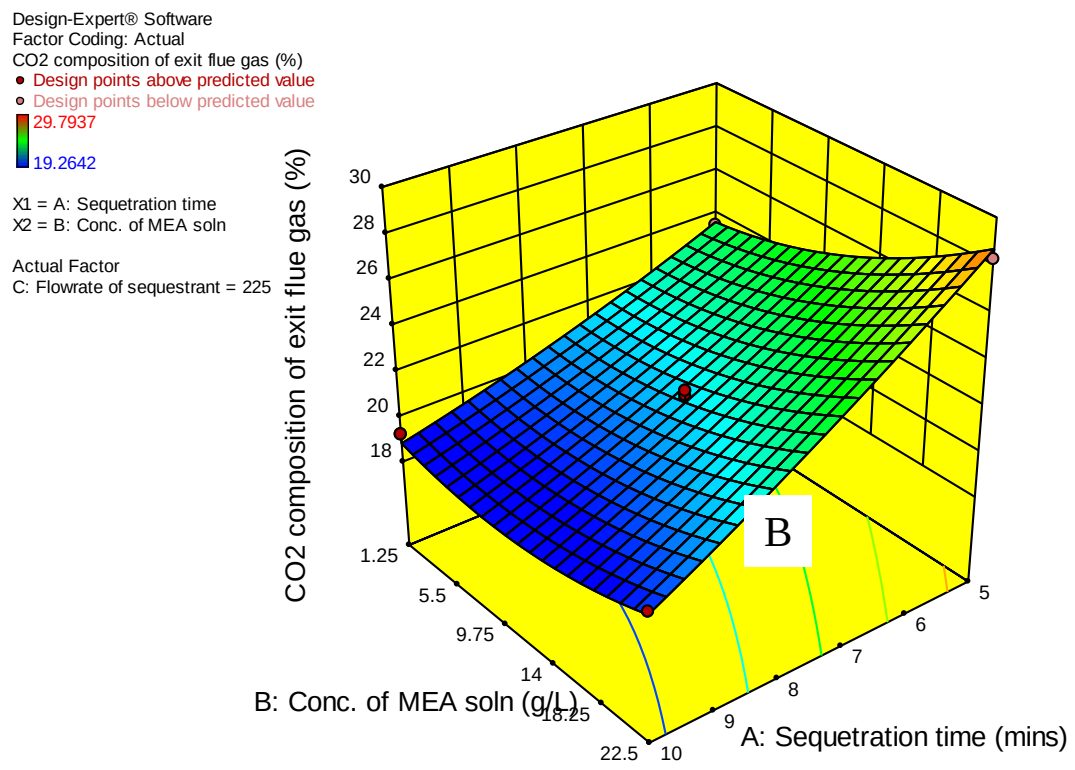

Figure4.13: Surface ¯ A ponse Plot (MEA Solution) – Using Concentration of MEA Solution (A, g/L) and Sequestration time (B, mins) as Factors, with ‘C B Composition of Exit Flue Gas’ as Response

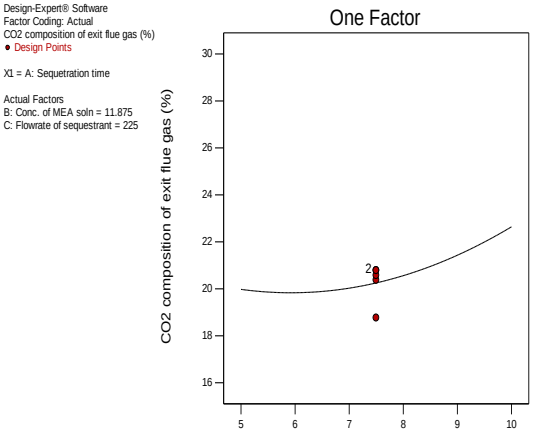

Figure 4.14: One Factor plot of CO_2 comp. against sequestration time

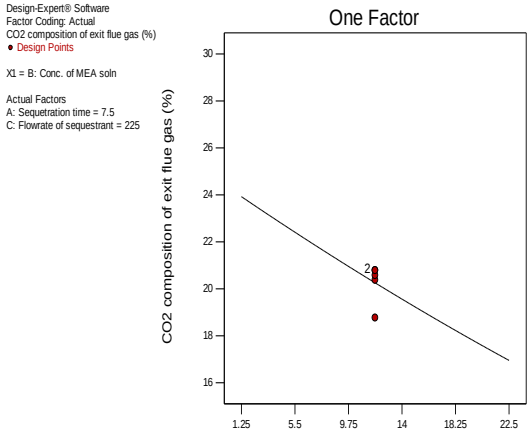

Figure4.15: One Factor plot of CO_2 comp. against concentration of MEA solution

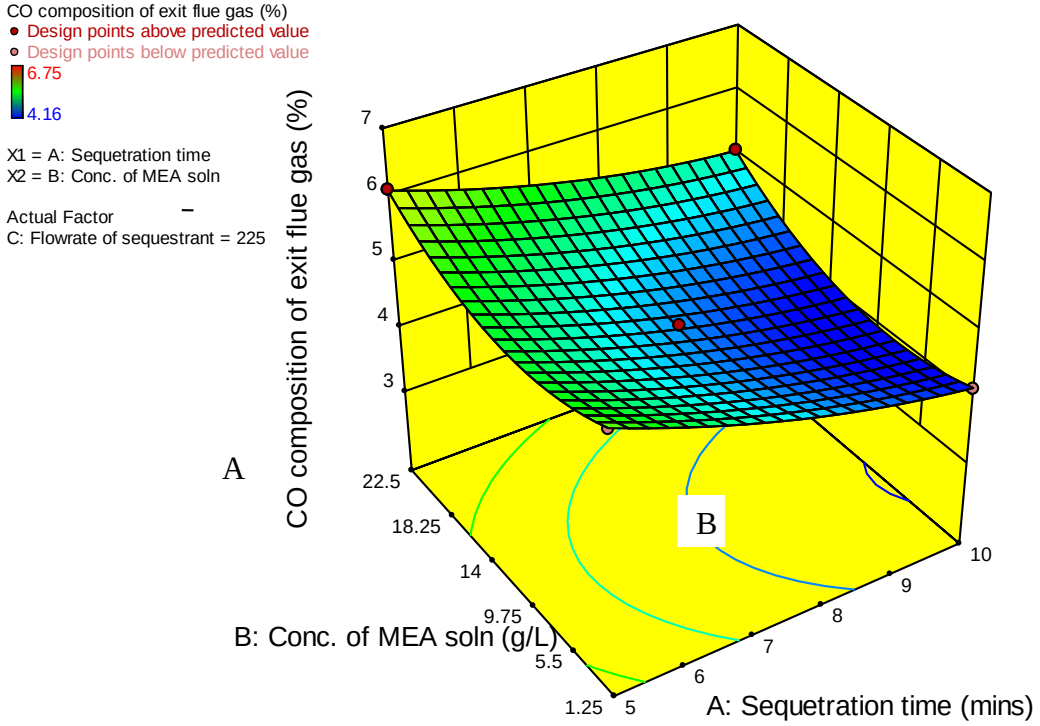

Figure 4.16: Surface Response Plot (MEA Solution) – Using Concentration of MEA Solution (A, g/L) and Sequestration time (B, mins) as Factors, with 'CO Composition of Exit Flue Gas' as Response

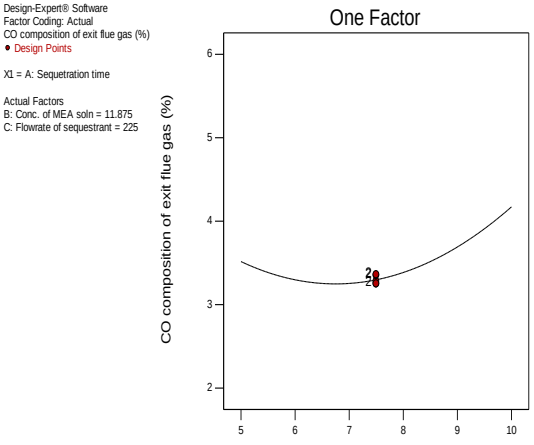

Figure4.17: One Factor plot of CO comp. against sequestration time

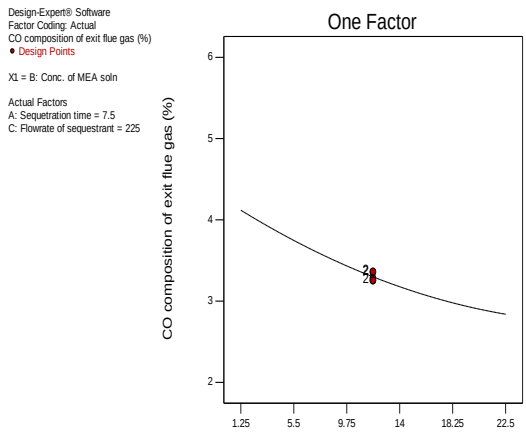

Figure4.18: One Factor plot of CO comp. against concentration of MEA solution

Figures4.13 to 4.18again show the 3D plot and its corresponding interactions for the effects of MEA concentration on composition ofCO_2 and CO in the exit flue gas stream. The graphs show that the least recorded value for $CO_2$and CO in the exit streams occur between 16.3g/L and 11.8g/L MEA concentration, which is in accordance with the model. As the MEA concentration is increased from 9.1g/L to 15.6g/L, the amount of CO_2 in the exit stream steadily decreases from 22.40% to 20.73% as seen in figure 4.15. This is similar to the report of several researchers (Moser et al., 2009) who agree that increase in MEA solution concentration results in decrease in CO_2 and CO composition of the exit flue gas stream. A similar trend was observed in the measurement of CO in the exit flue gas stream as seen figure 4.18.

It is evident that the MEA concentration has a significant effect on the response. Increasing the MEA concentration beyond 19.1g/L at all levels of sequestration time results in the increase of CO_2 and CO composition of the exit flue gas stream. As expected, the CO_2 and CO levels decreased linearly with increase in sequestration time (figures 4.14 and 4.17). This effect is independent of the MEA solution concentration as seen on the 3D plots of figures4.13 and 4.16.

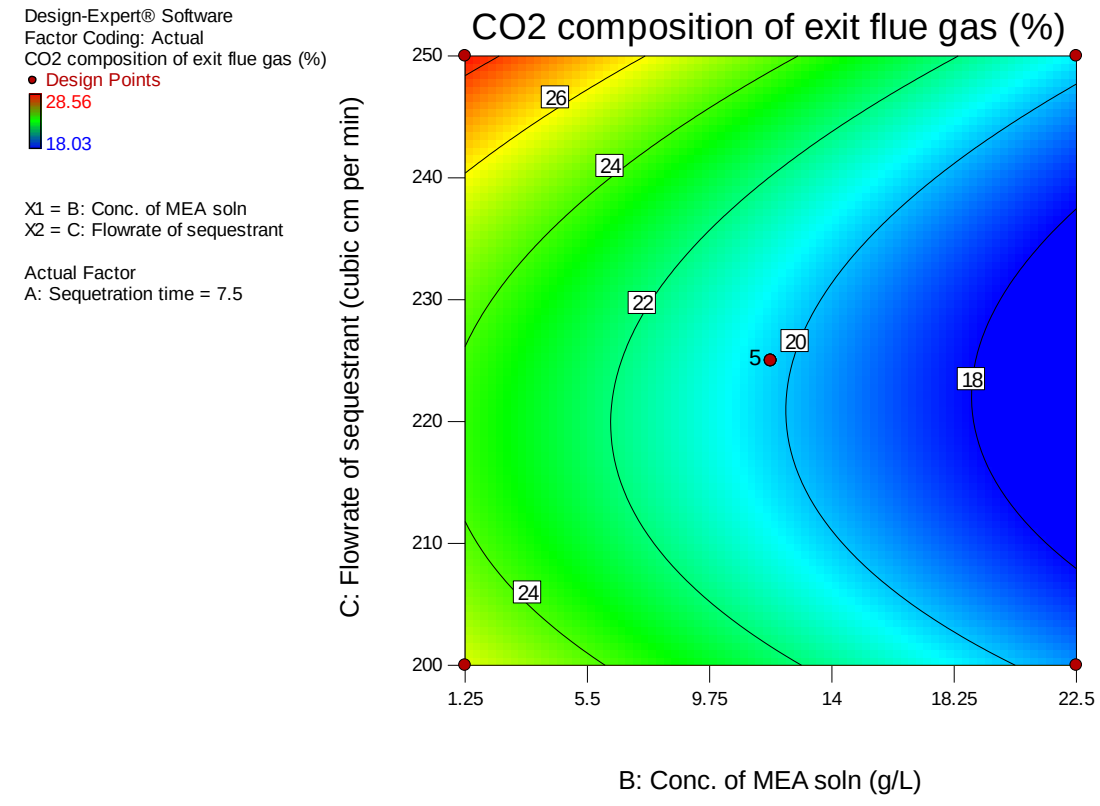

Figure 4.19: 2D contour plot for the effect of sequestrant flowrate and conc. of MEA solution on CO_2 composition of exit flue gas

The effect of MEA flowrate and sequestration time on the composition of $CO_2$of exit flue gas is shown on the 2D contour plot of fig. 4.19.

The process was carried out at sequestration time of 7.5 mins. The least CO_2composition of exit flue gas is found to be 18% at flowrate of 220 cubic centimeters per minute and 20g/L sequestrant concentration. Between 200 - 220 cm3/min flowrate, at all values of MEA concentration, the CO_2 composition decreased steadily as seen on isolines of the 2D contour plot. The decrease in CO_2composition of exit flue gas is associated with the the great affinity of the dissolved $CO_2$with the sequestrant. At higher values of flowrate (230cm^3/min - 250cm^3/min), the CO_2 composition increased steadily from 22 - 26% at 7.5 g/L MEA concentration. This increase can be attributed to insufficient interaction as a result of high turbulence due to increased flow rate.

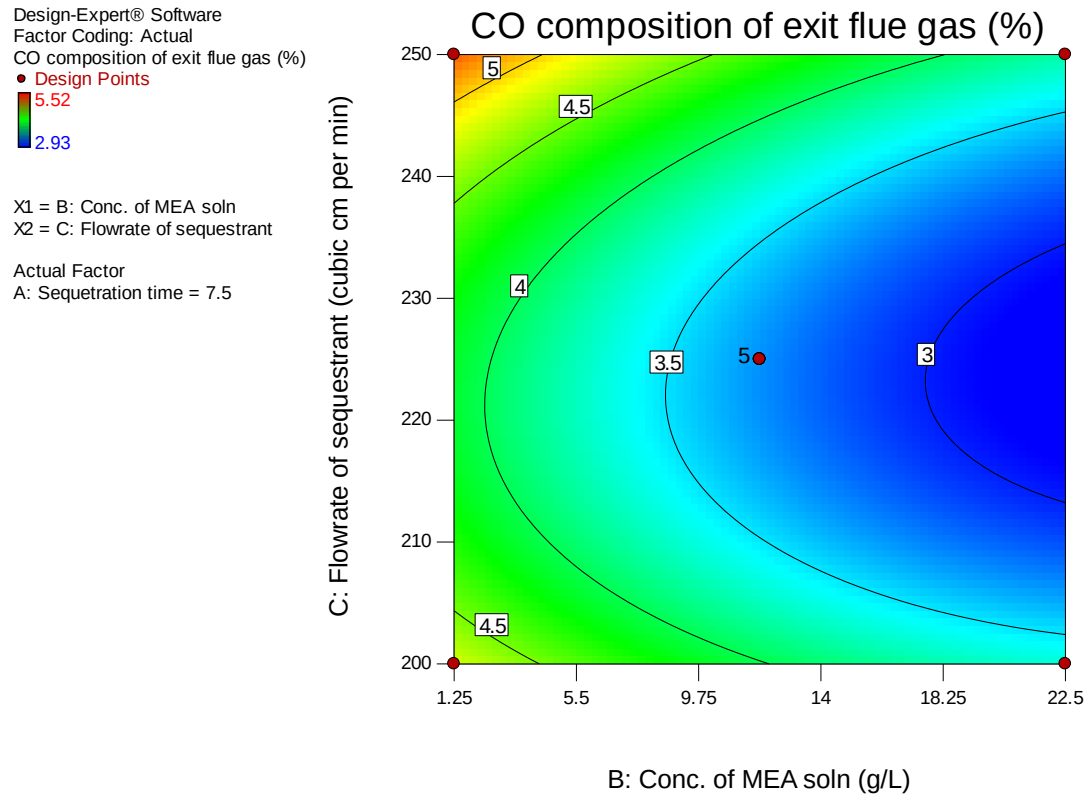

Figure 4.20: 2D contour plot for the effect of sequestrant flowrate and conc. of MEA solution on CO composition of exit flue gas

The effect of sequestrant flowrate and concentration of MEA on the CO composition of exit flue gas is shown on the 2D contour plot of fig. 4.20.

This process was carried out at sequestration time of 7.5 minutes. The least CO composition ofthe exit flue gas stream is found to be 3% at flowrate of 220 cubic centimeters per minute and 21g/LMEA concentration. Between 200 - 222cm^3/min flowrate, at all values of MEA concentration, the CO composition decreased steadily as seen on isolines of the 2D contour plot. At higher values of flowrate (225cm^3/min - 250cm^3/min) the CO composition increased steadily from 3.0 - 4.5% at 7.5 g/L MEA concentration. This increase can also be attributed to same reason as aforementioned in the case of CO_2.

Optimisation

Tables 4.20 and 4.21 outline the contraints and solutions for the optimisation results of the sequestration with MEA solution.

Table 4.20: Optimisation Contraints Values for Factors and Responses

Name	Goal	Lower Limit	Upper Limit	Lower Weight	Upper Weight	Importance
A: Conc. of MEA solution	is in range	1.25	22.5	1	1	3
B:Sequetration time	is in range	5	10	1	1	3
C:Flowrate of sequestrant	is in range	200	250	1	1	3
CO_2 composition of exit flue gas	minimize	19.2642	29.7937	1	1	3
CO composition of exit flue gas	minimize	4.16	6.75	1	1	3

Table 4.21: Optimisation Solutions Values for Factors and Responses

Number	Conc. of MEA	Sequestration time	Flowrate of sequestrant	CO_2 composition of exit flue gas	CO composition of exit flue gas	Desirability
1	20.044	5.666	223.721	18.959	4.139	1 Selected
2	21.101	6.521	223.848	18.493	4.027	1
3	21.615	6.319	222.546	18.361	4.023	1
4	18.958	6.500	221.667	19.092	4.122	1
5	20.17	6.638	216.988	18.830	4.148	1
6	21.615	6.319	227.454	18.498	4.016	1
7	22.146	5.417	229.167	18.685	4.095	1
8	21.709	5.267	223.415	18.713	4.152	1
9	20.028	6.834	218.681	18.798	4.120	1
10	21.069	7.262	222.064	18.470	4.078	1

Table 4.21 showsthe obtained and selected optimum values for the sequestration with MEA solution have CO_2 and CO composition of exit flue gas values of 18.959% and 4.139% as optima (i.e minima) respectively, at sequestrant concentration of 20.044g/L, sequestration time of 5.666mins and sequestrant flow rate of 223.848cm^3/min respectively.

CHAPTER FIVE

CONCLUSION AND RECOMMENDATIONS

5.1 Conclusion

There was more decrease in the CO_2 and CO composition of the flue gas during carbon sequestration with SDA leachate as compared to the MEA solution. The characterization showed that calcium ion was responsible for the sequestration due to its affinity for CO_2

Increasing the sequestrant concentration led to reduction in the CO_2 and CO compositions of the flue gas. However, concentration increase beyond 22.5g/L for SDA leachate proved impossible due to saw dust ash dissolution difficulty encountered in the process.

CO_2 and CO levels decreased linearly with increase in sequestration time while at higher values of sequestrant flowrate (230 cm^3/min - 250 cm^3/min), the flue gas CO_2 composition decreased steadily from 26 - 22% at 7.5g/L SDA leachate concentration. This decrease could be attributed to the improved interaction of the dissolved CO_2 with the ions in leachate, due to increased flow.

The optimization result showed about 8% reduction of flue gas better achieved by SDA leachate over conventional MEA under same working conditions. Central composite design was successfully used to model the carbon capture.

5.2 Recommendations

The following recommendations are put forward:

(1) More research should be geared towards regeneration of CO_2 from the CO_2 enriched leachate.

(2) Corrosion effect of use of SDA leachate as sequestrant in the absorber device can be worked upon in future work.

5.3 Contribution to knowledge

Findings from this research have added to existing knowledge in the following areas:

1) This research has establishedthat SDA leachate possess essential mineral that favors carbon sequestration. Equally, this has shown that SDA leachate is better than the conventional MEA for purpose of carbon sequestration.

2) The reaction mechanism of SDA with carbon dioxide was postulated and the kinetics obtained, which agreed with the experimentally determined rate law.
3) Models were also obtained for predicting carbon sequestration from flue gas. These models based on the operating conditions of the sequestration process can be used to predict the optimal conditions of the sequestration process.
4) A prototype absorber device was designed and fabricated.

REFERENCES

Aboudheir, A., Tontiwachwuthikul, P., Chakma, A. and Idem R. (2003). Kinetics of the reactive absorption of carbon dioxide in high CO_2 – loaded, concentrated aqueous monoethanolamine solutions. Chemical Engineering Science. Vol 58: pp 5195 – 5210.

Abu-Zahra, M., Feron, P., Jansens, P., Goetheer, E. (2009). New process concept for CO_2 post-combustion capture integrated with co-production of hydrogen. Internationa Journal of hydrogen energy. Vol.34., pp: 3992-4004.

Abu-Zahra, M., Niederer, J., Feron, P., Versteeg, G. (2007). CO_2 capture from power plants: Part II. A parametric study of the economical performance based on mono-ethanolamine. Int. J. GHG Con, 1 (2), 135-142.

Adėr, H.J. (2008). "Modeling", in Adėr, H.J. and Mellenbergh, G.J., Advising on Research Methodss: a consultant's companion, Huizen. The Netherlands: Johannes van Kessel Publishing, pp. 271-304.

Anderson, K,, Normann, F., Johnson, F. and Leckner, B. (2008). NO emission during oxy-fuel combustion of lignite.

Anderson, S. and Newell, R. (2004). Prospecs for carbon capture and storage technologies. Annual review of Environment and Resources. Volume 29, pp 109 – 142.

AOAC International (2016). Official methods of analysis. 20th Edition.

Arends, G.J., Donkersloot-Shouq, S.S. (1985). An overview of possible uses of sawdust. TOOL, Amsterdam, The Netherlands, pp197.

Aroonwilas, A. and Veawab, A.(2007). Integration of CO_2 capture unit using single and blended – amines into supercritical coal-fired power plants: implications for emission and energy management. International Journal of Greenhouse Gas control Vol 1: pp 143-150.

Aroonwilas, A. and Veawab, A. (2009). Integration of CO_2 capture unit using blended MEA-AMP solution into coal-fired power plants. Energy Procedia 1 (1) 4315 – 4321.

Aroonwilas, A., Veawab, A., Tontiwachwuthikul, P., Chakma, A. (2007). Performance and cost analysis for CO_2 capturefrom flue gas streams: absorption and regeneration aspects.In: *6th international conference on greenhouse gas controltechnologies*, Kyoto, Japan, 1-4 Oct 2002. Oxford, UK

Barker, D.J., Davison, J. and Turner, S. (2009). CO_2 capture in cement Industry. Energy procedia Vol.1 (1): pp 87 – 94.

Bausch, H. and Hartler, N. (1960). Determination of chip dimensions. Sven. Papperstidn. Vol. 63 (10): 319 – 326.

Bedell, S.A. (2009). Oxidative degradation mechanisms for amines in flue gas. Energy procedia Vol 1. Issue 1: pp 771 – 778.

Bergstrom, D., Israelsson, S., Ohman, M., Dahlqvistd, S.A., Gref, R., Boman, C. and Wasterlund, I. (2008). Effects of raw material particle size distribution on the characteristics of Scots pine sawdust fuel pellets. Fuel Process. Technol. 89 (12): 1324 – 1329.

Bishnoi, P. (2011). Experimental investigation of incipient equilibrium conditions for the formation of semi-clathrate hydrates from quaternary mixtures. Journal of Chemical Engineering Vol 21(1): pp 62- 69.

Bosoaga, A. and John, E. (2009). CO_2 capture technologies for cement industry. Energy procedia. Vol 1. Issue 1: pp 133 -140.

Bruder, P. and Svendsen, H.F. (2012). Capacity and kinetics of solvents for post-combustion CO_2 capture. Energy Procedia 23, 45 – 54.

Bublitz, W.J. and Yang, T.Y.. (1975). Pulping characteristics of scots pine sawdust fuel pellets. Fuel Process. Technol. 89(12): 1324 – 1329.

Caplow, M. (1968). Kinetics of carbamate formation and breakdown. Journal of the American Chemical Society. 90 (24), pp 6795 – 6803.

Chen, G.Q., Scholes, C.A., Stevens, G.W. and Kentish, S.E. (2010). Plasticization of Ultra – thin Polysulfone membranes by Carbon dioxide. Journal of membranes science Vol.46. No. 1: pp 208 – 214.

Chen, X.Y., Nik, O.G. and Kaliaguine, (2011). Amine- Functionalized Zeolite FAU/EMT – polyimide mixed matrix membranes for CO_2/CH_4 separation. Journal membrane Science.Vol.37.No 1: pp 468 – 478.

Cheng, S., Meisen, A., (1996). Predict amine solution properties accurately. Hydrocarbon

Chiao, C.H., Chen, J.L., Lan, C.R., Chen, S. and Hsu. H.W. (2011). Developments of CO_2 capture of storage technology. Taiwan power company perspective. Journal of sustainable Environment research, Vol 21:pp 1- 8.

Cullinane, J.T. and Rochelle, G.T. (2002). Carbon dioxide absorption with aqueous potassium carbonate promoted by Piperazine. Chemical Engineering. Science Vol. 59 (17): pp 3619 – 3630.

Cummings, R., Salazar, O. and Pelaez, F. (2007). Isolation and structure of platencion: a Fabtt and Fabf dual inhibitor with potent broad spectrum antibiotic activity. International Journal of Science Vol.46 (25): pp 4684 – 4688.

Danckwerts, P.V. (1970). Gas – liquid Reactions. McGraw – Hill, New York, U.S.A.

Davidson, R.M. (2007). *Post-combustion carbon capture from coal fired plants–solvent scrubbing*. CCC/125, UK, London,IEA Clean Coal Centre, pp58.

Davidson, R.M. (2009). *Post-combustion carbon capture–sold sorbents and membranes*. CCC/144, UK, London, IEAClean Coal Centre, pp 64.

Davidson, R.M. and Santos, S.O. (2007). *Oxyfuel combustion of pulverised coal*. CCC/168, UK, London, IEA Clean CoalCentre, pp 63.

Drew Shindell (2007). The Role of tropospheric ozone increases in 20th century climate change. Journal of Geophysics Research. Vol. (111). pp:342.

Epp, H. and Bathen, B. (2011). Comparison of membrane contractor and structured packings for CO_2 absorption. Energy procedia Vol 4: pp 1471 – 14 77.

Etiegni, L. and Mahler A.G. (1991). Physical and Chemical Characteristics of Wood Ash. *Resource Technology* 37:173-178.

Figueroa, D.J. and Rameshwar, D. (2008). Advances in CO_2 capture technology- The U.S Department of Energy's Carbon Sequestration program. International Journal of Greenhouse Gas control. Vol 2. Issue 1: pp 9- 20.

Gale, J. (2002). Overview of CO_2 emissions sources, potential, transport and geographical distribution of storage possibilities. Proceedings of the workshop on CO2 dioxide capture and storage, Regina, Canada, 18-21 November 2002, pp. 15-29.

Gielen, D.J. and Moriguchi, Y. (2003). Technological potentials for CO_2 emission reduction in the global iron and steel industry. *International Journal of Energy Technology and Policy*, 1(3), 229-249.

Goff, G.S., Rochelle, G.T. (2003). Oxidative degradation of aqueous monoethanolamine in CO_2 capture systems under absorber conditions. In: *6th international conference ongreenhouse gas control technologies*, Kyoto, Japan, 1-4. Oxford, UK, Elsevier Science, vol 1 pp115-119.

Hakkila, P. (1989) *Utilisation of Residual Forest Biomass.* (568 pp) Springer series in Wood Science -Springer Verlag, Berlin.

Herzog, H., Meldon, J., Hatton, A. (2009). *Advanced postcombustion capture*. Clean Air Task Force. Available at: web.mit.edu/mitei/docs/reports/herzog-meldon-hatton.pdf, pp 39.

Herzog, H.J. and Drake, E.M. (1996). Carbon dioxide recovery and disposal from large energy systems. Annual review of Energy and the Environment. Volume 21, pp 145 – 166.

Hikita, H. (2009) Absorption of carbon dioxide into aqueous sodium hydroxide and sodium bicarbonate solutions. The Chemical Engineering Journal. Vol. 11 (2): pp 120 – 123.

Huang, H., Campbell, A.G., Folk, R. and Mahler, R.L. (1992). Wood Ash as a Soil Additive and Liming Agent for Wheat: Field Studies. *Commum. Soil Sci. Plant Anal.* 12 (1&2):25-33.

IEO (2011). International Monetary Fund. Independent Evaluation Office Reports. 9781616351557/IEOREA2011001, 791 – 797.

Imai, N. (2003). Advanced solvent to capture CO_2 from flue gas. 2nd International forum on geological sequestration of CO_2 in deep, unmineable coal seams. *improve soil and tree condition in areas affected by air pollution.* National Swedish Environmental Protection Board, Report 518: 53-71.

Intergovernmental Panel on Climate Change (IPCC), (2005). Carbon dioxide capture and storage. Cambridge university press.

Isomaki, O. (1970). Research on the basic properties of sawdust. Pap Wood. 52 (9): 571 – 584.

Isotalo, I., Gottsching, L., Virkola, N.E. and Nordman L. (1964). The production of sawdust sulphate pulp and its use in printing paper manufacture I. Pap. Puu 46(3): 71 – 85.

Joshi, R.C., Bist, D.P.S., Jangalgi, N.R. and Kaul, S.S. (1982). Pulping studies on sawdust. Indian Pulp pap. 37(2): 12 – 19. Journal of Bio-technology, Vol. 15, No. 3, 2012, pp. 1 – 7.

Kittel, J., Idem, R., Gelowitz, D., Tontiwachwuthikul, P., Parrain, G. and Bonneau, A. (2009). Corrosion in MEA units for CO_2 capture: Pilot plant studies. Energy Procedia 1 (1): pp 791 – 797.

Korpinen, R., and Fradim, P. (2006). Characterisation of sawdust-like wood materials. 9th European workshop on Lignocellulosics and Pulp, at Vienna, Austria. August 2006.

Korpinen, R.I. (2002). On the potential utilization of sawdust and wood chip screenings. Thesis for: Doctor of Science in Technology.Natural Resources Institute Finland.

Kumar, R., Arya R.K., and Kaushik R. (2003). Periodate oxidation of aromatic amines: kinetics and mechanism of oxidation of N – ethylanilline in acetone water medium. Asian Journal of Chemistry. Vol. 12(4). pp:1229 – 1234.

Kvamsdal, H.M., Jakobsen, J.P.and Hoff, K.A. (2009). Dynamics modeling and simulation of a CO_2 absorber column for post- Combustion CO_2 capture. Chemical Engineering & Processing: process intensification Vol 48: pp 135 – 144.

Lawal, A., Wang, M., Stephenson, P. and Yeung, H. (2009). Dynamics modelling of CO_2 absorption for post -Combustion capture in Coal – fired power plants, fuel Vol. 88. Issue 12: pp 2455 – 2462.

Lee, S.C., Choi, B.Y., Ryu, C.K., Ahn, Y.S. and Kim, J.C. (2006).The effect of water on the activation and the CO_2 capture capacities of alkali metal- based sorbents. Korean journal. Chemical Engineering. Vol. 23: pp 374 – 379.

Liiri, E. (1979). Carbon Capture and Sequestration in power generation: review of impacts and opportunities for water sustainability. Energy sustainability of society8(1): pp 6 – 12.

Lukkari, T. (1998). From wood to refined. Finnish Forest Industries Federation, Finland. pp 75.

MacLeod, J.M. and Kingsland, K.A. (1990). Kraft-AQ pulping of sawdust. Tappi J. 73(1): 191 – 193.

Makino, K. (2006). Overview of the oxy-fuel combustion studies in Japan. In: *International Oxy-combustion Networkfor CO2 Capture. Report on inaugural (1st) workshop,* Cottbus, Germany, 29-30 Nov 2005. Report 2006/4, Cheltenham, UK, IEA Greenhouse Gas R&D Programme, p. 51-76 (Jul 2006) CD-ROM http://www.ieaghg.org/docs/ oxyfuel/w1/02W1Makino.pdf.

Marine Pollution Monitoring Manual (2009). 'A Training manual for Coastal and Marine Pollution Monitoring for the Guinea Current Large Marine Ecosystem Project'. Interim Guinea Current Commission. December 2009.

Mertens, K., Rengefors, K., Moestrrup, O. and Ellegaard, O. (2012). A review of recent freshwater dinoflagellate cysts: Taxonomy, phylogeny, ecology and palaecology. Phycologia Vol. 51 (6), 612 – 619.

Metz, B., Davidson, O., De Coninck, H.C., Loos, M., Meyer, L.A. (2005). *Intergovernmental Panel on Climate Change*. UK, Cambridge University Press, Cambridge pp: 442.

Miller D. C., Hariri M. H., Misovich M., Anklam M. and Artigue R. (2002). Proceedings of the American Society for Engineering Education Annual Conference and Symposium, pp 7.66.2 – 7.66.5.

Mimms, A., Kocurek, M.J., Pyatte, J.A. and Wright, E.E. (1995). Kraft pulping – A compiliation of Notes. Tappi, Atlanta (GA), USA, pp 181.

Mimura, T., Shimojo, S., Suda, T., Iijima, M., Mitsuoka, S. (1995). Research and development on energy saving technology for flue gas carbon dioxide recovery and steam system in power plant. Energy Convers. Mgmt. 36, 6-9, 397-400.

Misra, M., Raglund, K. and Baker, A. (1993) Wood ash composition as a function of furnace temperature. *Biomass and Bioenergy*, vol 4, No 2: 103-116.

Mitchell, M.J., Jensen O.E., Cliffe K.A. and Maroto-Valer, M.M. (2010). A model of carbon dioxide dissolution and mineral carbonation kinetics. *Proceedings of the Royal Society,* 466, 1265–1290.

Mohammad Songolzadeh, Mansooreh Soleimani, Maryam Takht Ravanchi and Reza Songolzadeh (2014). Carbon Dioxide Separation from Flue Gases: A Technological Review Emphasizing Reduction in Greenhouse Gas Emissions Vol. 2. pp: 4-5.

Moller, I. and Ingerslev, M. (2001). The need for and effects of wood-ash application in Danish forests. *SkogKorsk Report* no 2: 6-8.

Moser, P., Sandra, S. and Knut, S. (2011). Investigation of trace elements in the inlet and outlet streams of a MEA – based post – Combustion capture process result from the test programme at the Niederaussem pilot. Energy procedia, Vol 4: pp 473 – 479.

Moser, P., Schmidt, S., Sieder, G., Garcia, H., Ciattaglia, I., Klein, H. (2009). Enabling post combustion capture optimization – the pilot plant project at Niederaussem. In: *9th international conference on greenhouse gas control.*

Nguyen, T., Hilliard, M. and Rochelle, G.T. (2010). Amine Volality in CO_2 capture. International journal of Greenhouse Gas Control vol 4. No.5:pp 707 – 715.

Noves K.M. (2003). Integrated collaborative technology development program for CO_2 sequestration in geologic formations. Energy Conversion and Management. Vol. 41. pp:21-24.

Ohno, T. (1992). Neutralisation of soil acidity and release of phosphorous and potassium by wood ash. *J. Environ. Qual.* 21: 433-438.

Parham, P. (1983). A study on the reaction between CO_2 and alkanolamines in aqueous solutions. Chemical Engineering Science. Vol. 38 No. 9: pp 1411 – 1429.

Perry (2007). Chemical Engineers Handbook.

Pinsent, R.W. (2009). The Kinetics of Combination of Carbon dioxide with hydroxide ions. Journal of Engineering Sciences. Vol 52: pp 1956 – 1961.

Puxty, D.G., Dave N., Rowland, R., Feron, P.H.M., Attalla, M.I. (2009). CO_2 capture by aqueous amines and aqueous ammonia: A comparison. Energy Procedia 1(1), 949 – 954.

Rantasuo, P. (1976). Preparation of sawdust cellulose with Enso-Bauer M & D boiler, Norsk Skogind. 30 (6): 186 – 188.

Rao A.B., Rubin, E.S., Keith, D.W., Morgan, M.G. (2006). Evaluation of potential cost reductions from improved aminebasedCO_2 capture systems. *Energy Policy*; 34; 3765-3772.

Rao, A.B., Rubin, E.S. (2002). A technical, economic and environmental assessment of amine-based CO_2 capture technology for power plant greenhouse gas control. *Environmental Science and Technology*; 36; 4467-4475.

Reddy, S., Johnson, D., Gilmartin, J. (2008). Fluor's Econamine FG plusSM technology for CO_2 capture at coalfired power plants. Presented at: *Power plant air pollutantcontrol 'mega' symposium*, Baltimore, USA, 25-28 Aug 2008, 17 pp.

Richmond, V.A. (1993). Behaviour of radiocaesium in forest multilayered soils. *J. Environ. Radioactivity,* TAPPI Press, Atlanta. 18: 247-257.

Rikala, R. and Jozefek, H. (1990). Effect of dolomite lime and wood ash on peat substrate and development of tree seedlings. *Silva Fennica* 24(4) 323-334.

Rubin, E.S., Rao, A.B., Chen, C. (2012). Comparative assessments of fossil fuel power plants with CO_2 capture and storage. In: *Proceedings of the 7th international conferenceon greenhouse gas control technologies*, Vancouver, Canada, 5-9. UK, Oxford, Elsevier Ltd vol 1, 285-293.

Rühling, A. (1996). Effects of peat ash on fungi and vascular plants, and on heavy metal concentrations in berries and edible fungi. NUTEK, Ramprogram askåterföring R 1996: 49, Stockholm. pp 42.

Sander, M., and Mariz, C. (1992). The Fluor Daniel Econamine FG process: past experience and present day focus. Energy Conversion. Mgm. 33, 5-8, 341-348.

Schneilder, T.R., Hartmann, M. and Braus, G.H. (1999). Crystallization and preliminary X-ray analysis of 3-deoxy-D-arabino-heptulosonate-7-phosphate synthase (tyrosine inhibitable) from saccharomyces cerevisiae. Acta Crystallogr D Biol Crystallogr 55 (pt9): 1586-8.

Sexton, A.J. and Rochelle, G. (2009). Catalysts and inhibitors for MEA Oxidation. Energy Procedia Vol. 1, No. 1: pp 1179 – 1185.

Shao, M. (2009). Air Separation Unit (ASU) and CO_2 Processing Unit (CPU) for oxy-coal power plant. Paper presented at: *Asia Pacific Programme, oxyfuel working groupcapacity building*

course, Daejeon, South Korea, KEPRI, 5-6. Available at: http://www.co2captureandstorage.info/ networks/oxyfuelmeetings.htm, 18 pp.

Shindell, D. (2007). Estimating the potential for twenty-first century sudden climate change. Philosophical Transactions of the Royal Society of London A: Mathematical, Physical and Engineering Sciences, 365(1860), pp 2675 – 2694.

Sinnott, R.K. (2005). Engineering Design. Coulson and Richardson Vol 8: pp77 – 79.

Someshwar, A. (1996). Wood and combination wood-fired boiler ash characterisation. *J.Environ.Qual.* 25: 962-972.

Suda, T., Fujii, M., Yoshida, K., Lijima, M., Seto, T. (1992). Mitsuoka S, Development of flue gas carbon dioxide recovery technology. Energy Convers. Mgm. 33, 5-8, 317-324.

Supap, T., Idem, R., Tontiwachwuthikul, P., Saiwan, C. (2009). Kinetics of sulfur dioxide- and oxygen-induced degradationof aqueous monoethanolamine solution during CO_2absorption from power plant flue gas streams. *InternationalJournal of Greenhouse Gas Control*; 3; 133-142.

Surewicz, W. (1974). The processing of sawdust to bleached sulphate pulps. Zellst. Pap. 23(7): 196 – 203.

Svendsen, H.F.,Silva, D. and Goff, G.S. (2012). Ab-initio study of the reaction of carbonate formation from CO_2 and alkanolamine. Industrial & Engineering Chemistry Research. Vol 4(13): pp 3413 – 3418.

Svendsen, H.F., Tobiesen, F.A. and Hoff, K.A. (2011). Desorber Energy Consumption Amine Based Absorption Plants. International Journal of Green Energy.

Svendsen, P.L., Anderson, O.B. and Nielsen, A.A. (2016). Stable reconstruction of artic sea level for the 1950-2010 period. Journal of Geophysical Research. Volume 121, Issue 8, pp 5697 – 5710.

Taran, M. and Aghaie, E. (2015). Designing and optimization of separation process of iron impurities from kaolin by oxalic acid in bench – scale stirred- tank reactor. Applied Clay Science Vol 107: pp 109 – 116.

Taylor, G. (1977). Production of bleache kraft market pulp from sawdust, Research Gate. Annual Meeting of the Tech Sect, CPPA, 62nd.

Uusvaara, O. (1975). Industrial sawdust features. Publications of the Finnish Forest Research Institute 83. pp. 1 – 43.

Uyanga, I.J. and Idem, R.O. (2007). Studies of SO_2 - and O_2 - induced degradation of aqueous MEA during CO_2 capture from power plant flue gas streams. *Industrial and Engineering Chemical Research*; 48 (8); 2558-2566.

Vaidya, P.D. and Kenig, E.Y. (2007). CO_2 alkanolamine recation kinetics: A review of recent studies. Wiley online library. Chemical Engineering & technology. Volume 30, pp 1467 – 1474.

Veawab, A., Tontiwachwuthikul, P., Aroonwilas, A., Chakma, A. (2003). Performance and cost analysis for CO_2 capturefrom flue gas streams: absorption and regeneration aspects.In: *6th international conference on greenhouse gas controltechnologies*, Kyoto, Japan, 1-4 Oct 2002. Oxford, UK.

Voice, A., and Rochelle G. (2013). Aqueous 3 – (methylamino) propylamine for CO_2 capture. Internatural Journal of Greenhouse Gas control Vol 15: pp 70 -77.

Wang, M., Lawal, A., Stephenson, P., Sidders, J. and Ramshaw, C. (2011). Post Combustion CO_2 capture with Chemical absorption: a state-of-the-art review. Chemical Engineering Research and Design vol. 89 no. 9: pp 1609 – 1624.

Xu, E. and Rochelle (2009). Aqueous Piperazine as the new standard for CO_2 capture technology. Chemical Engineering Journal Vol 171(3): pp 725 – 733.

Zhao, L. Riensche, E., Menzer, R., Blum, L. and Stolten, D. (2008). A parametric study of CO_2/ N_2 gas separation membrane processes for post combustion capture. Journal of membrane science. Vol 325, no.1:pp 284 – 294.

Ziali, S. and Sahadu, S. and Saajid. (2009). Carbon capture and storage. European scientific Journal Vol 3(1): pp 1 – 7.

Zobel, B.J. and Sprague, J.R. (1998). Juvenile wood in forest trees. Springer-verlag, Berlin, Germany.

Zuo, G. and Hirsch, A. (2008). The trial of the top gas recycling blast furnace at LKAB's EBF and scale – up. Chinese journal of chemical Engineering. Vol.19:pp 615 – 620.

APPENDIX A

MATERIAL BALANCE CALCULATIONS FOR THE PROTOTYPE ABSORBER DESIGN

Table A1: Flue gas Components Compositions, Densities and Molecular Weights

S/N	COMPONENT	COMPOSITION	DENSITY (Kg/m^3)	MOLECULAR WEIGHT (kg/mol)
1	CO_2	12.6%	1.84	44
2	H_2O	6.2%	1000	18
3	O_2	4.3%	1.33	32
4	CO	50ppm	1.17	28
5	NO	420ppm	1.23	30
6	SO_2	420ppm	2.28	64
7	N_2	77%	1.17	28

Feed Stock Rate Basis = $20m^3/hr$

Volumetric Flow Rates of Feed Flue Gas Components

CO_2: 0.126×20 = $2.52m^3/hr$

H_2O: 0.062×20 = $1.24m^3/hr$

O_2: 0.043×20 = $0.86m^3/hr$

CO: $50 \times 10^{-6} \times 20$ = $0.001m^3/hr$

NO: $420 \times 10^{-6} \times 20 =$ $0.0084m^3/hr$

SO_2: $420 \times 10^{-6} \times 20 =$ $0.0084m^3/hr$

N_2: 0.77×20 = $15.40m^3/hr$

Mass Flow Rates of Feed Flue Gas Components (m^3/hr x kg/m^3)

CO_2: 2.52×1.84 = 4.637 kg/hr

H_2O: 1.24×1000 = 1,240 kg/hr

O_2: 0.86×1.33 = 1.1438 kg/hr

CO: 0.001×1.17 = 0.00117 kg/hr

NO: 0.0084×1.23 = 0.01033 kg/hr

SO_2: 0.0084x 2.28 = 0.01915 kg/hr

N_2: 15.40x 1.17 = 18.018 kg/hr

Molar Flow Rates (kg/hr by MW)

CO_2: $\frac{4.637}{44}$ = 0.1054 kgmol/hr

H_2O: $\frac{1,240}{18}$ = 68.89 kgmol/hr

O_2: $\frac{1.1438}{32}$ = 0.0357 kgmol/hr

CO: $\frac{0.00117}{28}$ = 0.00004179 kgmol/hr

NO: $\frac{0.01033}{30}$ = 0.000344 kgmol/hr

SO_2: $\frac{0.01915}{64}$ = 0.00030 kgmol/hr

N_2: $\frac{18.018}{28}$ = 0.6435 kgmol/hr

Total = 69.6753 kgmol/hr

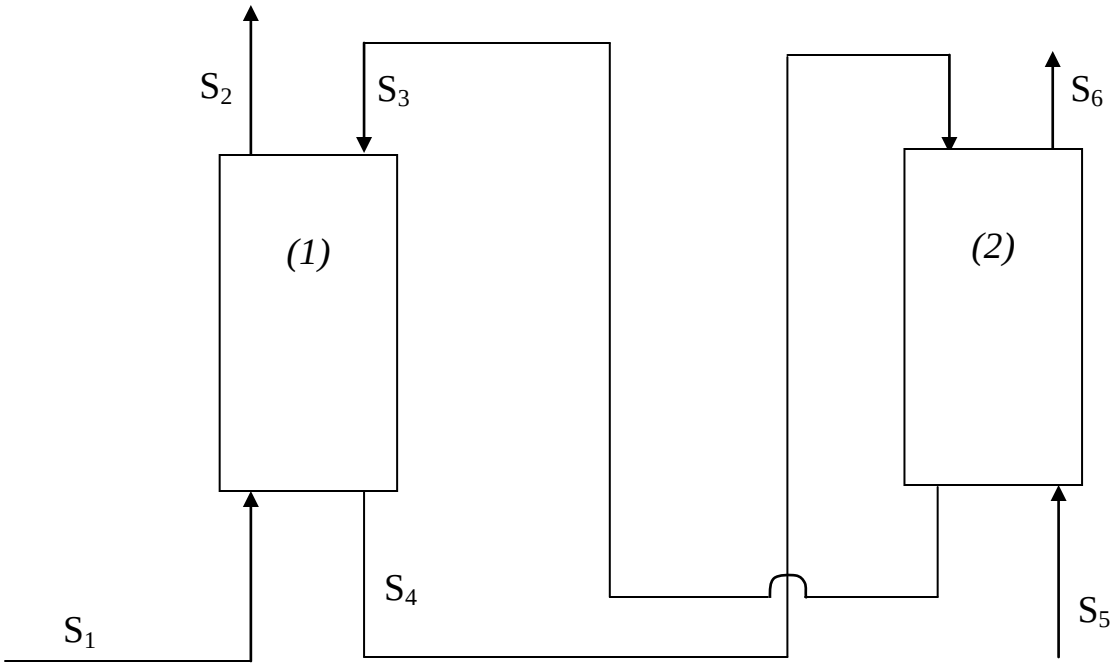

Fig A1: Block Flow Diagram of the prototype absorber (1), with an associating stripper (2)

COMPONENTS

CO_2	*(1)*
H_2O	*(2)*
O_2	*(3)*
CO	*(4)*
NO	*(5)*
SO_2	*(6)*
N_2	*(7)*

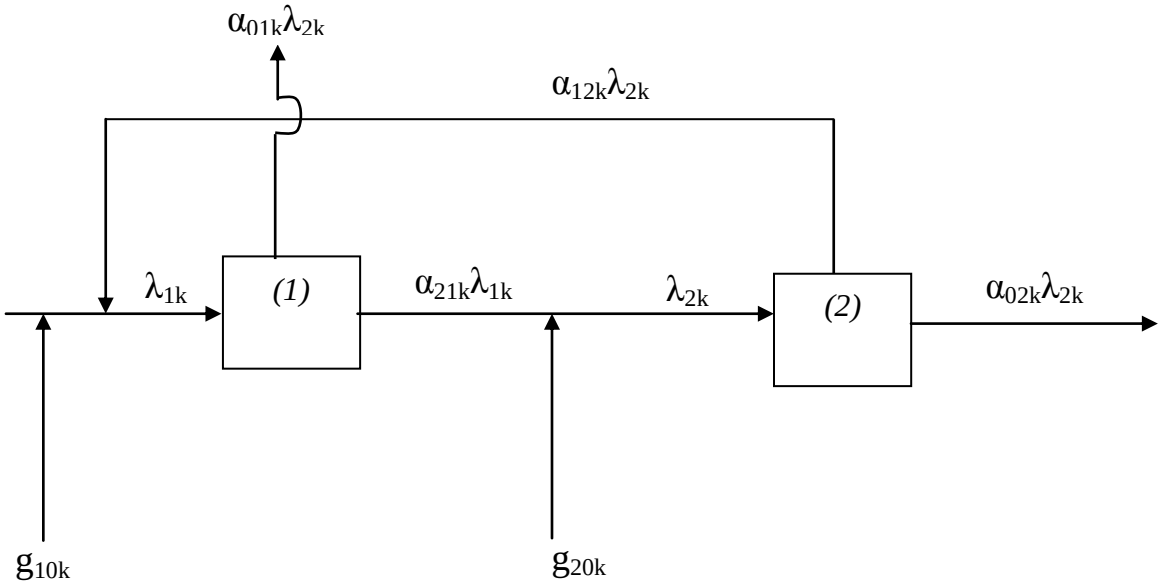

Fig A2: Process Flow Diagram showing Split fraction Co-efficients

Balances to generate the Matrix of Equations, for the Split Fraction Method

Note: Balances are made at the inlet of any unit.

Unit (1)	-	$g_{10k} + \alpha_{12k}\lambda_{2k}$	=	λ_{1k}		
Re-arranging;	$\lambda_{1k} - \alpha_{12k}\lambda_{2k}$		=	g_{10k}	. .	(i)
Unit (2)	-	$g_{20k} + \alpha_{21k}\lambda_{1k}$	=	λ_{2k}		
Re-arranging;	$-\alpha_{21k}\lambda_{1k} + \lambda_{2k}$		=	g_{20k}	. .	(ii)

GENERAL MATRIX OF EQUATIONS

$$\begin{bmatrix} 1 & -\propto_{12k} \\ -\propto_{21k} & 1 \end{bmatrix} = \begin{bmatrix} g_{10k} \\ g_{20k} \end{bmatrix}$$

Table A2: Summary of Values for Split Fractions and Fresh Feeds

Unit/Comp		***1***	***2***	***3***	***4***	***5***	***6***	***7***
1	α_{21K}	*0.95*	*0.90*	*0.30*	*0.98*	0.40	0.75	0.10
	g_{10k}	*0.1054*	*68.89*	*0.0357*	*0.00004179*	0.000344	0.00030	0.6435
2	α_{12K}	*0.03*	*1.00*	*0.20*	*0.10*	*0.15*	*0.30*	*0.00*
	g_{20k}	0.00	0.00	0.00	0.00	0.00	0.00	*2.00*

MATRIX OF EQUATIONS FOR EACH COMPONENT

CO_2

$$\begin{bmatrix} 1 & -0.03 \\ -0.95 & 1 \end{bmatrix} \begin{bmatrix} \lambda_{1,1} \\ \lambda_{2,1} \end{bmatrix} = \begin{bmatrix} 0.1054 \\ 0.000 \end{bmatrix}$$

$$\lambda_{1,1} = 0.1085 kgmol/hr \qquad \lambda_{2,1} = 0.1031 kgmol/hr$$

H_2O

$$\begin{bmatrix} 1 & -1.00 \\ -0.90 & 1 \end{bmatrix} \begin{bmatrix} \lambda_{1,2} \\ \lambda_{2,2} \end{bmatrix} = \begin{bmatrix} 68.89 \\ 0.000 \end{bmatrix}$$

$$\lambda_{1,2} = 68.89 kgmol/hr \qquad \lambda_{2,2} = 1{,}565.00 kgmol/hr$$

O_2

$$\begin{bmatrix} 1 & -0.20 \\ -0.30 & 1 \end{bmatrix} \begin{bmatrix} \lambda_{1,3} \\ \lambda_{1,3} \end{bmatrix} = \begin{bmatrix} 0.0357 \\ 0.000 \end{bmatrix}$$

$$\lambda_{1,3} = 0.0381 kgmol/hr \qquad \lambda_{2,3} = 0.0114 kgmol/hr$$

$$CO$$

$$\begin{bmatrix} 1 & -0.10 \\ -0.98 & 1 \end{bmatrix} \begin{bmatrix} \lambda_{1,4} \\ \lambda_{2,4} \end{bmatrix} = \begin{bmatrix} 0.00004 \\ 0.000 \end{bmatrix}$$

$$\lambda_{1,4} = 0.0000465 kgmol/hr \qquad \lambda_{2,4} = 0.00004565 kgmol/hr$$

$$NO$$

$$\begin{bmatrix} 1 & -0.15 \\ -0.40 & 1 \end{bmatrix} \begin{bmatrix} \lambda_{1,5} \\ \lambda_{2,5} \end{bmatrix} = \begin{bmatrix} 0.000344 \\ 0.000 \end{bmatrix}$$

$$\lambda_{1,5} = 0.000367 kgmol/hr \qquad \lambda_{2,5} = 0.000147 kgmol/hr$$

$$SO_2$$

$$\begin{bmatrix} 1 & -0.03 \\ -0.75 & 1 \end{bmatrix} \begin{bmatrix} \lambda_{1,6} \\ \lambda_{2,6} \end{bmatrix} = \begin{bmatrix} 0.00030 \\ 0.000 \end{bmatrix}$$

$$\lambda_{1,6} = 0.000387 kgmol/hr \qquad \lambda_{2,6} = 0.000291 gmol/hr$$

$$N_2$$

$$\begin{bmatrix} 1 & 0.00 \\ -0.10 & 1 \end{bmatrix} \begin{bmatrix} \lambda_{1,7} \\ \lambda_{2,7} \end{bmatrix} = \begin{bmatrix} 0.6435 \\ 2.00 \end{bmatrix}$$

$\lambda_{1,7} = 0.6435 gmol/hr$ $\lambda_{2,7} = 2.0644 kgmol/hr$

CALCULATIONS OF FLOW RATES IN EACH STREAM

STREAM 1

1. CO_2: g_{101} = *0.1054kgmol/hr* = *4.6376kg/hr*

2. H_2O: g_{102} = *68.89kgmol/hr* = *1,240.02kg/hr*

3. O_2: g_{103} = *0.0357kgmol/hr* = *1.1424kg/hr*

4. CO: g_{104} = *0.00004179kgmol/hr* = *0.00117kg/hr*

5. NO: g_{105} = *0.000344kgmol/hr* = *0.01032kg/hr*

6. SO_2: g_{106} = *0.00030kgmol/hr* = *0.0192kg/hr*

7. N_2: g_{107} = *0.6435kgmol/hr* = *18.018kg/hr*

Total=1,263.85kg/hr

%CO_2: = *4.6376/1,263.85x 100%* = *0.37%*

%H_2O: = *1,240.02/1,263.85x 100%* = *98.11%*

%O_2: = *1.1424/1,263.85x 100%* = *0.09%*

%CO: = *0.00117/1,263.85x 100%* = *0.000093%*

%NO: = *0.01032/1,263.85 x 100%* = *0.00082%*

%SO_2: = *0.0192/1,263.85 x 100%* = *0.0015%*

%N_2: = *18.018/1,263.85x 100%* = *1.46%*

STREAM 2

1. $CO_2 : \alpha_{011}\lambda_{11}$ = *0.05 x 4.774* = *0.2387kg/hr*

2. $H_2O: \alpha_{012}\lambda_{12}$ = *0.10 x 1240.02* = *124.0020kg/hr*

3. $O_2 : \alpha_{013}\lambda_{13}$ = *0.70 x 1.2192* = *0.85344kg/hr*

4. CO $: \alpha_{014}\lambda_{14}$ = *0.02 x 0.001302* = *0.00002604kg/hr*

5. NO $: \alpha_{015}\lambda_{15}$ = *0.60 x 0.01101* = *0.006606kg/hr*

6. $SO_2 : \alpha_{016}\lambda_{16}$ = *0.25 x 0.024768* = *0.006192kg/hr*

7. $N_2 : \alpha_{017}\lambda_{17}$ = *0.90 x 18.018* = *16.2162kg/hr*

Total = 141.3232kg/hr

%CO_2: = *0.2387/141.3232x 100%* = *0.17%*

%H_2O: = *124.002/141.3232x 100%* = *87.74%*

$\%O_2$: = 0.85344/141.3232x 100% = 0.604%

%CO: = 0.00002604/141.3232x 100% = 0.0000184%

%NO: = 0.006606/141.3232x 100% = 0.00467%

$\%SO_2$: = 0.006192/141.3232x 100% = 0.00438%

$\%N_2$: = 16.2162/141.3232x 100% = 11.47%

STREAM 3

1. CO_2 : $\alpha_{121}\lambda_{21}$ = 0.03 x 4.5364 = 0.1361kg/hr

2. H_2O: $\alpha_{122}\lambda_{22}$ = 1.00 x 28,170 = 28,170.00kg/hr

3. O_2 : $\alpha_{123}\lambda_{23}$ = 0.20 x 0.3648 = 0.0730kg/hr

4. CO : $\alpha_{124}\lambda_{24}$ = 0.10 x 0.001278 = 0.0001278kg/hr

5. NO : $\alpha_{125}\lambda_{25}$ = 0.15 x 0.00441 = 0.0006615kg/hr

6. SO_2 : $\alpha_{126}\lambda_{26}$ = 0.30 x 0.018624 = 0.005587kg/hr

Total = 28,170.2155kg/hr

$\%CO_2$: = 0.1361/28,170.2155 x 100% = 0.000483%

$\%H_2O$: = 28,170.00/28,170.2155 x 100% = 99.999%

$\%O_2$: = 0.0730/28,170.2155 x 100% = 0.000259%

%CO: = 0.0001278/28,170.2155 x 100% = 0.000000454%

%NO: = 0.0006615/28,170.2155 x 100% = 0.00000235%

$\%SO_2$: = 0.005587/28,170.2155 x 100% = 0.0000198%

STREAM 4

1. CO_2 : $\alpha_{211}\lambda_{11}$ = 0.95 x 4.774 = 4.5353kg/hr

2. H_2O: $\alpha_{212}\lambda_{12}$ = 0.90 x 1240.02 = 1116.018kg/hr

3. O_2 : $\alpha_{213}\lambda_{13}$ = 0.30 x 1.2192 = 0.3658kg/hr

4. CO : $\alpha_{214}\lambda_{14}$ = 0.98 x 0.001302 = 0.001276kg/hr

5. NO : $\alpha_{215}\lambda_{15}$ = 0.40 x 0.01101 = 0.004404kg/hr

6. SO_2 : $\alpha_{216}\lambda_{16}$ = 0.75 x 0.024768 = 0.0186kg/hr

6. N_2 : $\alpha_{217}\lambda_{17}$ = 0.10 x 18.018 = 1.8018kg/hr

Total = 1122.7452kg/hr

$\%CO_2$: = 4.5353/1122.7452x 100% = 0.404%

$\%H_2O$: = *1116.018/1122.7452x 100%* = *99.40%*

$\%O_2$: = *0.3658/1122.7452x 100%* = *0.0326%*

%CO: = *0.001276/1122.7452x 100%* = *0.000114%*

%NO: = *0.004404/1122.7452x 100%* = *0.00039%*

$\%SO_2$: = *0.0186/1122.7452x 100%* = *0.00166%*

$\%N_2$: = *1.8018/1122.7452x 100%* = *0.16%*

STREAM 5

7. N_2: g_{207} = *2.000kgmol/hr* = *56.000kg/hr*

$\%N_2$: = *100%*

STREAM 6

1. CO_2 : $\alpha_{021}\lambda_{21}$ = *0.97 x 4.5364* = *4.4003kg/hr*

2. H_2O: $\alpha_{022}\lambda_{22}$ = *0.00 x 28,170* = *0.00kg/hr*

3. O_2 : $\alpha_{023}\lambda_{23}$ = *0.80 x 0.3648* = *0.2918kg/hr*

4. CO : $\alpha_{024}\lambda_{24}$ = *0.90 x 0.001278* = *0.00115kg/hr*

5. NO : $\alpha_{025}\lambda_{25}$ = *0.85 x 0.00441* = *0.00375kg/hr*

6. SO_2 : $\alpha_{026}\lambda_{26}$ = *0.70 x 0.018624* = *0.01304kg/hr*

6. N_2 : $\alpha_{027}\lambda_{27}$ = *1.00 x 57.8032* = *57.8032kg/hr*

Total = 62.5132kg/hr

$\%CO_2$: = *4.4003/62.5132 x 100%* = *7.04%*

$\%H_2O$: = *0%*

$\%O_2$: = *0.2918/62.5132x 100%* = *0.47%*

%CO: = *0.00115/62.5132x 100%* = *0.0018%*

%NO: = *0.00375/62.5132x 100%* = *0.006%*

$\%SO_2$: = *0.01304/62.5132x 100%* = *0.021%*

$\%N_2$: = *57.8032/62.5132x 100%* = *92.47%*

Table A3: Calculated Mass Flow Rates of the Components across the Units (kgmol/hr)

		COMPONENTS						
Unit	***Mass flow (kgmol/hr)***	***1***	***2***	***3***	***4***	***5***	***6***	***7***
1	λ_{1K}	*0.1085*	*68.89*	*0.0381*	*0.0000465*	*0.000367*	*0.000387*	*0.6435*
2	λ_{2K}	*0.1031*	*1,565*	*0.0114*	*0.00004565*	*0.000147*	*0.000291*	*2.0644*

Table A4: Calculated Mass Flow Rates of the Components across the Units (kg/hr)

		COMPONENTS						
Unit	***Mass flow (kg/hr)***	***1***	***2***	***3***	***4***	***5***	***6***	***7***
1	λ_{1K}	*4.774*	*1240.020*	*1.2192*	*0.001302*	*0.01101*	*0.024768*	*18.018*
2	λ_{2K}	*4.5364*	*28,170*	*0.3648*	*0.001278*	*0.00441*	*0.018624*	*578032*

Table A5: Calculated Mass Flow Rates of the Components in the Process Stream(kg/hr)

STREAM	***CO_2 (1)***	***H_2O (2)***	***O_2 (3)***	***CO (4)***	***NO (5)***	***SO_2 (6)***	***N_2 (7)***
S_1	*4.6376*	*1240.02*	*1.1424*	*0.00117*	*0.01032*	*0.0192*	*18.018*
S_2	*0.2387*	*124.002*	*0.8534*	*0.00002604*	*0.006606*	*0.006192*	*16.2162*
S_3	*0.1361*	*28,170*	*0.0730*	*0.0001278*	*0.0006615*	*0.005587*	-
S_4	*4.5353*	*1116.018*	*0.3658*	*0.001276*	*0.004404*	*0.0186*	*1.8018*
S_5	-	-	-	-	-	-	*56.000*
S_6	*4.4003*	-	*0.2918*	*0.00115*	*0.00375*	*0.01304*	*57.8032*

Table A6: Calculated Percentage by Mass Flow Rates of Components in the Process Streams (%)

STREAM	***CO_2 (1)***	***H_2O (2)***	***O_2 (3)***	***CO (4)***	***NO (5)***	***SO_2 (6)***	***N_2 (7)***
S_1	*0.37*	*98.11*	*0.09*	*0.000093*	*0.00082*	*0.0015*	*1.46*
S_2	*0.17*	*87.74*	*0.604*	*0.0000184*	*0.00467*	*0.00438*	*11.47*
S_3	*0.00048*	*99.999*	*0.00026*	*0.000000454*	*0.00000235*	*0.00002*	-
S_4	*0.404*	*99.40*	*0.0326*	*0.000114*	*0.00039*	*0.00166*	*0.16*
S_5	-	-	-	-	-	-	*100*
S_6	*7.04*	-	*0.47*	*0.0018*	*0.006*	*0.021*	*92.47*

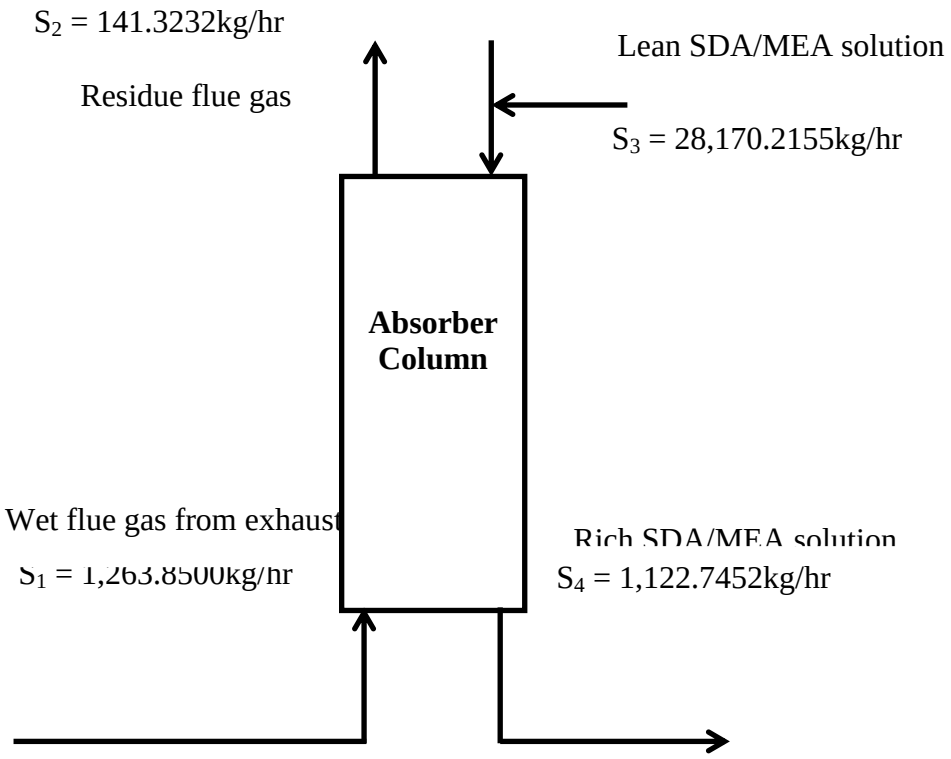

Fig A3: Material Balance around the Prototype Absorber Column

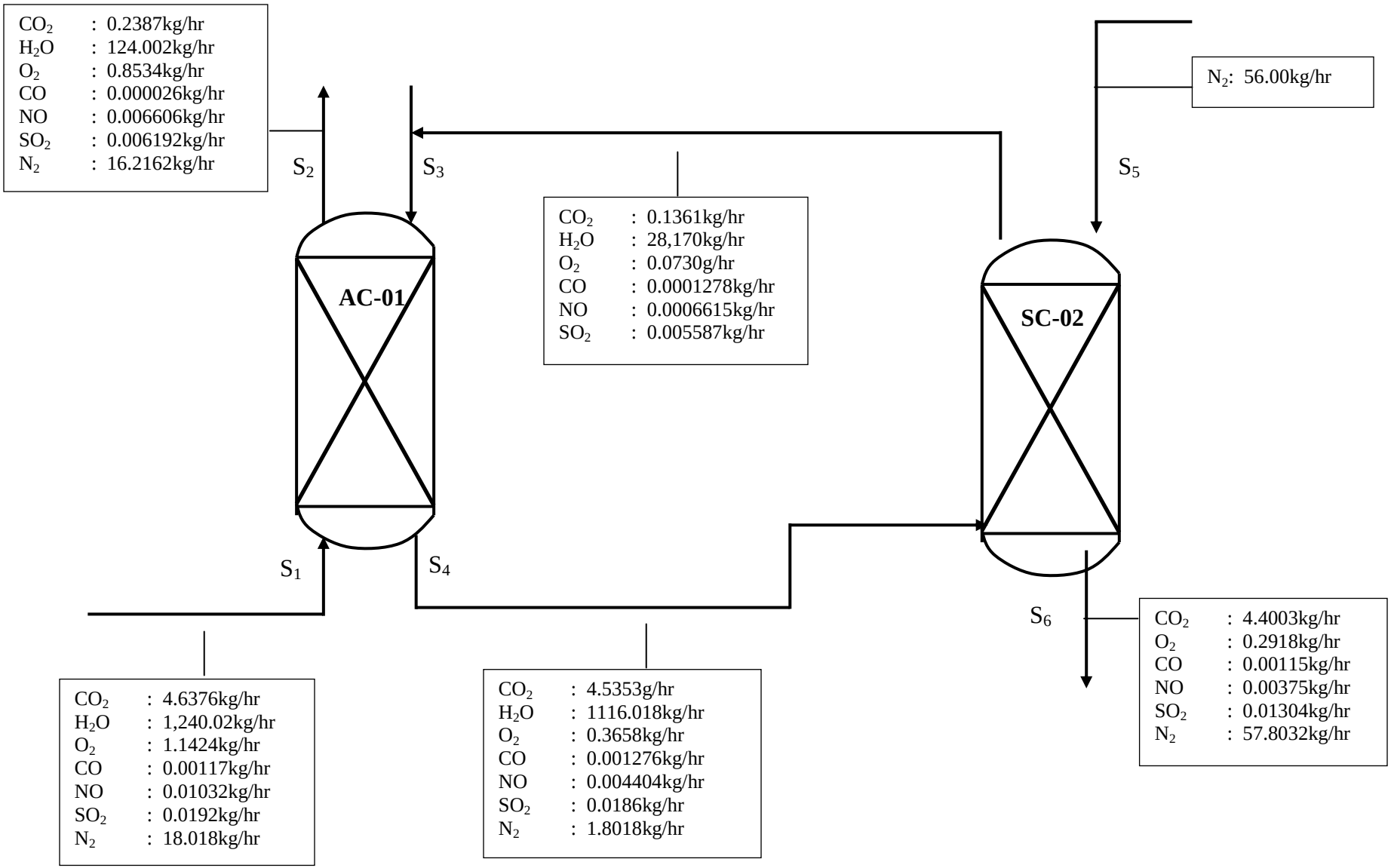

Fig A5: Quantitative flow sheet for the unit

APPENDIX B

ENERGY BALANCE CALCULATIONS

B1. DESIGN DATA

i. Reference Temperature , T_0 = 298K

ii. Reference Pressure, P_0 = 1atm (101.325KPa)

iii. Specific Heat Capacities of Components

$CO_2(g)$: $Cp = -8{,}304{,}300 + 104{,}370T - 433.33T^2 + 0.60052T^3$ (J/kmolK)

$H_2O(g)$: $Cp = 128{,}122 - 27{,}64.8T + 7.634T^2 - 0.01156T^3$ (J/kmolK)

$H_2O(l)$: $Cp = 276{,}370 - 2{,}090.1T - 8.125T^2 - 0.01412T^3$ (J/kmolK)

$O_2(g)$: $Cp = 175{,}430 - 6{,}T + 7.634T^2 - 0.01156T^3 + 9.37x10^6T^4$(J/kmolK)

$CO(g)$: $Cp = -8{,}304{,}300 + 104{,}370T - 433.33T^2 + 0.60052T^3$ (J/kmolK)

$NO(g)$: $Cp = -2{,}979{,}600 + 76{,}602T - 652.59T^2 + 1.8879T^3$ (J/kmolK)

$SO_2(g)$: $Cp = 85{,}743 + 5.7443T$ (J/kmolK

$N_2(g)$: $Cp = 281{,}970 - 12{,}281T + 248T^2 - 2.2182T^3 + 0.00749T^4$(J/kmolK)

Source: Perry's Chemical Engineers' Handbook.

B2. GENERAL ASSUMPTIONS

I. The processes are operating at steady state

II. There are negligible heat losses from process equipments and pipings. Adequate lagging ensures this.

III. Potential and Kinetic Energy contributions are neglected, as measured relative to the major forms of energy.

Accumulation = Energy in - Energy Out + Generation - Consumption

Where, at steady state, Accumulation = 0

Therefore, Energy = Energy In + Generation – Consumption

B3. ENERGY BALANCE AROUND THE UNITS

Calculations are done based on 1hour operation

1. ASORBER COLUMN (AC-X1)

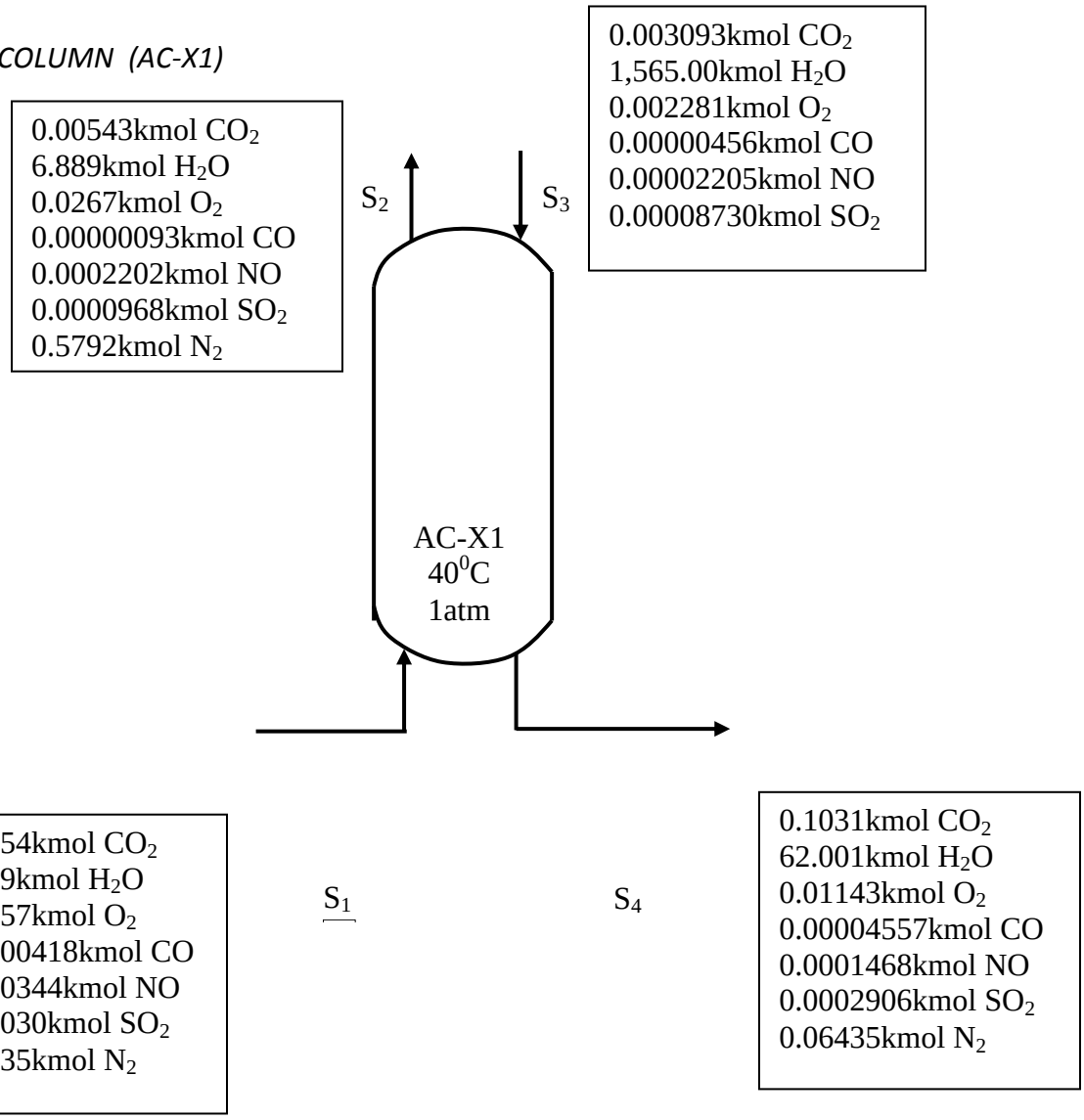

***Enthalpy In**: (Stream 1)* *T = 328K (55^0C)*

CO_2(g):

$$H = (0.1054)\int_{298}^{328}(-8{,}804{,}300 + 104{,}370T + 433.33T^2 + 0.60052T^3)dT$$

= 0.184MJ

H_2O(g):

$$H = (68.89)\int_{298}^{328}(128{,}122 - 27{,}640.8T + 7.634T^2 + 0.01156T^3)dT$$

= 10.922MJ

O_2(g):

$$H = (0.0267)\int_{298}^{328}(175{,}430 - 6{,}152.3T + 113.92T^2 - 0.92382T^3)dT$$

= 0.092MJ

CO(g):

$$H = (0.0000418)\int_{298}^{328}(65.429 + 28{,}723T - 847.39T^2 + 1{,}959.6T^3)dT$$

= 0.0002MJ

NO(g):

$$H = (0.000344)\int_{298}^{328}(-2{,}979{,}600 + 76{,}602T + 652.59T^2 - 1.8879T^3)dT$$

= 0.0039MJ

SO_2(g):

$$H = (0.00030)\int_{298}^{328}(85{,}743 + 5.7443T)dT$$

= 0.00785MJ

N_2(g):

$$H = (0.6435)\int_{298}^{328}(281{,}970 - 12{,}281T + 248T^2 - 2.2182T^3 + 0.00749T^4)dT$$

= 1.082MJ

***Enthalpy In**: (Stream 3)* *T = 313K (40^0C)*

CO_2(g):

$$H = (0.003093)\int_{298}^{313}(-8{,}804{,}300 + 104{,}370T + 433.33T^2 + 0.60052T^3)dT$$

= 0.042MJ

$H_2O(l)$:

$$H = (1{,}565.00)\int_{298}^{313}(\ 276{,}370\ - 2{,}090.1T - \ 8.125T2 - \ 0.01412T3)dT$$

= 43.273MJ

$O_2(g)$:

$$H = (0.002281)\int_{298}^{313}(175{,}430 - \ 6{,}152.3T\ +\ 113.92T^2 - \ 0.92382T^3)dT$$

= 0.039MJ

CO(g):

$$H = (0.00000456)\int_{298}^{313}(65.429\ + 28{,}723T - 847.39T^2 + 1{,}959.6T^3)dT$$

= 0.002MJ

NO(g):

$$H = (0.00002205)\int_{298}^{313}(-2{,}979{,}600 + 76{,}602T\ + 652.59T^2 - 1.8879T^3)dT$$

= 0.005MJ

$SO_2(g)$:

$$H = (0.00008730)\int_{298}^{313}(85{,}743\ + 5.7443T)dT$$

= 0.006MJ

Total Enthalpy In *= 55.658MJ*

***Enthalpy Out**: (Stream 2)* *T = 309K (36^0C)*

$CO_2(g)$:

$$H = (0.00543)\int_{298}^{309}(-8{,}804{,}300\ +\ 104{,}370T\ +\ 433.33T^2\ +\ 0.60052T^3)dT$$

= 0.038MJ

$H_2O(g)$:

$$H = (6.889)\int_{298}^{309}(128{,}122 - 27{,}640.8T\ +\ 7.634T^2 + 0.01156T^3)dT$$

= 14.683MJ

$O_2(g)$:

$$H = (0.0267)\int_{298}^{309}(175{,}430 - 6{,}152.3T + 113.92T^2 - 0.92382T^3)dT$$

= 0.080MJ

CO(g):

$$H = (0.00000093)\int_{298}^{309}(65.429 + 28{,}723T - 847.39T^2 + 1{,}959.6T^3)dT$$

= 0.00085MJ

NO(g):

$$H = (0.0002202)\int_{298}^{309}(-2{,}979{,}600 + 76{,}602T + 652.59T^2 - 1.8879T^3)dT$$

= 0.003MJ

SO_2(g):

$$H = (0.0000968)\int_{298}^{309}(85{,}743 + 5.7443T)dT$$

= 0.007MJ

N_2(g):

$$H = (0.5792)\int_{298}^{309}(281{,}970 - 12{,}281T + 248T^2 - 2.2182T^3 + 0.00749T^4)dT$$

= 1.052MJ

***Enthalpy Out**: (Stream 4)* *T = ?*

CO_2(g):

$$H = (0.1031)\int_{298}^{T}(-8{,}804{,}300 + 104{,}370T + 433.33T^2 + 0.60052T^3)dT$$

H_2O(g):

$$H = (62.001)\int_{298}^{T}(128{,}122 - 27{,}640.8T + 7.634T^2 + 0.01156T^3)dT$$

O_2(g):

$$H = (0.01143)\int_{298}^{T}(175{,}430 - 6{,}152.3T + 113.92T^2 - 0.92382T^3)dT$$

CO(g):

$$H = (0.00004557)\int_{298}^{T}(65.429 + 28{,}723T - 847.39T^2 + 1{,}959.6T^3)dT$$

NO(g):

$$H = (0.0001468)\int_{298}^{T}(-2{,}979{,}600 + 76{,}602T\ + 652.59T^2 - 1.8879T^3)dT$$

$SO_2(g)$:

$$H = (0.0002906)\int_{298}^{T}(85{,}743\ + 5.7443T)dT$$

$N_2(g)$:

$$H = (0.06435)\int_{298}^{T}(281{,}970\ - 12{,}281T\ + 248T^2 - 2.2182T^3 + 0.00749T^4)dT$$

Total Enthalpy Out *= 27.894 + $1.8x10^{-3}T^4$ – $0.49x10^{-1}T^3$ – $125.84T^2$ + $104.8T$ + $7.43x10^2$*

And Enthalpy In = Enthalpy Out

$15.864 = 770.894 + 104.8T - 125.84T^2 - 0.49x10^{-1}T^3 + 1.8x10^{-3}T^4$

Solving the polynomial for T, wehave;

$T = 311.7K = 38.7^0C = 39^0C$

B3. ENERGY BALANCE SCHEMATIC

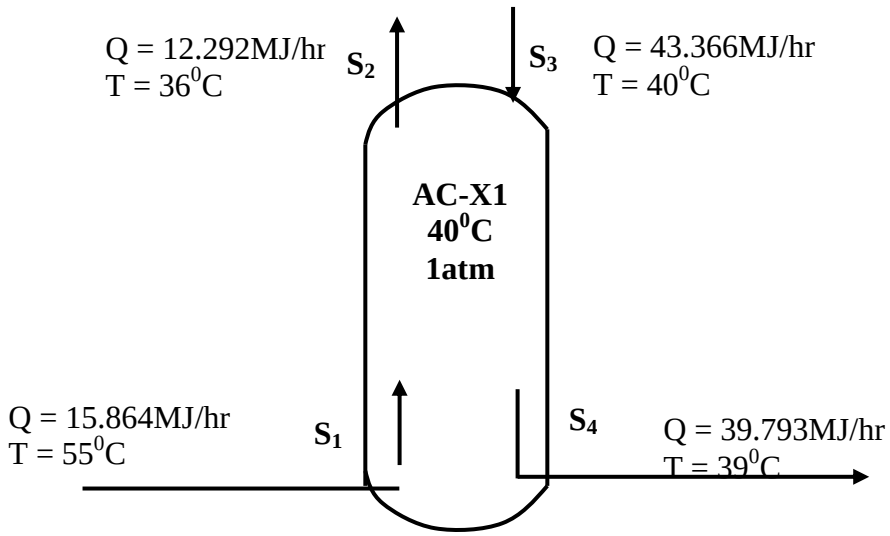

Fig B1: Energy Balance around the Prototype Absorber Column

Table B1: Energy Balance Table on Streams for the prototype absorber column

	Stream Code	Temp. ^{0}C	Stream Code	Temp ^{0}C	Stream Code	Temp. ^{0}C	Stream Code	Temp.	Total Energy Flow, MJ/hr
	S_1	55	S_2	36	S_3	40	S_4	39	
Input, MJ/hr	12.292				43.366				55.657
Output, MJ/hr			15.864				39.793		55.657

APPENDIX C

DETE

RMINATION OF SOMEKINETIC PARAMETERS

Determination of Experimental Rate Law for the Carbon Capture

The experimental rate law for the carbon capture with SDA leachate is determined using excerpts of the original phenomenal experimental trial runs:

Table C1: Result excerpts of carbon capture with SDA leachate

Experimental Serial Number	**Trial Number**	**CO_2 (M)$\times 10^{-3}$**	**H_2O (M)**	**Rate (M/min) $\times 10^{-3}$**
7	1	10.17	0.069	0.977
8	2	8.99	1.250	1.135
9	3	14.92	0.660	0.516

Rate = $k[CO_2(aq)]^x[H_2O]^y$

Trial 1: $0.977 \times 10^{-3} = k(10.17 \times 10^{-3})^x(0.069)^y$…… (i)

Trial 2: $1.135 \times 10^{-3} = k(8.99 \times 10^{-3})^x(1.250)^y$……. (ii)

Trial 3: $0.516 \times 10^{-3} = k(14.92 \times 10^{-3})^x(0.660)^y$…… (iii)

Equation (ii) divided by (i):

$1.162 = 0.884^x 18.116^y$ …….. (iv)

Equation (ii) divided by (iii):

$2.200 = 0.603^x 1.894^y$ …… (v)

Taking logarithm of equations (iv) and (v):

Log1.162 = xLog0.884+ yLog18.116 …….. (vi)

Log2.200 = xLog0.603+ yLog1.894 …… (vii)

Equations (vi) and (vii) result to:

0.065 = -0.054x + 1.258y …… (viii)

0.342 = -0.220x + 0.277 ……. (ix)

Solving the set of linear equations (viii & ix), for x and y:

$$\begin{bmatrix} -0.054 & 1.258 \\ -0.220 & 0.277 \end{bmatrix} \begin{bmatrix} x \\ y \end{bmatrix} = \begin{bmatrix} 0.065 \\ 0.342 \end{bmatrix}$$

$$x = 0.86 \quad ; \quad y = 0.88$$

$$x \approx 1 \quad ; \quad y \approx 1$$

Hence,

Experimental Rate Law: Rate = $k[CO_2]^1[H_2O]^1$ (C-1)

Determination of Overall Rate Constant (Second Order Rate Constant, k_2)

The overall rate constant *k* was determined by substituting values from the result excerpts of the carbon capture with SDA leachate (table C.1).

Choosing values for Trial 7, which represents an average of the three trials (or experimental serial numbers), and/or a mid-representative of the entire experimental trial runs, we have:

Rate = $k[CO_2]^x[H_2O]^y = k(CO_2)^{0.86}(H_2O)^{0.88}$

$0.977 \times 10^{-3} = k(10.17 \times 10^{-3})^{0.86}(0.069)^{0.88} = k(7.35 \times 10^{-2.58} \times 0.095)$

$0.977 \times 10^{-3} = k(1.836 \times 10^{-3})$

$k_2 = 0.53 M^{-1}min^{-1}$

Determination of Mass Transfer Coefficient

The mass transfer coefficient was determined by substituting appropriate values into eqn (2-45):

$K_L = \sqrt{(k_2[C_S]D_{CO2})}$

Where,

K_L is mass transfer coefficient (cms^{-1})

k_2 is the second order reaction rate constant = $0.53 M^{-1}min^{-1} = 8.83 \times 10^{-3} M^{-1}s^{-1}$

C_S is the optimal concentration of the solvent (sequestrant) = 22.5g/L = 1.25M

D_{CO2} is the diffusivity of CO_2 in mineralized water = $1.88 \times 10^{-5} cm^2s^{-1}$

Hence,

$K_L = \sqrt{(8.83 \times 10^{-3} M^{-1}s^{-1} \times 1.25M \times 1.88 \times 10^{-5} cm^2s^{-1})}$

$K_L = \sqrt{(20.75 \times 10^{-8} cm^2s^{-2})}$

$K_L = 4.56 \times 10^{-4} cms^{-1}$

APPENDIX D

PROTOTYPE ABSORBER DESIGN CALCULATIONS

Equilibrium Relationship: $y = 1.85x$

Diffusivity of carbon dioxide in the mineralized water, $D_{CW} = 1.88 \times 10^{-5}$ cm^2/s

Diffusivity of carbon dioxide in flue gas/air, $D_{CA} = 0.14$ cm^2/s

Kinematic viscosity of the mineralized water, $\mu_W = 0.653$g/cm.s

Kinematic viscosity of flue gas/air, $\mu_A = 0.18$g/cm.s

Mass density of the mineralized water, $\rho_W = 930$kg/m^3

Mass density of flue gas, $\rho_A = 1.15$kg/m^3

The Schmidt number for the liquid phase (mineralized water), $S_C = 410$

The Schmidt number for the gas phase (flue gas), $S_C = 1.14$

$$y_1 = \frac{\text{kmole CO2 in entry gas stream}}{\text{kmole of entry gas stream}} = \frac{0.1054}{69.6753} = 0.0015 \text{ or } 0.15\%$$

$$y_2 = \frac{\text{kmole CO2 in exitng gas stream}}{\text{kmole of exiting gas stream}} = \frac{0.00543}{7.5006} = 0.00072 \text{ or } 0.072\%$$

$y_{e,1} = mx_1$; $y_{e,2} = mx_2$

$$x_1 = \frac{\text{kmole CO2 in exiting liquid stream}}{\text{kmole of exiting liquid stream}} = \frac{0.1031}{62.1804} = 0.000166 \text{ or } 0.0166\%$$

$$x_2 = \frac{\text{kmole CO2 in entry liquid stream}}{\text{kmole of entry liquid stream}} = \frac{0.003093}{1565.0055} = 0.000002 \text{ or } 0.0002\%$$

$y_{e,1} = 1.85(0.000166) = 0.000307$

$y_{e,2} = 1.85(0.000002) = 0.0000037$

$\Delta y_1 = (y - y_e)_1 = 0.0015 - 0.000307 = 0.001193$

$\Delta y_2 = (y - y_e)_2 = 0.00072 - 0.0000037 = 0.0007163$

$$\Delta y_{lm} = \frac{\Delta y1 - \Delta y2}{\ln(\frac{\Delta y1}{\Delta y2})} = \frac{0.001193 - 0.0007163}{\ln(\frac{0.001193}{0.0007163})} = 0.0001656$$

And, number of Transfer Units is obtained as follows:

$$N_{OG} = \frac{y1 - y2}{\Delta ylm} = \frac{0.0015 - 0.00072}{0.0001656} = 4.71$$

To obtain the height of the Transfer Units, H_{OG} , the correlation for packed column flooding velocities are used, as can be related in existing log-log plots for the correlations;

$$\frac{L}{G}\sqrt{\left(\frac{\rho g}{\rho l}\right)} = \frac{G2(ap/\epsilon 3)(\text{⍰}L)0.2}{gc\rho g\rho l}$$

Where,

L = mass flow rate of the liquid

G = mass flow rate of the gas

ρ_G = mass density of the gas

ρ_L = mass density of the liquid

μ_L = kinematic viscosity of the liquid

g_C = gravitational acceleration

a_p/ϵ^3 = correlation factor for the stoneware raschig rings

$$\frac{L}{G}\sqrt{\left(\frac{\rho g}{\rho l}\right)} = \frac{3{,}342.287}{474.752}\sqrt{\left(\frac{1{,}15}{930}\right)} = 0.25$$

Checking the correlation chart

$$0.02 = \frac{G2(ap/\epsilon 3)(\text{⍰}L)0.2}{gc\rho g\rho l}$$

$$G^2 = \frac{(0.02)(1.27x10\wedge 8)(1.15)(930)}{(159)(0.653)\wedge 0.2} = \frac{27.17 \text{ x } 10\wedge 8)}{146.01} = 0.1861 \text{ x } 10^8$$

$G = \sqrt{(0.1861 \text{ x } 10^8)} = 4.31 \text{ x } 10^3 kg/m^2h$ at flooding.

The column is to operate at 60% of the flooding velocity = 0.60 x 4310 = $2586 kg/m^2h$

Tower Diameter, $D = \sqrt{\frac{(4)x(474.752)}{(3{,}14)x\ (3586)}} = 0.082m$

Height of the gas phase transfer unit, $H_G = \alpha G^{\beta} L^{\gamma} S_C^{0.5}$

where from tables; $\alpha = 6.41$, $\beta = 0.32$, $\gamma = -0.51$ and $S_C = 1.14$

$$H_G = (6.41)(474.752)^{0.32}(3{,}342.287)^{-0.51}(1.13)^{0.5}$$

$$= 0.0206m$$

Height of the liquid phase transfer unit, $H_L = \phi(L/\mu)^n S_C^{0.5}$

where from tables; $\phi = 0.010$, $\mu = 0.653$, $\eta = 0.22$ and $S_C = 410$

$$H_L = 0.01(3{,}342.287/0.653)^{0.22}(410)^{0.5}$$

$$= 0.0488m$$

The overall gas phase HTU is given by;

$$H_{OG} = H_G + \frac{MGm}{Lm}H_L$$

$$M = 1.85, \frac{Gm}{Lm} = \frac{2476.665}{184.657} = 13.412$$

$$H_{OG} = 0.0206 + (\frac{1.85}{13.412})0.0488 = 0.0242m$$

Then, the overall height of the column, Z is given by;

$$Z = H_{OG}N_{OG}$$

$$= 0.0242 \times 4.71$$

$$= 0.114m$$

The wetting rate for the Column is given by;

$$L_W = \frac{volumetric\ \ liquid\ \ rate\ \ per\ \ unit\ \ cross-sectional\ \ area\ \ of\ \ column}{\text{packing surface area per unit volume of column}}$$

$$= \frac{L}{A\rho lSB} = \frac{28{,}515}{1.65} = 17.28m^3/m.hr$$

The pressure drop in the column is given by;

$$\Delta P = \tfrac{1}{2}N\rho_G u_G^2 Z$$

where, ΔP is the pressure drop

ρ_G is the gas density

u_G is the superfacial gas velocity

Z is the height of column

N is the number of velocity heads lost per unit height of packing

$\Delta P = ½ \times 25 \times 1.15 \times 934.45 \times 0.114$

$= 1531.32 N/m^2$

The volumetric hold-up for the column is;

$HW = 0.0004(\frac{L}{d})^{0.6}$

$= 0.0004(\frac{5,786.786}{0.082})^{0.6} = 0.32 m^3$ Liquid/m^3 column